

UNIVERSITY OF CALGARY

Effects of nitric oxide on HIF-1 alpha following *Clostridium difficile* toxin exposure

By

Joshua Lee

A THESIS

SUBMITTED TO THE FACULTY OF GRADUATE STUDIES

IN PARTIAL FULFILLMENT OF THE REQUIREMENTS FOR THE

DEGREE OF MASTER OF SCIENCE

DEPARTMENT OF BIOCHEMISTRY AND MOLECULAR BIOLOGY

CALGARY, ALBERTA

JANUARY 2012

© Joshua Lee 2012



The University of Calgary Libraries and Cultural Resources supplies documents under the fair dealing and library exceptions of the Copyright Act. The documents are for individual research purposes only, with any further reproduction prohibited.

Abstract

Clostridium difficile (C.diff) is a toxin-secreting bacterium and leading cause of infectious colitis in humans. C.diff toxins (TcdA and TcdB) rapidly induce intestinal injury and inflammation via disruption of the intestinal epithelial barrier and induction of proinflammatory mediators. The hypoxia-inducible factor-1 (HIF-1 α) is a stress-induced transcription factor that impacts the expression of mucosal and barrier protective genes. Initial studies have demonstrated that C.diff toxins alter the expression and activity of the HIF-1 α . Nitric oxide (NO), reactive oxygen species (ROS), and the factor-inhibiting HIF-1 α (FIH-1) are well-known modulators of HIF-1 α stabilization and signaling. Therefore, we hypothesize that NO and ROS produced during C.diff toxin-induced intestinal injury act as an important signal to influence HIF-1 α and subsequent protection against intestinal damage. In the context of C.diff toxin exposure, it was determined both *in vitro* and *in vivo* that stabilization occurred via nitrosylation of HIF-1 α by NO. Inhibition of iNOS activity by selective inhibitors or genetic iNOS-deficiency in mice attenuated HIF-1 α stabilization, which identifies iNOS as an essential source of NO in this context. Studies performed with N-acetylcysteine (NAC, a well-known ROS scavenger) *in vitro* have demonstrated a potential for ROS involvement in the stabilization of HIF-1 α . Pre-treatment of cells with NAC followed by C.diff toxin exposure attenuated HIF-1 α expression despite the fact that nitrosylation still occurred. This study is the first to propose a synergistic action between NO and ROS to stabilize HIF-1 α in the context of C.diff toxin-mediated epithelial damage.

Acknowledgements

I would like to thank my supervisor, Dr. Justin MacDonald, for providing me with this opportunity to make a meaningful contribution to the world of research. None of this would have been possible without his guidance, immeasurable patience, and encouragement over the past 3 years. By demonstrating an unwavering faith in my abilities, he created the ideal environment for independent learning and personal growth.

I would also like to thank my committee members, Dr. Paul Beck and Dr. Michael Surette, for their critical input and helpful suggestions throughout the course of my research. Thanks to their involvement, I've come to appreciate the many different aspects of medical research.

For their generosity, I would like to thank my external collaborators Dr. Tom Louie and Dr. Sean Colgan. Without the C.diff cultures (Dr. Louie) and HIF-1 α siRNA cells (Dr. Colgan), this project would not be what it is today.

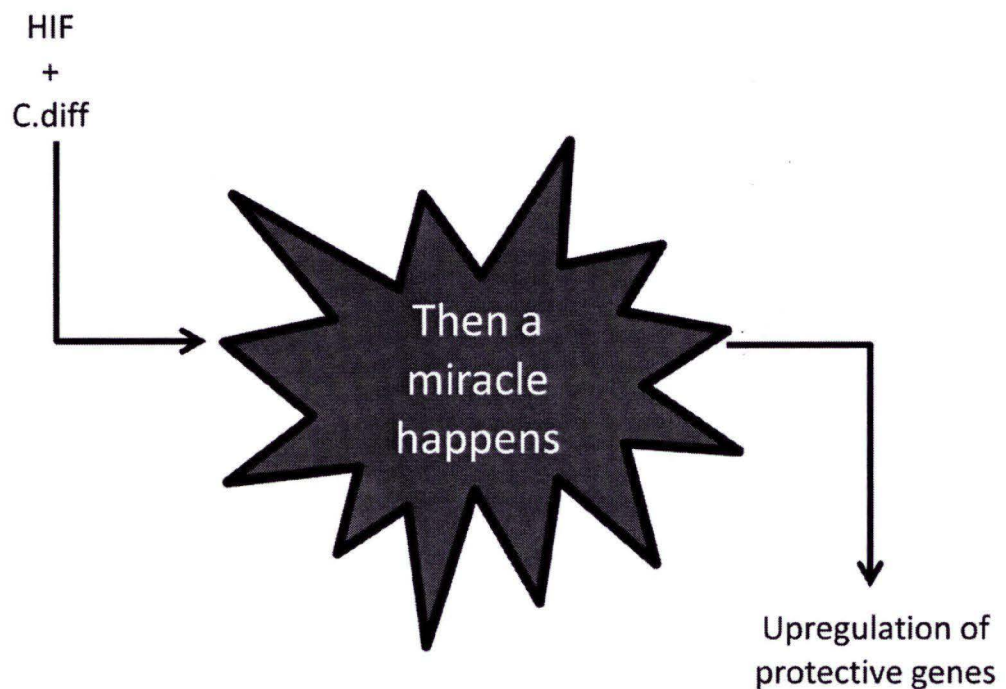
For their wealth of knowledge and technical assistance, I would like to thank Dr. Simon Hirota, Mona Chappellaz, and Annie Li. Many thanks go out to them for taking the time to teach the new kid how it's done. They've shown me all the ropes I currently know and it still doesn't even scratch the surface of everything they can do.

For the many helpful discussions and constant moral support, I would like to thank the guys that were in the trenches with me; Eric Butler, Mike Grassie, and Pat Schenck.

There were more than a few rough patches over the years, but misery had good company. Thanks guys.

A special thank you goes out to the people behind the scenes; CIHR and the Province of Alberta. Thanks to CIHR research funding and the Queen Elizabeth II scholarship, I was able to carry out my research while still living a relatively extravagant lifestyle.

Finally, I would like to thank my Caco-2 cells for teaching me a thing or two about parenting and how I'm definitely not ready for it.



Dedication

To my Savior, the author and finisher of my faith (...and this thesis). It was You who brought me through the desert and into the promised land. It's You and me, until the end.

To my family, who stood beside me. This wasn't so much about research as it was a lesson in adversity. Good days or bad, you were there throughout and believed in me when I didn't think I had anything left. For all I've been through, and all that's still to come, I can't thank you enough.

Table of Contents

Approval page.....	ii
Abstract.....	iii
Acknowledgements.....	iv
Dedication.....	vi
Table of Contents.....	vii
List of figures.....	xi
List of abbreviations.....	xiv
1 Introduction.....	1
1. – An overview of <i>Clostridium difficile</i>	
• i - Background and impact.....	2
• ii - <i>C. difficile</i> and the gastrointestinal environment.....	3
• iii – <i>C. difficile</i> toxins: structure and function.....	6
• iv - Mechanisms of barrier breakdown.....	7
2. – Hypoxia Inducible Factor – 1	
• i – Molecular composition: The α and β subunits of HIF-1.....	8
• ii - Activity of Hypoxia Inducible Factor-1 α	10
• iii - HIF-1 α in the context of inflammation and the GI tract.....	11
3. – An overview of nitric oxide	
• i - Nitric oxide synthase – Isozymes I, II and III.....	13
• ii - Formation and action of nitric oxide.....	15

•	iii - Nitric oxide in the context of the GI tract.....	17
•	iv - Interactions with HIF-1 α	22
4.	– An overview of reactive oxygen species	
•	i - Structure and production.....	26
•	ii - Reactive oxygen species in the context of the GI tract.....	29
•	iii - Interactions with nitric oxide.....	30
	Summary figure 1: Mechanisms of	
	HIF-1 α regulation.....	32
2	Hypothesis and objectives.....	34
1.	– Assess the effect of <i>C.diff</i> toxins on HIF-1 α on a post-translational level	
2.	– Assess the effects of NO on HIF-1 α in the presence of <i>C.diff</i> toxins	
3.	– Assess the relationship between reactive oxygen species and NO and how it affects HIF-1 α expression	
3	Materials and Methods.....	37
1.	– Inoculation of <i>C. difficile</i> cultures and production of toxin.....	38
2.	– <i>C. difficile</i> toxin purification.....	39
3.	– Cell culturing and maintenance of Caco-2 intestinal epithelial cells.....	40
4.	– Cell plating and experiment preparation.....	41
5.	– Light microscope images of Caco-2 cell monolayers.....	42
6.	– Caco-2 cell lysis with cytosolic and nuclear extract preparation.....	42
7.	– Bradford Assay for protein concentration.....	43
8.	– Electrophoretic Mobility Shift Assay.....	44

9. – Sodium Dodecyl Sulfate-Polyacrylamide	
Gel Electrophoresis (SDS-PAGE).....	45
10. – Immunoprecipitation of HIF-1 α from Caco-2 nuclear extracts.....	46
11. – Immunoblotting (Western blotting).....	47
12. – Biotin Switch Assay.....	48
13. – Nitric oxide detection assay.....	49
14. – Immunocytochemistry (ZO-1 staining).....	50
15. – Mouse surgical procedures.....	51
• Ileal-loop surgical protocol	
• Intra-rectal installation protocol	
16. – Statistics.....	53
4 Results.....	54
C.diff toxin disrupts epithelial monolayer morphology.....	55
C.diff toxin modulates HIF-1 α expression and signaling.....	55
C.diff toxin modulates HIF-1 α expression	
via iNOS-generated nitric oxide.....	65
C.diff toxin disrupts Caco-2 epithelial monolayer tight junctions.....	66
Effects of reactive oxygen species on C.diff toxin-mediated	
modulation of HIF-1 α	67
C.diff toxin modulates HIF-1 α expression via iNOS-generated	
nitric oxide in vivo.....	87

5 Discussion	92
1. – Analysis and interpretation.....	93
2. – Future directions.....	108
 Summary Figure 2: Mechanisms of <i>Clostridium difficile</i> -mediated HIF-1 α regulation.....	110
 6 References	113

List of Figures

- Summary Figure 1: Mechanisms of HIF-1 α regulation
- Figure 4.1: Evaluation of Caco-2 cell monolayer morphology following application of *C. difficile* toxin
- Figure 4.2: Assessment of HIF-1 α stabilization in Caco-2 cells exposed to *C. difficile* toxin
- Figure 4.3: Electrophoretic Mobility Shift Assay of HIF-1 DNA binding activity following exposure to *C. difficile* toxin
- Figure 4.4: Examination of iNOS expression and HIF-1 α nitrosylation in Caco-2 cells exposed to *C. difficile* toxin
- Figure 4.5: Purification of TcdA and TcdB from *C. difficile* crude toxin isolate: Chromatographic purification (A) and assessment of toxin purity (B)
- Figure 4.6: Examination of HIF-1 α expression in Caco-2 cells exposed to purified *C. difficile* toxin B
- Figure 4.7: Examination of iNOS expression and nitric oxide concentration in Caco-2 cells exposed to purified *C. difficile* toxin B
- Figure 4.8: Assessment of iNOS inhibition on HIF-1 α stabilization in Caco-2 cells exposed to *C. difficile* toxin

- Figure 4.9: Examination of iNOS-selective inhibition on iNOS expression and nitric oxide concentration in Caco-2 cells exposed to *C. difficile* toxin exposure
- Figure 4.10: Examination of iNOS inhibition on HIF-1 α nitrosylation (biotinylation) in Caco-2 cells exposed to *C. difficile* toxin
- Figure 4.11: Immunocytochemistry of ZO-1 staining and epithelial monolayer integrity following *C. difficile* toxin exposure and iNOS inhibition
- Figure 4.12: Quantification of Caco-2 epithelial monolayer integrity following *C. difficile* toxin exposure and iNOS inhibition
- Figure 4.13: HIF-1 α protein expression in scrambled and knockdown Caco-2 cells upon stimulation with CoCl₂
- Figure 4.14: Assessment of N-acetylcysteine on HIF-1 α stabilization in HIF-1 α scrambled (A) and knockdown (B) Caco-2 cells exposed to *C. difficile* toxin
- Figure 4.15: Examination of N-acetylcysteine on iNOS expression and nitric oxide concentration in HIF-1 α scrambled (A) and knockdown (B) Caco-2 cells exposed to *C. difficile* toxin
- Figure 4.16: Examination of N-acetylcysteine on HIF-1 α nitrosylation (biotinylation) in HIF-1 α scrambled (A) and knockdown (B) Caco-2 cells exposed to *C. difficile* toxin

- Figure 4.17: Immunocytochemistry ZO-1 as an indicator of epithelial monolayer integrity following exposure to *C. difficile* toxin and N-acetylcysteine in HIF-1 α scrambled cells (A) and knockdown (B) cells
- Figure 4.18: Quantification of Caco-2 epithelial monolayer integrity following *C.difficile* toxin and N-acetylcysteine in HIF-1 α scrambled (A) and knockdown (B) cells
- Figure 4.19: Ileal-loop surgical procedure – HIF-1 α Immunoprecipitation in toxin versus PBS-treated WT mice
- Figure 4.20: Ileal-loop surgical procedure – HIF-1 α Immunoprecipitation in toxin-treated WT versus iNOS $^{-/-}$ mice
- Figure 4.21: Intra-rectal surgical procedure – HIF-1 α protein expression and nitrosylation in PBS versus Toxin-treated C57/Bl6 mice
- Summary Figure 2: Mechanisms of *Clostridium difficile*-mediated HIF-1 α regulation

List of Abbreviations

AP-1	Activator protein 1
Arnt	Aryl hydrocarbon receptor nuclear translocator
Caco-2	Colorectal adenocarcinoma-derived intestinal epithelial cell line
CBP	CREB-binding protein
CDAD	Clostridium difficile-associated disease
C.diff	Clostridium difficile
cGMP	Cyclic guanosine monophosphate
cNOS	Constitutive nitric oxide synthase
CTAD	C-terminal transactivation domain
EDTA	Ethylene diamine tetraacetic acid
EGTA	Ethylene glycol tetraacetic acid
eNOS (NOS III)	Endothelial nitric oxide synthase
FIH-1	Factor Inhibiting Hypoxia-Inducible Factor 1
GC	Guanylate cyclase
GSNO	S-nitrosogluathione
GTP	Guanosine triphosphate
GTPase	Guanosine triphosphate hydrolase
HIF	Hypoxia-Inducible Factor
HIF-KD	Hypoxia-Inducible Factor 1 α knockdown siRNA
HIF-Scr	Hypoxia-Inducible Factor 1 α scrambled siRNA

HRE	Hypoxia Response Element
IFN- γ	Interferon- γ
IKK α	Inhibitor of Nuclear Factor kappa-B kinase subunit α
IL	Interleukin
iNOS (NOS II)	Inducible nitric oxide synthase
iNOS-KO	Inducible nitric oxide synthase knockout
L-NAME	L-N ^G -Nitroarginine methyl ester
L-NMMA	L-N ^G -monomethyl arginine citrate
LPS	Lipopolysaccharide
NAC	N-Acetylcysteine
NADPH	Nicotinamide adenine dinucleotide phosphate
NF- κ B	Nuclear Factor kappa-light-chain-enhancer of activated B cells
nNOS (NOS I)	Neuronal nitric oxide synthase
NO	Nitric oxide
NTAD	N-terminal transactivation domain
ODDD	Oxygen-dependent degradation domain
PHD	Prolyl hydroxylase
PMC	Pseudomembranous colitis
ROS	Reactive oxygen species
RNI	Reactive nitrogen intermediates
RNS	Reactive nitrogen species
siRNA	small interfering ribonucleic acid

SNAP	S-nitroso-N-acetylpenicillamine
SOA	Superoxide anion
SOD	Superoxide dismutase
TcdA/B	Crude toxin (mixture of Clostridium difficile toxins A and B)
TcdA	Clostridium difficile toxin A
TcdB	Clostridium difficile toxin B
TJ	Tight Junction
TNF- α	Tumor necrosis factor- α
UDP	Uridine diphosphate
VHL	von Hippel-Lindau protein
ZO	Zonula Occludens
1400W	N-(3-(Aminomethyl)benzyl)acetamidine

1.0

introduction

1.0 Introduction

1.1 An overview of *Clostridium difficile*

i) Background and Impact

Clostridium difficile (C.diff) is an anaerobic gram-positive, rod-shaped, bacterium that is a leading cause of severe hospital-acquired colitis and diarrhea; otherwise known as C.diff-associated disease (CDAD) [1-3]. C.diff-related mortality rates are steadily rising in the United States and Canada. C.diff-related deaths in the US have increased from 5.3 per million population (1999) to 23.7 per million (2004) over the course of only 5 years throughout which the rates have also been steadily climbing. In Quebec, Canada there have also been reports of increased CDAD incidence especially among the elderly population over 65 years of age. The rate of incidence has increased from 35.6 per 100,000 population in 1991 to 156.3/100,000 in 2003 [4, 5]. Our current understanding of C.diff containment and elimination requires immediate attention as outbreaks of hypervirulent strains are still occurring. Such was the case in Quebec in 2003 and to a lesser extent in Calgary, Alberta in the same year. Hospitals in Quebec City and Calgary battled with the antibiotic-resistant infections for at least 18 months before bringing C.diff incidence levels close to baseline [5, 6]. C.diff infection rates are continuously rising and US hospitals are reporting anywhere between 250,000 to 300,000 cases of CDAD a year and associated health care costs of up to \$1 billion US per year. A typical C.diff patient requires anywhere between 1-2 weeks of treatment totaling up to \$10,000

in health care costs [7]. This cost assumes that the patient is successfully treated without relapse, which is becoming an increasing problem especially among elderly populations [4, 7]. With *C.diff* becoming increasingly resistant to antibiotic treatments and with health care costs steadily rising, alternative methods of combating this infectious bacteria are needed.

ii) *C. difficile* and the gastrointestinal environment

C.diff itself is an opportunistic colonizer, with infections often occurring in patients following broad-spectrum antibiotic treatments (such as clindamycin [1, 2], cephalosporins [1] and fluoroquinolones [1, 5]) and chemotherapeutic agents [1, 3]. Studies have shown *C.diff* to be the primary isolate in the feces of clindamycin-treated patients [2, 3]. By eliminating the majority of healthy bacterial flora within the colon, the antibiotics and chemotherapeutic agents create ideal conditions for *C.diff* bacteria to out-compete other bacterial strains [2, 3, 7]. Two important characteristics of *C.diff* are its ability to produce toxins and form spores [1-3]. When conditions are unfavorable for the growth and proliferation of the bacteria, they begin forming spores and enter into a dormant state that allows for survival until more favorable environmental conditions occur. *C.diff* spores are highly resistant to adverse conditions including acidic environments (thus they cannot be destroyed by gastric secretions), chemical cleaning agents and many alcohol-based sanitizers which are commonly used in hospitals. As a result of this resilience, *C.diff* spores can survive on surfaces for extended periods (e.g.,

months), allowing *C.diff* outbreaks and infections to persist [3, 7, 8]. Once spores are ingested, they survive the harsh conditions of the stomach [3, 7] to enter into the intestine where pH is approximately 6 (still slightly acidic) providing a favorable environment for the beginning of germination. Spores continue to travel to the large intestine where they rapidly germinate and outcompete other bacterial species [8]. Once *C.diff* begins to colonize the large intestine it begins producing potent toxins which are the effectors of CDAD and mucosal inflammation.

In order to thoroughly understand the effects of *C.diff* within the gastrointestinal environment, we must first investigate the environment itself as well as the cells most directly affected by the bacteria. The entire intestinal tract is lined with a single, continuous layer of columnar cells known as epithelial cells. These cells are an integral part of the barrier which regulates the absorption of material from the lumen of the intestine into the tissues themselves. The intestinal epithelial cells are situated atop a bed of loose connective tissue perfused with capillaries and lacteals known as the lamina propria, and the combination of these two structures is collectively known as the intestinal mucosa. The epithelial cell layer along with secreted layers of mucus serve to separate the intestinal lumen from the underlying lamina propria and the subsequent layers of intestinal tissue [9, 10]. The epithelial barrier is a dynamic structure which is regularly replaced approximately every 2 to 5 days. Regular maintenance of this barrier is absolutely essential for maintaining homeostasis, normal intestinal function, and protection from disease [9, 11].

An extremely important aspect of the epithelial barrier are the junctions between the epithelial cells. The most apical portion of these junctions are collectively known as tight junctions (TJs) and they are comprised of a number of different proteins that are associated with the plasma membranes of the epithelial cells. Membrane proteins such as the claudins, occludins, and junctional adhesion molecules (JAMs) span the inter-membrane space and form tight connections between adjacent epithelial cells. Plaque proteins such as the zonula occludens (ZO) family of proteins (i.e., ZO-1, -2, and -3), function to anchor the membrane proteins together within the cell and connect them to an intracellular structure known as the actomyosin ring [9, 10, 12]. The actomyosin ring is a belt-like structure that is situated at the apical end of the epithelial cell and is composed of actin and myosin II. This structure is capable of contracting and is known to be involved in regulating the TJ. During contraction, it is able to pull adjacent cells together in order to maintain barrier integrity [10]. These contractions are also involved in the regular maintenance of the barrier by “squeezing out” dead epithelial cells and closing the gaps that are left behind [10, 13]. The ZO family of proteins can directly interact with protein filaments of the actin cytoskeleton; which is a structure that is composed of actin filaments and is present throughout the cytosolic component of all eukaryotic cells. One of its primary functions is to maintain the structure of the cell as a whole [10, 14, 15]. Both the TJ and the adherens junction (located beneath the TJ and is involved in cell to cell adhesion) interact directly with the actin cytoskeleton, effectively linking the structure of an individual cell with its connections to adjacent cells [10, 14].

The TJ, along with the epithelial cells, acts as a selectively permeable barrier that determines which molecules enter the gut based on their size and charge [12]. It is this crucial barrier that acts as the primary target for *C. diff* toxins, and it is the disruption in barrier which subsequently results in massive cellular damage and uncontrolled inflammation [2, 3, 11, 16].

iii) *C. difficile* toxins: structure and function

The two primary toxins produced by *C. diff* are Toxin A (TcdA) and Toxin B (TcdB), which both exhibit cytotoxic effects. TcdA and TcdB have been classified as large clostridial toxins as they are long, single-chain proteins with sizes of 308 kDa and 270 kDa respectively [2, 3, 16, 17]. Encoded on the same pathogenicity locus of *C. diff*, TcdA and B both contain 4 key domains; the biologically active N-terminal domain, the C-terminal oligosaccharide receptor binding domain, the autocatalytic cysteine protease domain, and the hydrophobic transmembrane domain [3, 7, 16, 17]. Once the toxins have been released from the bacteria, the C-terminal receptor binding domains bind to oligosaccharide-type receptors (usually containing galactose β 1-4 linkages) and are taken up into the mucosal cells via endocytosis [3, 17]. Within the acidic endosome, a conformational change occurs whereby the transmembrane domain is inserted into the endosome and the active N-terminal domain (which contains glucosyltransferase activity) is cleaved off and exits through a pore in the endosome [3, 7, 17]. Although the structure of the transmembrane domain is largely unknown at this point, it is thought to

be involved in formation of the endosomal pore [17]. Acidification of the endosome is crucial in order for the toxins to be able to undergo the necessary conformational change. Also, preventing the fusion of a lysosome with the newly formed endosome has been shown to attenuate TcdB activity [3].

iv) Mechanisms of barrier breakdown

Once inside the cytosol, the glucosyltransferase activity of the C.diff toxin protein proceeds to remove a glucose moiety from UDP-glucose (which acts as a co-substrate) and transfers it to small GTPase proteins such as Rho, Rac, and Cdc42 [2, 3, 7, 16, 17].

These proteins are involved in cell cycle pathways and their inhibition causes an increase in two different types of cell death, known as apoptosis and necrosis [3, 16]. While both result in the death of cells, necrosis is characterized by the release of cytoplasmic contents which initiates a local inflammatory response [16]. In addition, Rho proteins are also known to control the structure of the actin cytoskeleton within cells.

Inactivation of Rho proteins results in condensation of actin (i.e., the breakdown or depolymerization of actin filaments), destabilization of the cytoskeleton and eventual change in cell morphology (i.e., cell rounding) [3, 16, 17]. Rho proteins also maintain the tight junctions between epithelial cells, and when combined with the apoptotic effects of TcdA/B, the mucosal layer becomes compromised as its permeability to various fluids becomes increased. This results in an increase in fluid influx into the mucosal layer [2, 3, 7, 16, 17]. The toxins are also responsible for causing an increase in pro-inflammatory

cytokines from intestinal epithelial cells such as Interleukin-8 (IL-8) and other inflammatory mediators such as Tumor Necrosis Factor- α (TNF- α). This leads to neutrophilic infiltration and the stimulation of the mucosal immune system to initiate a key inflammatory response, a primary effector of intestinal injury [18, 19]. As the colonization of *C.diff* continues, severe inflammation results as well as the formation of pseudomembranous plaques, which are composed of mucous and necrotic epithelial cells. This condition is known as pseudomembranous colitis (PMC) and it is the primary pathogenic condition resulting from *C.diff* infection [2].

1.2 *Hypoxia-Inducible Factor-1*

i) Molecular composition: The α and β subunits of HIF-1

Within the intestinal epithelial cells, there are many different genes which are responsible for encoding proteins that are directly (or indirectly) involved in barrier maintenance and repair. Proteins known as transcription factors have been shown to bind to specific regions of these genes (known as response elements) in order to activate the subsequent production of mRNA transcripts which eventually lead to the formation of these proteins. The hypoxia-inducible factors, or HIFs, are important regulatory transcription factors made up of α and β subunits which are members of the basic helix-loop-helix/PAS (per-arnt-sim homology) family of transcription factors. The α and β subunits must combine to form a heterodimer in order to become

transcriptionally active and modify gene expression (Summary Figure 1). The β subunit of HIF is also referred to as the aryl hydrocarbon receptor nuclear translocator (Arnt1), and it is a constitutively expressed nuclear protein. There are 3 different forms of the β subunit termed Arnt1, Arnt2, and Arnt3. There are also 3 different isoforms of the α subunit known as, HIF-1 α , HIF-2 α , and HIF-3 α [20-23]. The α subunit of HIF, unlike the β subunit, is regulated in a manner directly dependent on oxygen availability. Despite the fact that HIF- α is expressed at a constant rate, the cellular levels of HIF- α tend to be extremely low in normoxic conditions. When oxygen is readily available, the HIF- α subunit is targeted for proteosomal degradation and this usually happens in a very rapid manner as HIF- α remains in the cell for less than 10 minutes. This proteosomal degradation is controlled by a domain which exists within the HIF- α structure known as the Oxygen-Dependent Degradation Domain (ODDD). Within this domain reside two key proline residues (P-402 and P-564) that are targeted for hydroxylation by enzymes (prolyl hydroxylases – PHD) that are specific for the HIF- α subunit [20, 24-26]. It is important to note that the PHDs which are specific for HIF- α are oxygen-dependent themselves. Thus, when oxygen is abundant, the enzymes are stable and able to carry out the hydroxylation of the HIF- α subunit [25]. The hydroxylation of the key proline residues on the HIF- α subunit creates a binding site for the von Hippel-Landau (VHL) protein which is part of the VHL ubiquitin ligase complex (an E3 ubiquitin ligase). The VHL complex binds to HIF- α by forming hydrogen bonds with the two hydroxylated proline residues. Upon binding, the VHL complex proceeds to polyubiquitinate the HIF- α

subunit; thus, marking the transcription factor for proteosomal degradation [25, 27]. In contrast, under conditions of low oxygen levels within the cell, a general stabilization of HIF- α levels occurs. When the cell experiences hypoxia, the PHDs are no longer able to hydroxylate HIF- α subunits due to inhibition from low oxygen concentrations, thus preventing the subsequent proteosomal degradation [28].

ii) Activity of Hypoxia-Inducible Factor-1 α

In the event that HIF- α is stabilized, it is able to translocate into the nucleus of the cell [20, 28]. Once inside the nucleus, it proceeds to dimerize with the HIF-1 β subunit to form an active HIF transcription factor. This heterodimerization step is essential for allowing HIF to bind to a domain on target genes known as the Hypoxia Response Element (HRE) with a core sequence of 5'-TACGTG-3'. Once bound, HIF would go on to modify gene transcription in response to hypoxic conditions [20, 21, 24]. As opposed to HIF-1 α and -2 α , HIF-3 α while still able to form a heterodimer with HIF-1 β , appears to have an inhibitory role. HIF-3 α is thought to accomplish this by sequestering the available HIF-1 β , thus preventing the subsequent gene transcription that usually accompanies HIF dimerization and activation [20].

Both α and β subunits of the HIF complex contain two transactivation domains which are also important in regulating the activity of HIF. The C-terminal transactivation domain (CTAD) and the N-terminal transactivation domain (NTAD) recruit the help of transcriptional coactivators, p300 and CREB binding protein (CBP). These coactivators

are necessary in order to form complexes with other coactivators and transcriptional machinery. Once the complex is formed it is able to effectively upregulate transcription of downstream genes. A key regulator of the CTAD is an asparaginyl hydroxylase known as Factor Inhibiting HIF-1 α (FIH-1). In normoxic conditions, the oxygen-dependent enzyme FIH-1, inhibits the CTAD's ability to recruit p300/CBP by hydroxylating an asparagine residue (asn 803), thus providing another level of oxygen-dependent control [20, 21, 27-29].

iii) HIF-1 α in the context of inflammation and the GI tract

In early experiments carried out *in vivo* with animals exposed to hypoxia, an increase of HIF-1 α mRNA transcription was observed [30]. In the HIF-1 α studies that followed it was determined that, depending on the conditions used, many substances were able to influence HIF-1 α transcription. These results defied the convention that HIF-1 α stabilization and modification were strictly post-translational events. In studies performed in human monocytes (both differentiated and undifferentiated), stimulation with bacterial lipopolysaccharide (LPS) was found to increase the HIF-1 α mRNA transcription as well as protein concentration in normoxic conditions [30, 31]. LPS activity influences HIF-1 α directly at the transcriptional level since the inhibition of transcription eliminates LPS effects on HIF-1 α under normoxic conditions. With respect to inflammatory pathways, this is important since LPS, which binds to surface receptors, is also known to induce immune response-related transcription factors NF- κ B and AP-1.

Analysis of upstream promoters of HIF-1 α revealed binding sites for both of these transcription factors and without NF- κ B, continuous transcription of HIF-1 α mRNA is not possible. In studies relating to downstream HIF-1 effects, it was found that p65 (an NF- κ B subunit) and IKK α (a kinase which phosphorylates NF- κ B inhibitors causing their dissociation from NF- κ B) are both gene targets of the HIF-1 complex suggesting that the interaction between NF- κ B and HIF-1 is part of a hypoxia and inflammation-induced enhancing cycle [30].

These findings are particularly relevant to inflammatory diseases such as colitis. Epithelial tissues in the intestines are known to be somewhat hypoxic due to the large oxygen gradient formed between epithelial tissues and subepithelial tissues. This gradient is formed as a result of the distance between the epithelium and the vascular blood flow, which causes most of the oxygen to be taken up by the subepithelial layer. Epithelial tissues demonstrate a nearly 2-fold increase in the expression of HIF-1 target genes relative to surrounding tissues [32, 33]. At the tissue level, it has been shown that inflammation and hypoxia are closely associated with each other, which is perhaps why Crohn's disease (an inflammatory disease) is characterized by alterations in tissue oxygen and energy levels [33, 34]. Without adequate oxygen and energy, the epithelial transport and barrier functions can quickly become compromised. A clinically important symptom shared by Crohn's disease, ulcerative, ischemic, and C.diff-mediated colitis seems to be the loss of barrier function via disruption of tight junctions [16, 32-34]. HIF-1 however, demonstrates a protective function in the epithelium. Through murine

models of colitis, it has been observed that mice that had decreased levels of HIF-1 also experienced the most severe symptoms. If HIF-1 was constitutively active, loss of epithelial barrier function was decreased *in vivo* and therefore damage to the mucosa was decreased. Further studies in colons that constitutively expressed HIF-1 also showed an increased expression of HIF-1 target genes including CD73, CD55, intestinal trefoil factor (ITF), multidrug resistance gene-1, and the adenosine A2B receptor; all of which are involved in increasing the protection afforded by the epithelial barrier [33, 34]. It is important to note that despite the heavy influence of oxygen on the regulation and control of HIF-1 α , other factors, such as nitric oxide (NO) have also been found to play an essential role in mediating HIF-1 α activity [24, 27, 35].

1.3 *An overview of nitric oxide*

i) Nitric oxide synthase – isozymes I, II, and III

NO is produced in the tissues by an enzyme known as nitric oxide synthase (NOS).

Depending on the cellular location within the body, NO can be produced by one of three different NOS isozymes; neuronal (nNOS, NOS I), endothelial (eNOS, NOS III) or inducible (iNOS, NOS II) nitric oxide synthase [36, 37].

The first enzyme to be purified, nNOS, is a constitutively active enzyme in the body. Despite its constant expression, nNOS is only capable of producing very small

quantities of NO, typically within the picomolar range [36, 38]. In terms of regulation, nNOS activity is highly dependent upon Ca^{2+} concentrations within the cell [36].

The third isozyme to be purified, eNOS, shares certain key features in common with the nNOS isozyme. The eNOS isozyme is also constitutively expressed, but like nNOS, it is short-lived and produces a very small (picomolar) amount of NO [36, 38]. Also, eNOS activity is dependent on intracellular Ca^{2+} concentrations, but to an even greater extent than nNOS in their respective tissue types. The eNOS protein is primarily found in the particulate (membrane-bound) fraction, whereas nNOS and iNOS are primarily in the soluble fraction [36].

The second isozyme to be purified, iNOS, demonstrates key differences from both nNOS and eNOS. Unlike the other two isozymes, iNOS is not a constitutively active enzyme, and was originally purified from murine macrophages. In addition to macrophages, iNOS can also be induced in epithelial cells, eosinophils, neutrophils, hepatocytes, and smooth muscle cells. Unlike nNOS and eNOS, iNOS is long-lived and produces NO at much higher concentrations; nanomolar as opposed to picomolar levels. Another key difference between the constitutively active NOS enzymes (cNOS) and iNOS is their sensitivity to Ca^{2+} . Regulation of iNOS is Ca^{2+} independent and induction of iNOS typically occurs in the presence of bacterial endotoxins (such as LPS) and inflammatory cytokines (such as IL-1 β , TNF- α , and IFN- γ); thus making it clinically relevant in pathological conditions [37-39]. The presence of iNOS in normal intestine is to be expected as the intestinal tissues often make "first contact" with respect to foreign

antigens. Also, the intestine is home to many different species of bacteria whose byproducts can act as potent stimulators for the induction of iNOS in the tissues [40]. Due to the relative volumes of NO produced by the three enzymes, iNOS has often been associated with inflammation and damage. Whereas, the smaller volumes of NO produced by cNOS have been deemed beneficial in maintaining homeostasis [40, 41]. To reiterate and summarize the roles of each NOS isozyme, cNOS is typically associated with normal regulatory functions within the cell, whereas iNOS is associated with disease-state or pathological conditions [36-39].

ii) Formation and action of nitric oxide

It is believed that the mechanism of generating the small NO radical is quite likely to be consistent across all three isozymes of NOS due to similar cofactor requirements [36]. The NOS enzyme, in conjunction with molecular oxygen and NADPH as co-substrates, carries out an oxidation of the terminal guanido nitrogen from the amino acid, L-arginine. The final result of the aforementioned reaction are the two products, NO and L-citrulline [37, 38, 42, 43]. This enzymatic reaction is highly specific as structural analogs of L-arginine, such as L-N^G-monomethyl-arginine (L-NMMA) and L-N-nitro-arginine methyl ester (L-NAME) act as competitive inhibitors of NOS [38, 44]. NO is quite lipophilic, which allows it to pass through cell membranes, but it also has a very short biological half-life (3-5 seconds); therefore it has a rapid, localized effect on surrounding tissues [44]. The action of NO however is quickly attenuated by the

conversion to either NO_2^- or NO_3^- , which are both much less potent in terms of regulating specific biological processes [42, 44]. The majority of NO (90%) undergoes a spontaneous oxidation to form NO_2^- and the remaining NO is converted to NO_3^- in a reaction with the superoxide anion (O_2^-). It is important to mention that NO_2^- can also be oxidized to NO_3^- . The presence of NO_3^- is rare due to the fact that superoxide dismutase enzymes typically keep levels of O_2^- very low; however this may change and have an increased relevance in various pathological conditions [44]. It is important to note that both NO and NO_2^- are able to react with thiol groups in order to form more chemically complex nitroso-donating compounds such as S-nitrosothiols. These compounds are potentially relevant in clinical applications as they are known to have a much longer biological half-life than NO (anywhere from 30 seconds to 1 hour depending on the compound) [27, 44]. The actual biological action of NO is based on the use of various NO donating compounds such as Deta-NONOate, S-nitrosoglutathione (GSNO), S-nitroso-N-acetylpenicillamine (SNAP), or sodium nitroprusside (SNP) [24, 27, 35, 45]. Many of these NO derivative compounds (as mentioned above) are able to nitrosylate (post-translational protein modification with NO), nitrate (addition of a nitro group, NO_2 , on a chemical compound), nitrosate (addition of NO group on an organic compound), or even oxidize various target molecules/proteins. This can lead to changes in gene transcription and/or translation. NO, however, is not consistent in its action on the cell as its effects can vary depending on the timing of NO action, NO concentrations,

and even redox states of the cell. One important example of varying NO effects deals with its interaction with HIF-1 α in normoxic versus hypoxic environments [24, 35].

iii) Nitric oxide in the context of the GI tract

Before we explore the different interactions of NO with HIF-1, it is important to understand the role of nitric oxide in the context of the gastrointestinal tract. There is definitely an extensive body of work which implicates the three isoforms of NOS as critical contributors to many physiological processes throughout the body. However, for the purposes of this thesis, only the functions relating to the GI tract will be discussed, particularly those of iNOS.

One of the first studies to characterize the role of NO in the intestine involved the use of ⁵¹Cr-labeled EDTA in feline ileum. This study successfully demonstrated that NO plays a role in regulating intestinal permeability. A local intra-arterial infusion of the broad spectrum NOS inhibitor (i.e. acts as a competitive inhibitor of all three isoforms of NOS), L-NAME, caused a significant increase in the blood-to-lumen clearance of ⁵¹-Cr EDTA. This increase in permeability was nearly six times that of the control treatment and was such that the presence of macromolecules (such as fluorescently-labeled dextran) was increased from the interstitial space to the lumen. These effects of L-NAME on intestinal permeability were effectively countered by the addition of L-arginine (which would compete against L-NAME for the active site on the NOS enzyme) or the nitric oxide donating compound, sodium nitroprusside (SNP). In addition, the infusion of a

structural isomer of L-NAME, D-NAME, had no effect on permeability in the feline small intestine. It is important to note however that the increase in permeability due to NO inhibition was not necessarily the result of increased injury to the epithelium. In this particular study, there was no evidence of overt intestinal damage such as the presence of blood or mucosal lesions [46].

In terms of NO's direct effects on intestinal permeability, it has been previously postulated that the relaxation mechanisms of cells may be involved. It has been well-characterized that one of NO's main functions is the activation of the enzyme guanylate cyclase (GC). GC activity involves the conversion of guanosine triphosphate (GTP) into cyclic guanosine monophosphate (cGMP). The formation of cGMP has been implicated in a number of physiological processes as it reacts together with cGMP-dependent protein kinase and triggers an important signaling cascade. This signaling event is known to be involved in altering the phosphorylation state of many different proteins, which includes the dephosphorylation of myosin light chain. This dephosphorylation is responsible for inducing a relaxation response in the cells [47, 48]. Therefore, by inhibiting NO synthesis and preventing the activation of GC, this results in cell constriction and the increase in the interepithelial spaces. Also, this can prevent the stimulation of certain gastric mucus secretions by soluble GC. Through these mechanisms, it is possible that NO may be directly involved in regulating intestinal epithelial permeability [37, 49, 50].

Studies which investigated the role of NO synthesis inhibitors in rat intestinal permeability have demonstrated a potential role of reactive oxygen species and mast cells [49]. In this study, permeability was once again determined to increase roughly sixfold in rats that were treated with the NOS inhibitor, L-NAME. Along with an increase in permeability, the tissues also demonstrated a significant increase in mast cell degranulation; which has been associated with the release of a number of inflammatory mediating factors such as oxidants, platelet-activating factor (PAF), and histamine. Pretreatment of rat jejunum with Superoxide dismutase (SOD – an antioxidant enzyme), dexamethasone (causes mast cell depletion), PAF inhibiting compounds, or mast cell stabilizing compounds, prior to the addition of L-NAME all resulted in an attenuation of the increased permeability that was seen with L-NAME treatment alone.

Another important role for NO is its association with neutrophils. Neutrophils act as a source of oxidant molecules and their recruitment to sites of inflammation are a regular occurrence in many different inflammatory pathologies [39]. Studies performed in postischemic tissue have demonstrated that NO is capable of inhibiting neutrophil adhesion and emigration by inhibiting the expression of various molecules required for adhesion [51, 52]. Furthermore, NO has also been shown to act specifically on the enzymatic processes in neutrophils which are responsible for oxidant production. In a cell-free system, it was demonstrated that exposing plasma membrane elements of the NADPH-oxidase enzyme complex prior to assembly of the entire complex, resulted in a

significant reduction in the amount of ROS generated by the enzyme upon stimulation with NADPH [53].

It is important to mention that many of these studies investigating the role of NO in the intestine, particularly the studies which focus on NO synthesis inhibition, only look at the general effects of the NOS enzymes as a whole. As mentioned previously, L-NAME and L-NMMA are broad spectrum inhibitors which, at best, implicate all three isozymes of NOS in regulating epithelial permeability. One study, which examined the effects of endotoxin in rats, found interesting results pertaining to iNOS and its role in affecting intestinal permeability. When exposing rat colonic tissues to LPS, it was found that co-incubation with EGTA (a calcium chelating agent) suppressed NOS activity only up until the 3 hour mark, beyond which EGTA provided only partial suppression of NOS activity suggesting the presence of a calcium-independent NOS enzyme (a primary characteristic of iNOS) after 3 hours of LPS exposure. In this same study, if the NO synthesis was inhibited with L-NMMA prior to the initial induction of NOS activity (i.e. 0-3 hours) it proved to have detrimental effects with respect to the endotoxin-induced colonic damage. However, if the L-NMMA was added prior to the induction of iNOS, the damage was attenuated and it seemed to have a protective effect. Therefore, it was suggested that the larger quantities of NO that are produced by iNOS are associated with exacerbated intestinal injury [54]. However, the debate on the contribution of iNOS to intestinal injury does not end there. There have been studies published which investigate the effects of iNOS in iNOS-deficient ($iNOS^{-/-}$) mice with exposure to different

strains of bacteria. For example, one group investigated the effects of LPS on iNOS^{-/-} mice and found that at higher concentrations of LPS, there were no differences in the levels of inflammation and injury between the wild-type and deficient mice. Also, when mice were pretreated with heat-inactivated bacteria prior to exposure with LPS, the overall mortality rate of iNOS^{-/-} mice was no different than that of the wild-type mice [55]. There have been a number of other studies that have shown contrasting results with respect to LPS treatment in mice. Some studies have demonstrated an increase in resistance to LPS in iNOS^{-/-} mice, and yet other studies have shown no resistance iNOS^{-/-} mice. However, a consistent finding across each of these studies has been the fact that lethal doses of bacterial exposure have been at least 5-10 fold lower in iNOS^{-/-} mice than in wild type mice (reviewed in [39] and [41]). In terms of the infection model, it would seem that results tend to favour the presence of iNOS in mice with respect to maintaining intestinal integrity and permeability. One possible explanation for this effect in mice is the microbicidal effects of NO. Although the NO radical itself is ineffective with respect to certain organisms, it has been shown that S-nitrosothiols, peroxynitrite (NO₃⁻), or even RNI can have bacteriostatic, antimicrobial, and DNA-altering effects depending on the species of bacteria [56, 57]. These effects of NO, in combination with the fact that iNOS produces far more NO than cNOS (as mentioned previously), may offer a possible explanation for the role of iNOS in the context of pathogen-induced intestinal injury. This brief overview of NO with respect to infection however has been greatly simplified as the literature supporting opposing views is

certainly extensive. Although the effects of NO in the gut have been fairly well-studied, the relative contributions of the different NOS enzymes, especially iNOS, have not been definitively characterized as different conditions can result in vastly different responses.

iv) Interactions with HIF-1 α

It comes as no surprise that NO, with its ability to affect a vast number of essential physiological responses, has also been shown to have implications with respect to oxygen sensing and hypoxic signaling. It was determined that HIF-1 and its associated proteins contained thiol groups which act as targets for NO-related interactions. Also, the transport of NO from the hemoglobin complexes has also been shown to be dependent on oxygen availability [45]. Thus, studies pertaining to the effects of NO on HIF-1 and its related proteins began to emerge. Early experiments have shown that NO has an inhibitory role with respect to stabilization and activation of HIF-1 α [35].

However, more recent studies have demonstrated that NO donors which are chemically diverse (such as GSNO for example) or increased endogenous NO (produced via iNOS) in normoxic conditions have been found to enhance HIF-1 α stabilization, DNA-binding, and transcriptional activation of target genes [27, 35, 45, 58].

Since the HIF-1 α subunit must translocate to the nucleus and dimerize with HIF-1 β in order to become transcriptionally active, samples of nuclear extracts should contain detectable amounts of HIF-1 α . Metzzen et al., using cultured Human Embryonic Kidney cells (HEK293), exposed the cells to CoCl₂ (which is used as a hypoxia mimic and

stabilizes the HIF-1 α subunit, thus acting as a positive control), and the NO-donating compound, GSNO. The control cells, as expected, demonstrated a lack of HIF-1 α (as it is degraded in normoxic conditions). However, the GSNO treated cells demonstrated an almost equipotent response with the CoCl₂ positive control. It is important to note that these results were observed using a constant concentration of GSNO (1mM) [58]. Park et al. conducted similar experiments in HeLa cells (immortalized cervical cancer cells) using NO-donors to induce HIF-1 α in both normoxic and hypoxic conditions. They demonstrated that each of these NO-donors were able to induce HIF-1 α in both conditions [27].

Experimentation proceeded to determine whether or not HIF-1 α induction was influenced in a dose- and time-dependent manner. Metzen et al., demonstrated that HIF-1 α signal increases with increasing concentrations of GSNO but also with prolonged exposure to constant GSNO. Park et al. demonstrated similar findings using SNAP and that the intensity of the HIF-1 α signal was equal (if not slightly greater) to that of the hypoxic response [27, 58]. Palmer et al., also illustrates similar results using bovine pulmonary artery endothelial (BPAE) cells. The BPAE cells were exposed to an NO donor and this resulted in a stabilization of HIF-1 α in a dose- and time-dependent manner, but also an increase in HIF-1 β (similar to HIF-1 α) [45]. These findings provide evidence that the HIF-1 subunits, especially HIF-1 α , are stabilized in the cell by NO in a dose- and time-dependent manner under normoxic conditions (as HIF-1 α is normally undetectable in normoxic conditions).

Park et al. went on to test the DNA-binding stability of HIF-1 in HeLa cells. The HeLa cells experienced increases in HIF-1 DNA-binding in a dose- and time- dependent manner using SNAP. Metzen et al., performed a similar experiment with GSNO. HIF-1 DNA binding activity was measured at one 16 hour time point and showed a doubling of activity in GSNO and CoCl_2 compared to control cells [58]. Also, to add to the evidence supporting stabilized DNA-binding, Park et al. also performed quantitative real-time PCR on the mRNA of known HIF-1 targets; vascular endothelial growth factor (VEGF) and carbonic anhydrase 9 (CA9). Levels of VEGF and CA9 were shown to increase in a dose- and time-dependent manner with respect to SNAP [27]. This suggests that in spite of normoxic conditions of the cell, HIF-1 DNA-binding is also stabilized by NO, since these proteins would not normally be transcribed at all by HIF-1 under these conditions.

There are two other important levels of control for HIF-1 α which include interactions with PHD and VHL protein complexes. HIF-1 α degradation depends on its hydroxylation at two key proline residues by PHD enzymes and then subsequent binding to the VHL protein complex. Metzen et al. postulated that NO was able to prevent hydroxylation by inhibiting PHD enzymes [58], however more recent studies performed by Park et al., demonstrate this to be false with data gathered via mass spectrometry. PHD2 enzyme was added to a biotin-HIF-1 α peptide and a single peak (which represented a hydroxylated form of HIF-1 α) was observed. Despite the addition of increasing concentrations of SNAP, this peak remained the same suggesting that NO-donors could not interfere with the hydroxylation of HIF-1 α [27]. These results have not fully

answered the question concerning hydroxylation-dependent binding of VHL and subsequent polyubiquitination. Both Metzen et al. and Park et al., in similar studies using co-immunoprecipitation of HIF-1 α and ubiquitinated HIF-1 α provided evidence that NO-donors were indeed able to downregulate the ubiquitination of HIF-1 α to levels similar to that of cells which were not exposed to ubiquitin, or were administered with ubiquitination blockers. The protease inhibitor, MG132, was also administered to make it possible to precipitate the ubiquitinated proteins [27, 58]. Park et al., using bacterially expressed and purified HIF-1 α with ³⁵S labeled VHL, introduced SNAP and PHD2. The results of this experiment showed that PHD2 was still able to hydroxylate HIF-1 α , however, in the absence of reducing agents (Fe(II) and vitamin C), SNAP was able to inhibit recruitment of VHL to HIF-1 α . In order to determine whether this inhibition was based on S-nitrosylation, the cysteine 520 residue was mutated to alanine. This point mutation eliminated the effects of SNAP on HIF-1 α with respect to VHL recruitment suggesting that cysteine 520 is indeed nitrosylated at this point, thus preventing the VHL recruitment and subsequent degradation. Although this indicates that NO-donors can prevent the polyubiquitination by VHL, it also indicates that these interactions are redox dependent as SNAP could not inhibit VHL recruitment unless reducing agents were in limiting amounts (low vitamin C in this case). Similarly, Metzen et al. observed that GSNO stabilization of HIF-1 α could be inhibited by addition of Dithiothreitol (a reducing agent) in the middle and at the end of the incubation with GSNO [58]. As demonstrated

in these two studies, NO is able to interact and stabilize HIF-1 α on many different levels of control.

In an interesting set of data presented by Metzen et al., it was found that by analyzing total RNA levels in cells treated with CoCl₂ and GSNO after 2 hour incubation (to coincide with their protein treatments), levels of mRNA showed no change in response. Also, in a second experiment, Metzen et al. inhibited transcription by incubating with actinomycin D (30 min), followed by 4 hour incubation with GSNO. The levels of HIF-1 α protein present did not appear to change relative to cells that were not treated with actinomycin D. From these results, Metzen et al. concluded that elevated HIF-1 α levels due to GSNO were not influenced by transcription of HIF-1 α mRNA. In similar experiments performed by Palmer et al., it was determined that other NO donors had no effect on HIF-1 α stabilization in a transcriptional manner. It is important to note that these results however, do not completely eliminate the possibility of mRNA's influence on HIF-1 α , or its clinical importance.

1.4 *An overview of reactive oxygen species*

i) Structure and production

The phrase "reactive oxygen species" functions as a blanket term to describe a number of different molecules that can act as oxidants [59, 60]. It was not until the discovery of superoxide dismutase (i.e. an enzyme specifically designed to breakdown superoxide

radicals) that the effects of ROS were linked to a multitude of cellular events [59].

Although UV and ionizing radiation both contribute to the formation of oxidative free radicals, the primary source of ROS actually originates from a number of different reactions ranging from enzyme-mediated catalysis to electron leak from certain enzyme complexes. Originally thought to be just a byproduct of oxygen metabolism (via cytochrome enzymes) in the mitochondria, it was later found to be a primary effector molecule of certain immune-related cells such as neutrophils (via NADPH oxidase – NOX) [53, 59-62]. Many of the protein complexes involved in respiration will leak electrons to oxygen, resulting in the formation of ROS [59-62]. Another well-documented source of ROS is the enzyme, xanthine oxidase, which is primarily located in the serum and pulmonary tissue [59-61, 63]. Typically formed by the reduction of oxygen by a single electron, the superoxide anion ($\text{SOA} - \text{O}_2^{\bullet-}$) acts as a mediator in many oxidative reactions and is a well-known precursor for the majority of different ROS and even Reactive Nitrogen Species (RNS). Due to the instability and reactivity of the SOA, the enzyme SOD can convert the free radical into the less damaging hydrogen peroxide (H_2O_2). This conversion to H_2O_2 has also been known to occur spontaneously. H_2O_2 has two possible fates in that it can either be further reduced to water (H_2O) or partially reduced into an even more powerful oxidant, the hydroxyl radical (OH^{\bullet}) [60].

ROS are also involved in a number of important antimicrobial defenses within the body. Phagocytic cells (e.g. polymorphonuclear neutrophils and macrophages) for example, contain an important enzyme complex located on the cell membrane known

as the NOX enzyme. These enzymes are composed of regulatory subunits, flavoproteins, and cytochrome b. Once the cells are activated in response to infection or inflammation, the NOX complex begins to assemble on the cell membrane where they reduce oxygen to form SOA. These newly formed species are released into the phagosomal space where they are then converted by enzymes like myeloperoxidase (MPO) into more powerful oxidants such as hypochlorous acid. These acidic compounds are some of the most effective oxidants in a neutrophil's antimicrobial arsenal [53, 59, 60, 62, 64].

It is important to note that basal levels of ROS (i.e., what is normally produced by respiration and other sources) are not toxic to the cells, and small fluctuations in their levels have been known to influence cell signaling events. If the steady-state level of SOA increases, this increased production leads to interactions with other effector molecules such as transition metals or NO. These subsequent reactions cause the formation of some of the most powerful oxidants in nature such as OH• and peroxynitrite respectively [60]. Although minute amounts of these oxidants are not particularly harmful, increases in their levels during certain chronic inflammatory conditions can have deleterious effects. The dysfunctional regulation of ROS production leads to a condition known as "oxidative stress" and is typically associated with increased levels of SOA, OH•, and NO₃⁻, which are capable of indiscriminately targeting proteins, lipids and DNA with damaging consequences [59-62, 65]. These instances of oxidative stress and injury have been associated with a number of different intestinal

pathologies such as ischemia-reperfusion injury and inflammatory bowel disease. The increased presence of oxygen radicals has also been implicated in the increased permeability of the endothelium and mucosa [61, 66, 67].

ii) Reactive oxygen species in the context of the GI tract

Within the GI environment, ROS can play a significant role in mediating both infection and inflammation. As previously described, NOX enzymes (namely, NOX2) are heavily involved in the antimicrobial actions of phagocytic cells. However, ROS production is not limited to phagocytic cells of the intestine. In a recent study [68], the expression of another member of the NOX family, NOX4, was found to be expressed in the intestinal epithelial cells themselves. In this study, intestinal epithelial cell monolayers were exposed to *Listeria monocytogenes* (LM). Upon infection, the cells began producing ROS in a NOX4-dependent fashion as early as 5 minutes following bacterial exposure. The group suggests that these data are in accordance with previous data that link the production of ROS with the activation of MAP kinase and the initiation of certain signaling events. These events are thought to be involved in horizontal cell-to-cell communication and the coordination of innate immune responses with neighbouring cells against bacterial challenge. Another study investigated ROS production in epithelial cells in response to signals from enteric commensal bacteria [62]. Using intestinal epithelial cells, this group focused on the induction of ROS by bacterial exposure and the subsequent effects on wound repair. The results of this study

demonstrated that when exposed to enteric commensal bacteria, ROS generation was increased in the epithelial cells. The increase in ROS resulted in the inactivation of the redox-sensitive tyrosine phosphatase proteins, which subsequently led to the increased activation of focal adhesion kinase (which is required for epithelial mobility in wound repair) [62].

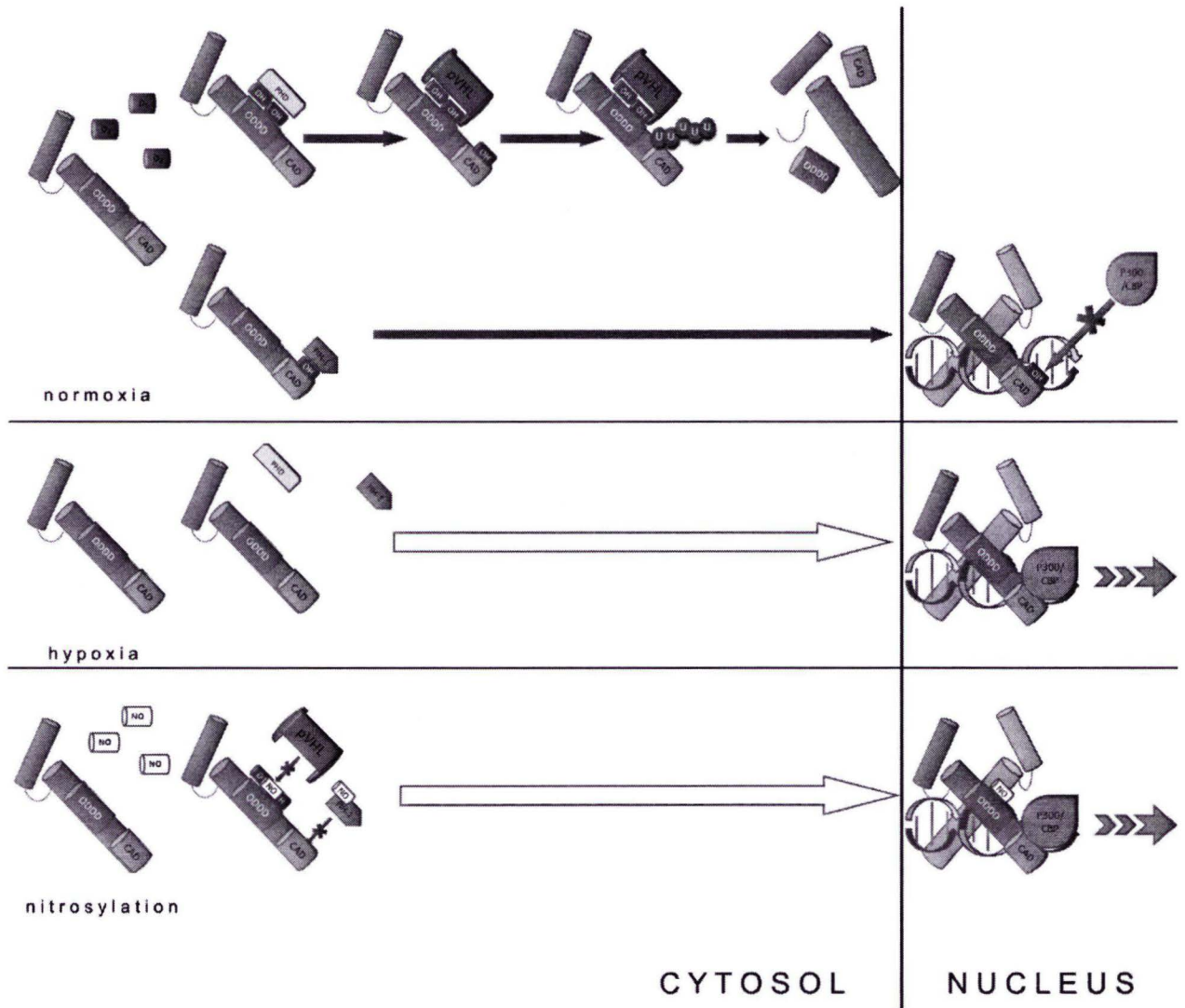
iii) Interactions with nitric oxide

There have been a number of studies that have investigated the often opposing effects of ROS and NO. As stated previously, NO can, through its interactions with proteins in the NOX complex, prevent the generation of ROS [65]. Elevated concentrations of NO have been associated with many different (patho)physiological states (e.g. certain inflammatory conditions or ischemic injury). Moreover it is important to note that the elevations in NO can occur concurrently with increased ROS production [63, 65]. Studies investigating the effects of ROS on Chinese hamster lung fibroblasts and primary cultures of rat mesencephalic neurons demonstrated deleterious effects in each cell type when incubated with H₂O₂ or xanthine oxidase. The damage caused by ROS was significantly attenuated when co-incubated with an NO-donating compound. The NO-donating compound alone (at 1 mM concentrations) did not cause any damage to the cells but demonstrated a protective effect against ROS. This suggests that even at higher concentrations, NO alone does not seem to be sufficient to cause any real damage [63]. This is however an *in vitro* effect and does not necessarily depict what

would happen *in vivo* where NO is free to diffuse into many surrounding tissues [65].

Also, *in vivo*, NO is the only biological molecule that is present in high enough concentrations to actually compete with SOD for the SOA [63, 65].

It has been well-characterized that SOA, at physiological conditions, will readily react with NO to form peroxynitrite. This highly reactive product has also been shown to nitrosylate tyrosine residues of many different proteins, including structural proteins such as actin [65]. This tyrosine nitrosylation of structural proteins can have seriously deleterious effects, and these nitrotyrosine residues (that often act as a marker or footprint) have been found in many different pathological conditions including inflammatory bowel disease [65, 69]. Individually, ROS and NO appear to have beneficial if not necessary effects in maintaining homeostasis. This delicate balance however can easily be upset with the introduction of an infection or the initiation of an inflammatory response. Since both have been closely associated with GI tract, it is important to consider the interactions between these two crucial effector molecules when dealing with intestinal injury.



Summary Figure 1 – Mechanisms of HIF-1 α regulation

Summary Figure 1 – Mechanisms of HIF-1 α regulation. The purpose of this figure is simply to summarize the regulatory mechanisms of HIF-1 α discussed in the introduction. The alpha subunit of the HIF-1 transcription factor exists in the cytosol and is regulated by an Oxygen-dependent degradation domain (ODDD) and a C-terminal transactivation domain (CAD). Under [**normoxia**] - Proline hydroxylation occurs in the ODDD via Prolyl hydroxylase (PHD) and Asparagine hydroxylation occurs in the CAD via Factor-Inhibiting HIF-1 (FIH-1). Proline hydroxylation allows for the recruitment of the Von-Hippel Lindau protein complex (pVHL, an E3 ubiquitin ligase), which results in the polyubiquitination and proteosomal degradation of HIF-1 α . Asparagine hydroxylation still allows HIF-1 α to enter the nucleus, dimerize with HIF-1 β and bind to target genes. However, the hydroxylated asparagine prevents recruitment of transcriptional co-activators (p300/CBP), thus preventing downstream target gene activation. Under [**hypoxia**] – Since oxygen concentrations are low, neither PHD nor FIH-1 have the necessary co-factor requirement to carry out hydroxylation of HIF-1 α . This allows HIF-1 α to translocate to the nucleus and dimerize with HIF-1 β in order to regulate transcription of downstream genes. During [**nitrosylation**] – Nitric oxide concentrations are increased in the cell allowing NO to nitrosylate HIF-1 α on cysteine residues (S-nitrosylation). This prevents the recruitment of ubiquitin ligating enzymes (pVHL). Nitrosylation is also thought to interfere with FIH-1. Nitrosylated HIF-1 α is considered stabilized from ubiquitination and asparagine hydroxylation. It can now enter the nucleus, dimerize with HIF-1 β , and initiate transcription of downstream target genes

2.0

hypothesis & objectives

2.0 Hypothesis and objectives

As stated previously, HIF-1 is a highly regulated transcription factor that demonstrates protective functions within intestinal inflammatory pathologies such as colitis. Its activity as a transcription factor influences key target genes such as VEGF, ITF, MDR-1, and CD73 which are involved in mucosal barrier maintenance and restitution. Since the majority of regulatory control lies with the α -subunit, it would be advantageous to keep the studies specifically focused on the various control mechanisms that potentially regulate its expression and biological activity. HIF-1 α levels were tested in patients with C.diff-mediated injury and the findings have shown an upregulation of HIF-1 α levels. In addition, studies performed by Hirota et al. [70] have demonstrated the protective effects of HIF in the context of C.diff toxin-mediated damage in mice. Moreover, mice that were genetically deficient in HIF-1 α were more susceptible to C.diff-induced damage when compared to wild type mice. **These results implicate an essential role for HIF-1 α in modulating the innate protective functions of the intestinal epithelial mucosa in response to C.diff-mediated intestinal injury.** Due to the suggested importance of the HIF-1 transcription factor, studies were performed to determine key mechanisms of stabilization (i.e. interactions with NO). For the intents and purposes of this thesis, **it was hypothesized that NO and ROS produced during C.diff toxin-induced intestinal injury may act as important signals to influence HIF-1 α and initiate protection against C.diff toxin-induced intestinal damage.**

The 3 primary objectives of this study are as follows:

- 2.1 *Assess the effect of C.diff toxins on HIF-1 α on a post-translational level*
- 2.2 *Assess the effects of NO on HIF-1 α in the presence of C.diff toxins*
- 2.3 *Assess the relationship between reactive oxygen species and NO and how it affects HIF-1 α expression.*

3.0

materials & methods

3.0 Materials and Methods

3.1 *Inoculation of C. difficile cultures and production of toxin*

The bacterial toxin used in these experiments was extracted from the NAP-1/027 strain of *C.diff* (positive for both TcdA and TcdB), which was obtained from Dr. Tom Louie's laboratory at the Foothills Hospital, Calgary, AB, Canada. The toxin production and extraction protocol was previously described by Sullivan et al. 1982 [71], where cultures were inoculated in brain-heart infusion media and grown in sterile, anaerobic conditions. Approximately 5 days after inoculation, *C.diff* cultures were harvested by centrifugation at 10,000 x g for 1 hour. The culture supernatant (i.e. the mixture of toxins A and B – TcdA/B) was placed in a Steriflip® Filter Unit (Millipore, USA) in order to remove any remaining bacteria or bacterial spores. The supernatant (containing TcdA and TcdB) was then transferred to an Amicon Ultra-15 Centrifugal Filter Unit with a 100-kDa cutoff filter (Millipore, USA) in order to exclude anything below the size of the large clostridial toxins. The remaining filtrand (i.e., any protein above 100-kDa) was carefully extracted from the filter. Approximately half of the concentrated supernatant was set aside for the purification of individual toxins TcdA and TcdB. The protein concentration of the final TcdA/B mixture was determined by Bradford assay, and the TcdA/B mixture used as the toxin source for both *in vitro* and *in vivo* experiments.

3.2 *C. difficile* toxin purification

The toxin purification protocol using ion exchange chromatography was described previously in Sullivan et al. 1982 [71]. Concentrated TcdA/B supernatant (500 μ L) was injected onto a DEAE Sepharose CL-6B anion exchange column at 4°C that was previously equilibrated in Buffer A (50 mM Tris, 0 M NaCl, pH 7.4). Clostridial proteins were eluted with a linear gradient of Buffer B (50 mM Tris, 1 M NaCl, pH 7.4) at a flow rate of 0.3 mL/min. Fractions (0.9 mL) were collected over a total time of 3 hours. The fractions which appeared around 0.10 – 0.25 M NaCl and the fractions which appeared around 0.3 – 0.6 M NaCl were analyzed on an 8% SDS-PAGE (recipe described in Section 3.9). The gels were stained with Coomassie Brilliant Blue G-250, and the 0.10-0.25M NaCl fractions containing high molecular weight bands (i.e. >250KDa) were pooled and concentrated using 100-kDa cutoff centrifugal filters. This concentrated supernatant was immunoblotted with anti-TcdA antibody (Meridian Bioscience, UK) and confirmed to be *C.diff* TcdA. The same procedure was carried out for fractions containing 0.3-0.6 M NaCl to generate a pure pool of *C.diff* TcdB. Again, the purity was confirmed by immunoblotting with antibody specific for TcdB protein (Meridian Bioscience, UK).

3.3 Cell culturing and maintenance of Caco-2 intestinal epithelial cells

The *in vitro* experiments were carried out on the Caco-2 colorectal adenocarcinoma cell line (ATCC, USA - cell #: HTB-37, designation: Caco-2). Cells were cultured in Dulbecco's Modified Eagle Medium (DMEM; Invitrogen, USA) with 20% Fetal Bovine Serum (FBS; Invitrogen, USA), 1% Penicillin-Streptomycin solution (PenStrep; Invitrogen, USA), 1% non-essential amino acid solution (NEAA; Invitrogen, USA) and 1% sodium pyruvate solution (Invitrogen, USA). Cell cultures were incubated at 37 °C under 5% CO₂ in 75 cm² culture flasks or 10 cm petri dishes (BD Biosciences, USA).

The cells were passaged every 4-5 days by decanting the cell media, washing twice with 1x sterile PBS and adding 1 mL of 0.25% trypsin-EDTA solution (Invitrogen, USA). The cells were incubated at 37°C (with trypsin still added) in order to allow the adherent cells to be separated from the flask/plate. Cells were then re-suspended with 9 mL of culture media (described above) and diluted to the desired concentration (typically 1:10). The culture media and trypsin-EDTA solutions were heated to 37 °C prior to coming in contact with the cells.

Stably expressing HIF-1 α siRNA knockdown Caco-2 cells (Caco-2^{HIF-KD}) were obtained from the laboratory of Dr. Sean Colgan (University of Colorado, Denver, USA) and used as control cells for some experiments. The siRNA in these Caco-2 cells functions to decrease the transcription of HIF-1 α within the cell. Caco-2^{HIF-KD} cells were cultured in DMEM (Cellgro – Mediatech, Inc. USA), with 10% FBS, 1% PenStrep, 1% L-glutamine (Invitrogen, USA) and 3 μ g/mL of puromycin (Invitrogen, USA). The

puromycin, which is an inhibitor of protein translation, is needed for the specific selection of cells containing the appropriate siRNA. Maintenance of the Caco-2^{HIF-KD} cells followed the same protocol as described for the wild-type (WT) Caco-2 cells.

3.4 Cell plating and experiment preparation

Caco-2 IECs were plated onto 6-well and 12-well plates (BD Falcon, USA) or 8-well chamber slides (Lab-Tek - Nalgene Nunc, USA) depending on which experiments were to be performed. Cells were seeded by harvesting a 125 μ L volume of cells ready for passaging (i.e., cells suspended in 1 mL of trypsin-EDTA solution and 9 mL of cell media). At this dilution, cells grew to 85 – 95% confluence in approximately 3 days. Confluence was determined qualitatively, where experiments were carried out upon formation of a Caco-2 monolayer which covered 85 – 95% of the well. The treatments that were added to the cells were as follows; C.diff toxin mixture (contains both TcdA and TcdB), 1400W dihydrochloride (1400W, dissolved in PBS; SIGMA-Aldrich, USA), and N-acetyl L-cysteine (NAC, dissolved in PBS and pH adjusted to 7.0 with 10 M sodium hydroxide; SIGMA-Aldrich, USA). Treatments were added directly to the cell media and plates were then lightly agitated to ensure an even distribution of the treatment. For the majority of the experiments, C.diff toxin was added at a concentration of 70 μ g/mL. Treatments (i.e., 1400W, 100 μ M and NAC, 25 mM) were added 1 hour prior to exposure with C.diff toxin. For example, if an experiment was testing the effects of a 4 hour C.diff toxin exposure, the drug would be placed on the cells for a total of 5 hours; therefore the

control for the drug (i.e. the cells treated with the drug alone) would also have to be treated for 5 hours in order to accommodate for the 1 hour pre-treatment.

3.5 *Light microscope images of Caco-2 cell monolayers*

Digital images of Caco-2 cell monolayers were captured with a standard light microscope (Nikon, USA) using a digital camera (Canon Powershot SD-1000). Caco-2 cells that were plated and treated with different conditions (control, toxin, drug, etc.) on the multi-well plates were viewed under a light microscope at 20X magnification. Images were taken with the following digital camera settings: optical zoom (3X) exposure level (0), auto white balance, evaluative capture mode, superfine quality, 2048 x 1536 resolution and auto ISO. The digital camera images were used to qualitatively analyze the integrity of the monolayer; for this reason, images were inverted (i.e., a negative image was created) in Adobe Photoshop to provide a better contrast with respect to the cell-to-cell junctions.

3.6 *Caco-2 cell lysis with cytosolic and nuclear extract preparation*

The treated media was decanted from the cells in the sterile hood using a vacuum pump and a Pasteur pipette. Cells were washed once with an equal volume of sterile PBS to ensure all the serum and growth factors of the media did not contaminate the cell extract. Once the PBS was decanted from the cells, HEN/2 lysis buffer (125 mM HEPES, pH 7.7, 0.5 mM EDTA, and 0.05 mM neocuproine with 0.2% (v/v) NP-40 and Complete

Protease Inhibitor) at 150 μL /well for a 12-well plate was added to each well in accordance with (Jaffrey et al, 2001). The lysis buffer was allowed to incubate at room temperature for 2-3 minutes, after which the cells were stirred with an inverted 10 μL pipette tip. Cell extracts were placed into a pre-chilled 1.5 mL Eppendorf tube and flash frozen with liquid nitrogen or dry ice. The extracts were stored at $-80\text{ }^{\circ}\text{C}$ for 12 hours. The extracts were allowed to thaw completely on ice and then were clarified with centrifugation at $17,500 \times g$ at $4\text{ }^{\circ}\text{C}$ for 5 minutes. The supernatants (i.e., cytosolic fraction) were removed and placed into a separate pre-chilled tubes. The pellet was then reconstituted in 150 μL nuclear extract buffer (20 mM HEPES, pH 7.9, 0.4 M NaCl, 1 mM EDTA, 10% (v/v) glycerol, and 0.1 mM Neocuproine). As with the lysis buffer, Complete Protease Inhibitor was added to the buffer just prior to use. The reconstituted pellets were then incubated for at least 2 hours at $4\text{ }^{\circ}\text{C}$, followed by high-speed centrifugation at $17,500 \times g$ for 5 minutes at $4\text{ }^{\circ}\text{C}$. The resulting supernatant represented the nuclear fraction of the cell extract. These samples were also stored at $-80\text{ }^{\circ}\text{C}$ until use. Due to the light-sensitive nature of nitric oxide and its associated modifications, the Eppendorf tubes used in the cell extraction were amber-colored.

3.7 *Bradford Assay for protein concentration*

Bradford protein assay reagent (Bio-Rad, USA) was diluted 1:10 (v/v) and used with BSA as a standard to measure the protein concentrations of cell extracts. Absorbance readings of samples and standards (0 – 10 $\mu\text{g}/\mu\text{L}$ BSA in PBS) were taken using a

spectrophotometer set to 600 nm. The equation of the linear regression analysis of the corresponding BSA standard curve was used to calculate the concentration of unknown protein samples.

3.8 *Electrophoretic Mobility Shift Assay (EMSA)*

The EMSA protocol used for these experiments was previously described by Hellman and Fried 2007 [72]. The DNA sequences used were derived from the human erythropoietin (EPO) gene that contains a known HRE sequence (as characterized by Semenza et al, 1992 [73]). Both a wild type (WT; GCCCTACGTGCTGTCTCA) and mutant (M18; GCCCT**AAA**AGCTGTCTCA) were used, where the sequence written represents the sense strand. The underlined portion represents the 8bp HRE and the bolded portions represent the nucleotides that are mutated in the M18 strand. Oligonucleotides were synthesized at the University of Calgary DNA sequencing labs.

During the preparation of the binding reaction, a large size, 5% native gel (without stack gel) was cast and run using the Protean II gel system (Bio-Rad, USA). At a constant 300 V setting, the gel was pre-run for 30 minutes. In the actual binding reaction, 15 µg of nuclear extract was used. The tube was tapped lightly and left to incubate at room temperature for 5 minutes to eliminate any non-specific binding that may occur. After the incubation, 1 µL of the [γ 32 P]-labeled probe was added and the mixture was incubated at room temperature for 20 minutes. The samples were then loaded onto the pre-run 5% native gel and run at 300 V until the bromophenol blue

dye (dark blue) was approximately 4 cm from the bottom of the gel. The gel was then vacuum dried onto a proportionately-sized piece of Wattman filter paper (VWR, Canada) and placed into an autoradiography cassette (Kodak, USA) with a phosphor screen (Kodak, USA) for 12 hours. The phosphor screen was imaged using a STORM scanner (Amersham biosciences/GE healthcare, USA).

3.9 *Sodium Dodecyl Sulfate-Polyacrylamide Gel Electrophoresis (SDS-PAGE)*

Gels 8 –10% acrylamide (with 33:1.8 ratio of acrylamide:bisacrylamide) were cast using the Bio-Rad Mini PROTEAN gel casting system (Bio-Rad Inc., USA). Once polymerized, the gels were placed into the Bio-Rad mini protean gel system (Bio-Rad, USA) and the gel box was filled to the top with SDS-PAGE running buffer (25 mM Tris, 192 mM glycine, and 0.1% SDS). In preparation for running samples through SDS-PAGE, 1 of 2 different types of sample buffer were used depending on the experiment:

For standard SDS-PAGE and Western blotting

4X Laemmli sample buffer (2.4 mL 1 M Tris pH 6.8, 0.8 g SDS, 4 mL 100% glycerol, 0.01% bromophenol blue, 0.5 mL β -mercaptoethanol, 3.3 mL water)

For the Biotin Switch Assay

2X non-reducing buffer (2.4 mL 1 M Tris pH 6.8, 0.8 g SDS, 4 mL 100% glycerol, 3.3 mL water)

The buffers were added to the sample so that their final concentration is 1X. The sample Eppendorf tubes were boiled on a heating block for 10 minutes, placed briefly

on ice, and then centrifuged at 17,500 x g for 2 minutes. Samples were then loaded in the wells of the gel and run at a constant voltage of 150 V until the dye front ran off (approx. 1.5 – 2 hrs).

For standard SDS-PAGE (i.e. no Western blotting), gels were stained overnight using the Coomassie brilliant blue solution (0.2% w/v Coomassie blue, 7.5% glacial acetic acid, and 50% ethanol – in 500mL).

3.10 *Immunoprecipitation of HIF-1 α from Caco-2 nuclear extracts*

In 1.5mL Eppendorf tubes, Protein G agarose bead slurry (25 μ L; diluted 1:2 with the HEN/2 buffer) was combined with 100 μ L of nuclear extract sample. These samples were gently rocked at 4 °C for 15 minutes in order to remove any proteins that may bind non-specifically to the beads. The samples were then centrifuged at 17,500 x g for 5 minutes at 4 °C. The protein concentration of the resulting supernatant was determined by the Bradford assay and samples were normalized according to their protein concentrations. HIF-1 α antibody (1 μ g; H1alpha67 (ab1), Abcam, USA) was added to each sample followed by gentle rocking at 4°C for at least 12 hours. Protein G agarose bead slurry (25 μ L) was added, and the samples were incubated again at 4 °C for 4 hours. The beads were collected by centrifugation at 12,879 x g. The supernatant was carefully extracted and discarded, and the beads were washed 4 times with cold PBS. After the last wash, the beads were stored in cold PBS. At this stage, the samples were used for either immunoblotting or the biotin-switch assay.

3.11 Immunoblotting (*Western blotting*)

The Mini Trans-Blot system from Bio-Rad (Bio-Rad, USA) was used for Western blotting. The SDS-PAGE gels were placed into transfer cassettes along with 0.2µm Nitrocellulose membranes (GE Healthcare, USA). Transfer cassettes were submerged in chilled transfer Buffer (25 mM Tris, pH 8.3, 192 mM glycine and 20% methanol) and run at 100 V for 2 hours at 4 °C. The membranes were then placed blocked with 5% w/v milk (non-fat dry milk powder) in Tris-buffered saline with Tween (TBST; 25 mM Tris, 150 mM NaCl, 2 mM KCl and pH-adjusted to 7.4) for 1 hour on the rocker at room temperature. Membranes were then incubated with a specific primary antibody diluted 1:1000 in TBST containing 5% milk overnight at 4°C. The following primary antibodies were used: HIF-1 α (ab1/h1alpha67 – Abcam, USA), iNOS (ab3523 – Abcam, USA), FIH-1 (ab63163/HIF1AN – Abcam, USA), and β-actin (A5316/AC-74 – SIGMA Aldrich, USA). The membranes were given 5, 3-minute washes with TBST and then incubated with a specific secondary antibody (anti-mouse or anti-rabbit depending on in the source of the primary antibody) for 1 hour at room temperature. The following secondary antibodies were used: HRP conjugated goat anti-mouse IgG (Bio-Rad, USA) and HRP-conjugated donkey anti-rabbit IgG (GE Healthcare, UK). The membranes were then given 10, 3-minute washes with TBST and developed with enhanced chemiluminescent reagent (ECL) and exposed to Hyperfilm (GE Healthcare, USA) in the darkroom.

3.12 *Biotin Switch Assay*

The biotin switch assay was conducted using the S-nitrosylated protein detection kit (Cayman Chemical, USA). Although the assay had been optimized for use in a kit, the protocol follows the original method as published by Jaffrey et al. 2001 [74]. The protocol was performed in very low-light conditions to protect the light-labile, nitrosylated residues. The manufacturer's suggested protocol was modified slightly to incorporate the HIF-1 α IP samples instead of whole cell extracts. In brief, the PBS-suspended HIF-1 α IP samples were centrifuged (200 x g, 4 °C) to pellet the G protein agarose beads. The PBS was slowly decanted off the beads, and the samples were placed on ice. Blocking Buffer was added to each sample (250 μ L of Blocking Buffer for 25 μ L of beads) prior to incubation at 4 °C for 30 minutes. The blocking buffer contained methyl methanethiosulfonate (MMTS), which methylates all free thiol residues. The beads were then washed extensively with ice-cold PBS before incubation with Reducing and Labeling Buffer for 1 hour at room temperature. The reducing agent (ascorbate) functions to remove NO groups from nitrosylated thiol residues, and the labeling agent (Biotin-HPDP) covalently tags the previously nitrosylated residues with a biotin moiety. After extensive washing with PBS, the supernatant was decanted from the beads and discarded. An equal volume of 2X Non-reducing Buffer was added to the samples and then heated to boiling for 5 minutes, placed on ice for 5 minutes, and then centrifuged at 17,500 x g. The supernatant was carefully decanted from the beads and then loaded onto a 10% SDS-PAGE gel. The gel was then subjected to standard immunoblotting

protocol (see Section 3.11) onto 0.2 μm Nitrocellulose membranes up until the blocking step. In this case, membranes were blocked overnight in 5% (w/v) bovine serum albumin (BSA) in TBST. After washing with TBST, the membranes were incubated with Streptavidin-HRP (Millipore, USA) at 1:1000 dilution in 5% (w/v) BSA in TBST. Membranes were developed using ECL and film as previously described.

3.13 *Nitric oxide detection assay*

For detection of NO in cytosolic cell extracts, the Bioxytech Nitric Oxide Assay kit (OXIS Health Products Inc., USA) was used. Although the assay had been optimized for use in a kit format, the protocol follows the well-established Griess reaction for detection of nitrite in a sample (described in [75]). A standard concentration curve of KNO_3 (0 – 100 μM) was prepared. Both standards and samples were added in duplicate to a 96-well plate to a total volume of 85 μL . In each well, nitrate reductase (10 μL) and 2 mM NADH (10 μL) were added followed by a 20-minute incubation at room temperature with continuous shaking. After the incubation, sulfanilamide (Color reagent #1, 50 μL) was added to each well followed by a brief 10-second mixing. N-(1-Naphthyl) ethylenediamine dihydrochloride (Color Reagent #2, 50 μL) was then added to each well followed by a 5-minute incubation at room temperature with continuous shaking. Absorbance values at 540nm were recorded with a plate reader. The concentration of nitrite in each sample of cell extract was determined from the standard curve and then

related to the initial protein concentration of each sample as determined previously by the Bradford assay.

3.14 Immunocytochemistry (ZO-1 staining)

Caco-2 cells were grown to confluence in 8-well chamber slides as previously described (Section 3.4). The DMEM media was aspirated, and the cells were washed twice with ice-cold PBS. Cells were fixed with methanol (400 μ L/well) for 30 minutes at 4 °C. Briefly, cells were incubated overnight at 4 °C with rabbit anti-ZO-1 primary antibody (Zymed, USA) diluted 1:200 in 2% FBS in PBS. Cells were washed twice with cold PBS and then incubated with CY-3 conjugated AffiniPure goat anti-rabbit secondary antibody (Jackson ImmunoResearch labs Inc., USA), diluted 1:200 in 2% FBS in PBS for 1 hour at room temperature. After a final 2 washes with cold PBS, chambers were carefully removed from the slides and a glass coverslip was placed on top of the cells using a slide mount solution. The glass coverslips were allowed to adhere to the slides overnight. Cells on each slide were excited using a mercury fluorescent lamp (Nikon, USA) and cell images were captured using the Nikon Digital Sight and NIS-elements capture system (Nikon, USA). Using the NIS-elements software, ZO-1 fluorescence intensity was quantified according to the method described by Zehendner et al. 2011 [76]; where the intensity was measured at two points on the periphery of the cell, expressed as an average intensity and then divided by the overall intensity between the two points.

3.15 *Mouse surgical procedures*

Two different surgical procedures were used – the ileal-loop method and the intra-rectal installation method. Although both methods have been described in previous studies, the specific protocols used herein were characterized by Dr. Simon Hirota while working in the Beck/MacDonald labs.

Ileal-loop surgical protocol – a laparotomy is performed on the mouse (under isofluorane anesthetic) in order to gain access to the intestine. To keep the surgery as clean as possible, the cecum was quickly located and the terminal end of the ileum was exposed. A small suture was placed on the anal/rectal end of the ileum and 100 μ L of treatment solution (sterile PBS or TcdA/B – 100 μ g) was injected towards the oral end of the ileum using a 1cc syringe. While simultaneously removing the syringe, the suture was tied tight to close off access to the cecum and colon. The intestine was then gently placed back into the peritoneum of the mouse and the abdominal wall was sutured closed. The skin was also closed over the sutures using surgical grade staples. Mice were laid down on a heating pad and placed on oxygen to facilitate recovery from the surgery. The treatments were left to incubate for 4 hours in the mice before they were sacrificed and ileal tissue was harvested for analysis. Mice were briefly placed under anesthesia and a cervical dislocation was quickly performed to euthanize the mouse. The abdominal cavity was then re-exposed at the suture site and the ileal tissue sample was removed and sectioned into pieces for various analyses. The samples were immediately placed in round-bottom culture tubes on dry ice to snap freeze the tissue.

The tissues were stored at -80 °C prior to analysis. The ileal loop method was performed on both WT mice for PBS vs Toxin treatments, and iNOS KO mice (with appropriate controls) for WT toxin vs iNOS KO toxin treatments.

Intra-rectal installation protocol – a non-invasive method which involved placing a lubricated feeding tube approximately 2cm into the rectum of the mouse. The treatment solution (sterile PBS or TcdA/B - 100µg) was then injected using a 1cc syringe. The anus was then tilted upwards and slight pressure was applied to the rectal area to increase rectal retention of the treatment. The treatment was left to incubate for 4 hours and the mice were quickly euthanized using the cervical dislocation method. Colonic tissue was then removed and sectioned into pieces for various analyses. Samples were placed in round-bottom culture tubes on dry ice to snap freeze the tissue. Tissues were stored at -80 °C. It is important to note that these steps were performed by Dr. Simon Hirota, whereas I carried out the subsequent tissue processing and analysis. The intra-rectal installation method was only performed on the WT strain of mice.

Most of the studies involved wild-type (WT) mice of the C57BL/6N strain (general multipurpose model – strain code 027) obtained from Charles River Laboratories. The studies involving mice that were genetically deficient for iNOS (iNOS KO) were obtained from Jackson Laboratories and were the standard iNOS KO mouse of the strain B6.129P2-*Nos2*^{tm1Lau}/J (Stock number 002609). The corresponding controls for the iNOS

KO mice were also obtained from Jackson Laboratories in the B6 background of the strain C57BL/6J (Stock number 000664).

3.16 *Statistics*

All numerical data are reported as the mean \pm standard error of the mean (SEM). All graphical data and associated statistical analyses were generated with GraphPad PRISM 4 (GraphPad, USA). Statistics for experiments comparing 2 sets of parametric data were calculated using the Student's t-test. Experiments comparing more than 2 sets of parametric data were calculated using a 1-way ANOVA followed by the Neuman-Keuls post-hoc test. Statistical significance was assigned to values where $p < 0.05$ between groups.

4.0

results

4.0 Results

C.diff toxin disrupts epithelial monolayer morphology

It has been previously shown that C.diff toxins can act on intestinal epithelial cells to cause a disruption of the cell monolayer. In order to verify the activity of our isolated bacterial toxin, Caco-2 intestinal epithelial cells were exposed to 70 µg/mL of the crude toxin preparation (i.e., TcdA/B). As demonstrated in Figure 4.1, the Caco-2 monolayer experienced increasing disruption as exposure to TcdA/B was prolonged. This qualitative assessment of the toxin's temporal effects not only verified the action of the toxin but also provided an approximation of the toxin's potency at a given concentration.

C.diff toxin modulates HIF-1α expression and signaling

In a previous study performed by Hirota et al. 2010 [70], it was determined that HIF-1α expression and signaling were possibly linked to the nitric oxide generated by iNOS. In order to establish a point of origin for further investigation, it was necessary to recapitulate these results. To confirm the association between HIF-1α and iNOS expression, Caco-2 cells were exposed to TcdA/B over a time course of 12 hours. Looking at HIF-1α stabilization, HIF-1α expression was elevated 2-fold compared to control at 4 hours (Figure 4.2A). Since HIF-1 is a transcription factor, it was necessary to determine whether or not increases in its expression translated into increases in its DNA

binding capability. FIH-1, a known inhibitor of HIF-1 signaling, was also analyzed when cells were exposed to toxin. Over the course of a 12 hour toxin exposure, cells experienced a significant 2-fold decrease in FIH-1 expression compared to control beginning at the 4 hour mark, and continuing through to 12 hours (Figure 4.2B). This initial decrease at 4 hours suggested that the increase in HIF-1 α expression may be associated with an increase in downstream signaling. This was confirmed by EMSA data (Figure 4.3), which demonstrated an increase in HIF-1 α binding activity to ³²P-radiolabeled DNA with prolonged exposure to TcdA/B (most notably between 4-8 hours). A typical EMSA can only determine whether an increase in general DNA binding has occurred. The supershift experiment however (Figure 4.3, bottom panel) identifies the binding partner to be HIF-1 α due to the presence of the supershift band. This band represents a complex between the DNA probe, HIF-1 α , and the HIF-1 α antibody as opposed to just HIF-1 α and the probe itself (HIF-DNA band). Due to the nature of the EMSA and its requirement for smaller volumes, it was necessary to maximize the amount of viable cell protein (i.e. live cells) in a given volume for use in the assay. Therefore, the TcdA/B preparation was applied to the cells at a reduced concentration (50 μ g/mL) in order to increase the levels of protein harvested from cells that were exposed for longer periods of time.

With respect to iNOS expression, a 2-fold increase relative to control was also observed at 4 hours indicating a possible correlation with HIF-1 α expression (Figure 4.4A). As mentioned previously, NO is capable of nitrosylating HIF-1 α on specific cysteine

residues, which results in the stabilization of the α subunit. In order to determine if this was the case with *C.diff* toxin exposure, the nitrosylation of HIF-1 α was determined by the Biotin switch assay (Figure 4.4B). Levels of nitrosylated HIF-1 α reached a peak at 4 hours suggesting that the nitrosylation events were happening in concordance with iNOS expression. At this point, we immediately turned our attention to the toxin itself and the presence of secondary metabolites which may be in the crude preparation. Before continuing any further, it was necessary to establish these protein effects as being toxin-specific, and not those of other Clostridial metabolites. Fractions of pure TcdB were generated (Figure 4.5) and applied to Caco-2 cell monolayers (Figure 4.3a, b, c). As demonstrated previously with the TcdA/B preparation, expression levels of both HIF-1 α (Figure 4.6) and iNOS (Figure 4.7A) were elevated by a factor of approximately 2-fold compared to control. Elevated levels of NO (Figure 4.7B) were also detected in these cells suggesting that the increase in iNOS was linked to a direct increase in NO concentration.

The effect of C. difficile toxin on Caco-2 epithelial cell monolayers

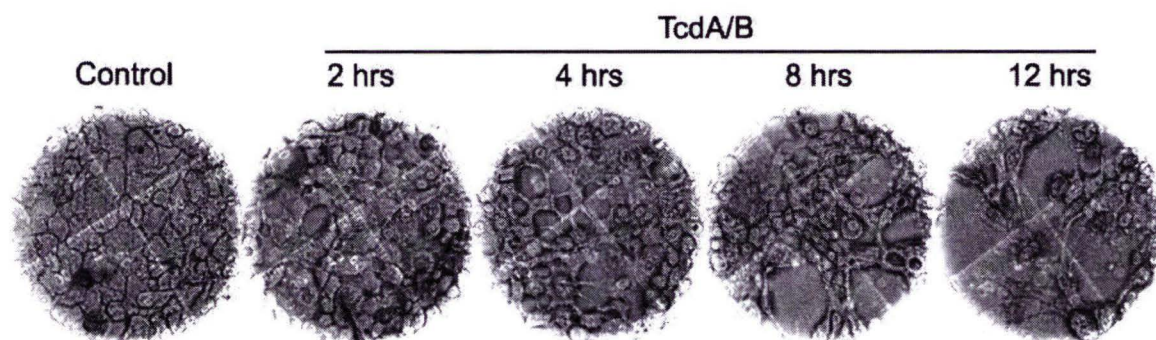


Figure 4.1 - Evaluation of Caco-2 cell monolayer morphology following application of *C. difficile* toxin. Light microscope images of Caco-2 cell monolayers that were exposed to *C. difficile* toxin (TcdA/B – 70 $\mu\text{g}/\text{mL}$) over a period of 12 hours (n=3). These images were taken at 20X magnification.

The temporal effect of C.difficile toxin on HIF-1 α expression and signaling

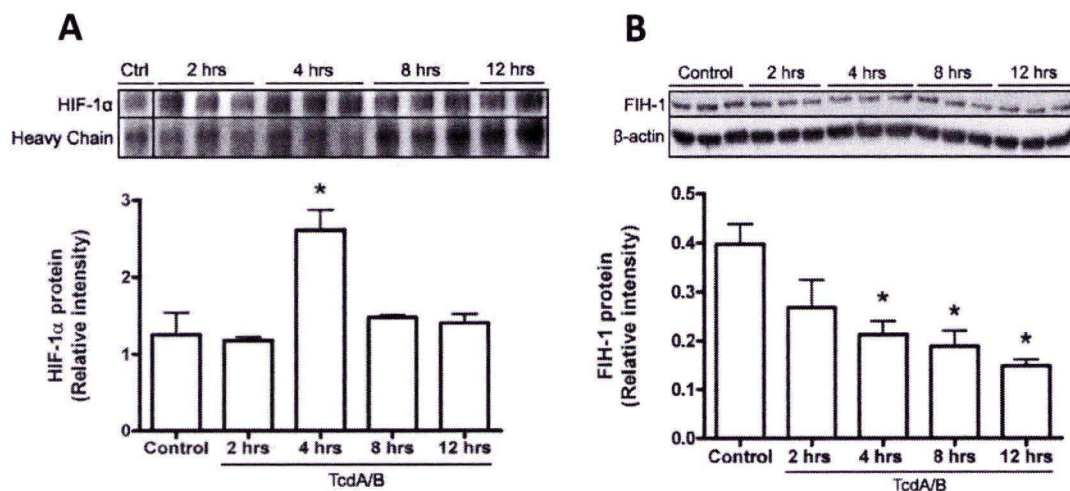


Figure 4.2 - Assessment of HIF-1 α stabilization in Caco-2 cells exposed to *C. difficile*

toxin. Caco-2 cells were exposed to *C.difficile* toxin (TcdA/B – 70 μ g/mL) and harvested at 2, 4, 8 and 12 hours with control cells being harvested at the 12 hour mark. Cytosolic and nuclear cell extracts were prepared for each sample (n=3). **(A)** HIF-1 α was immunoprecipitated from the nuclear extracts and then immunoblotted for HIF-1 α and expression levels were measured relative to antibody heavy chain. **(B)** Cytosolic fractions of each sample were immunoblotted for FIH-1 and expression levels were measured relative to β -actin. Statistical analysis involved a one-way ANOVA followed by Neuman-Keuls post-hoc test where * represents $p < 0.01$ compared to control.

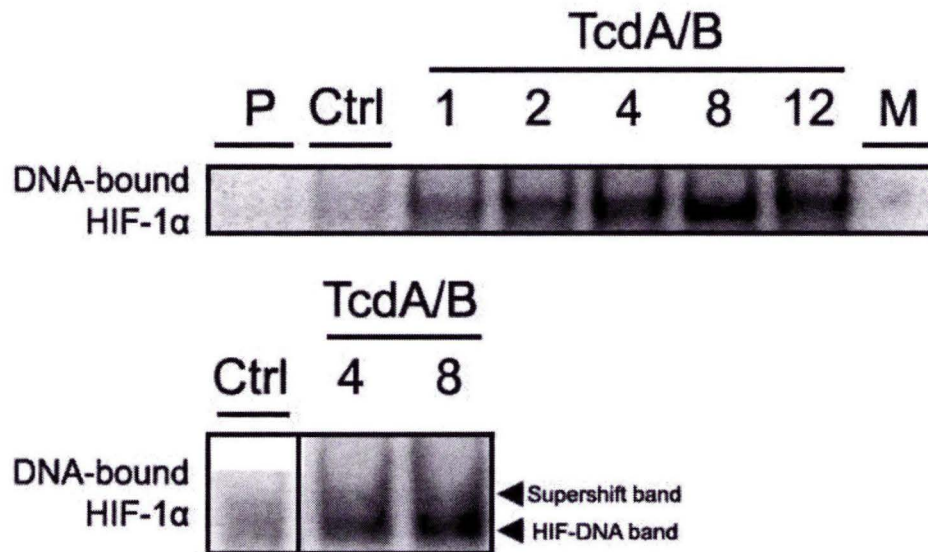


Figure 4.3 – Electrophoretic Mobility Shift Assay of HIF-1 DNA binding activity

following exposure to *C. difficile* toxin. Caco-2 cells were exposed to TcdA/B over a period of 12 hours (n=2). Nuclear extracts were generated and used in an EMSA and compared to the probe alone (P), a 12-hour control (Ctrl), *C. difficile* toxin (TcdA/B)-exposed cells (1, 2, 4, 8 and 12 hours – 50 µg/mL), and a 12-hour TcdA/B treatment incubated with a mutated DNA binding sequence (M). The supershift experiment followed the same protocol as the standard EMSA along with 1 µg of anti-human HIF-1α antibody.

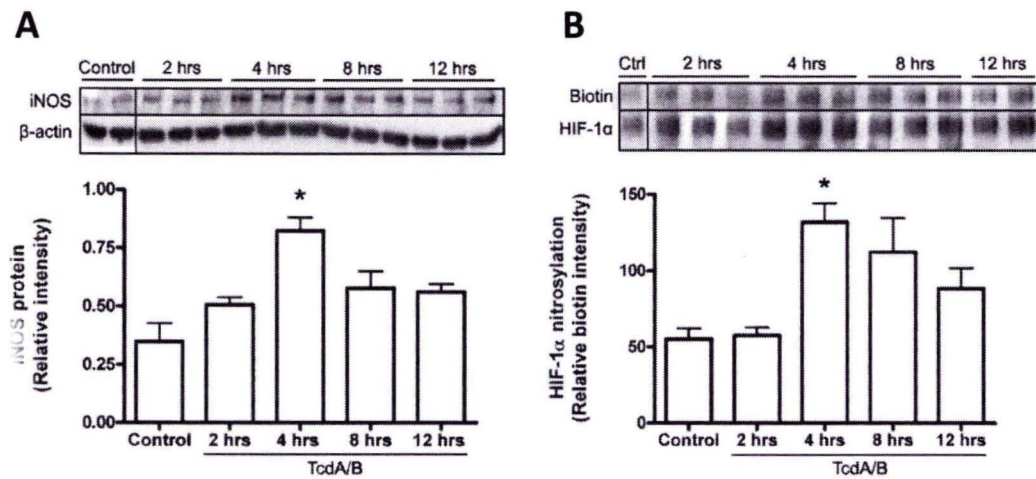


Figure 4.4 - Examination of iNOS expression and HIF-1 α nitrosylation in Caco-2 cells exposed to *C. difficile* toxin. Caco-2 cells were exposed to *C. difficile* toxin (TcdA/B – 70 μ g/mL) and harvested at 2, 4, 8 and 12 hours with control cells being harvested at the 12 hour mark. Cytosolic and nuclear cell extracts were prepared for each sample (n=3). **(A)** Cytosolic fractions of each sample were immunoblotted for iNOS where expression levels were measured relative to β -actin. Statistical analysis involved a one-way ANOVA followed by Neuman-Keuls post hoc test, where * represents $p < 0.01$ compared to control. **(B)** HIF-1 α was immunoprecipitated from the nuclear extracts and subjected to the biotin switch assay where nitrosylated residues were biotinylated. Immunoblot quantification is presented as biotin signal relative to HIF-1 α protein levels.

Purification of TcdA and TcdB from C. difficile crude toxin isolate

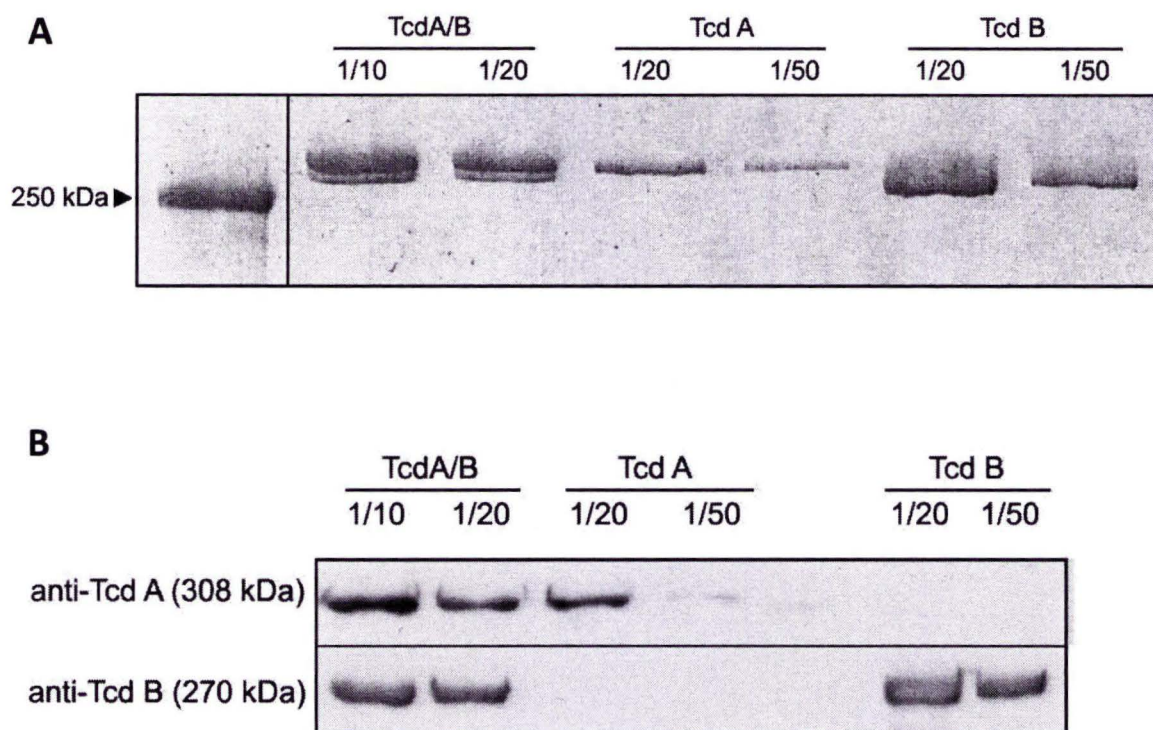


Figure 4.5 – Purification of TcdA and TcdB from *C. difficile* crude toxin isolate: (A)

Chromatographic purification of TcdA and TcdB – FPLC fractions of TcdA and TcdB were resolved on an 8% SDS-PAGE at two separate dilutions (1/20, 1/50) and compared to two dilutions of TcdA/B preparation (1/10, 1/20). **(B)** Assessment of Toxin purity with TcdA and TcdB antibodies – Fractions containing crude and purified toxin were separated with 8% SDS-PAGE and then immunoblotted using anti-TcdA (308 kDa) or anti-TcdB antibodies (270 kDa) to confirm the purity of each fraction.

Verification of toxin-specific response with purified Toxin B in Caco-2 cells

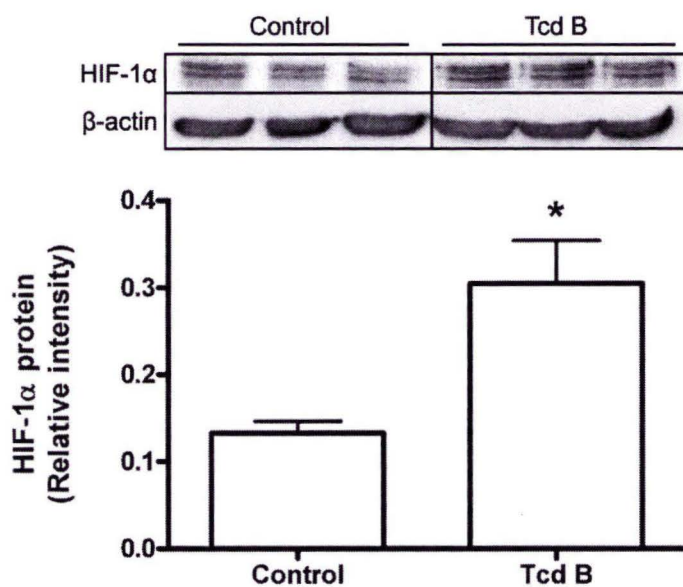


Figure 4.6 - Examination of HIF-1 α expression in Caco-2 cells exposed to purified *C. difficile* toxin B. Caco-2 cells were exposed to purified Tcd B (10ng/mL) for a period of 4 hours. Cells were harvested and whole cell extracts were generated (n=3). Samples were immunoblotted for HIF-1 α where expression levels were measured relative to β -actin. Statistical analysis involved the Student's t-test where * represents $p < 0.05$ compared to control.

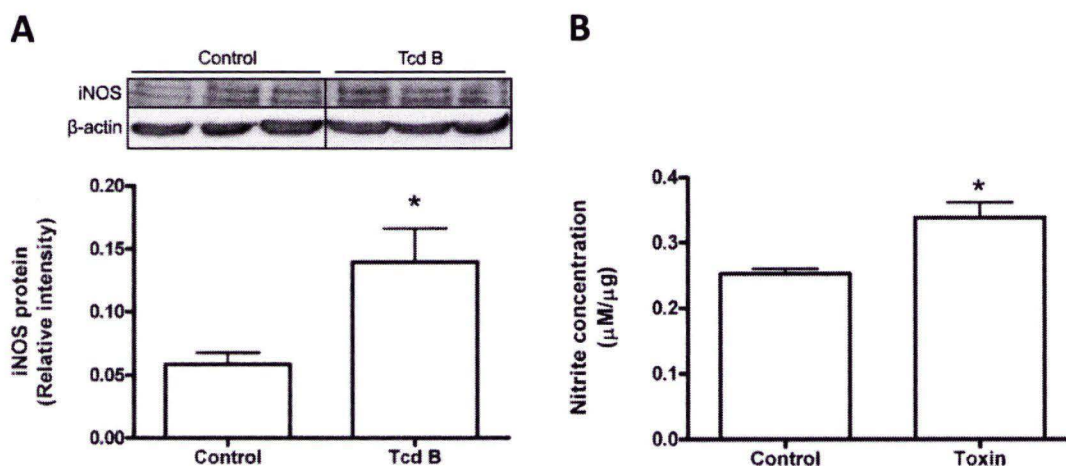


Figure 4.7 - Examination of iNOS expression and nitric oxide concentration in Caco-2 cells exposed to purified *C. difficile* toxin B. Caco-2 cells were exposed to purified Tcd B (10ng/mL) for a period of 4 hours. Cells were harvested and whole cell extracts were generated (n=3). **(A)** Samples were immunoblotted for iNOS where expression levels were measured relative to β-actin. **(B)** NO levels were detected in the whole cell extract using the colorimetric Griess assay. Detected nitrite concentration in the cells were measured relative to total protein content of the extract used in the assay. Statistical analysis involved the Student's t-test where * represents $p < 0.05$ compared to control.

C.diff toxin modulates HIF-1 α expression via iNOS-generated nitric oxide

The results of experiments presented in Figure 4.8 - 4.10 suggested that the TcdA/B effects on iNOS expression could influence HIF-1 α stabilization. The highly selective iNOS inhibitor, 1400W [77], was applied in order to verify that HIF-1 α nitrosylation, and therefore HIF-1 α protein stabilization, was directly linked to NO derived from iNOS. Similar to previous experiments, we observed significant stabilization (2-fold above control) of HIF-1 α protein following exposure of IECs to TcdA/B for 4 hours. FIH-1 expression was suppressed approximately 3-fold relative to control with TcdA/B exposure. However, when cells were pre-incubated with 1400W then exposed to TcdA/B, HIF-1 α expression was suppressed (to control levels) but FIH-1 expression was elevated to control (Figure 4.8). These results suggest that the levels of FIH-1 protein might also be influenced by iNOS-generated NO.

With respect to iNOS expression and subsequent NO concentration within the cells, TcdA/B exposure resulted in 2-fold and 3-fold increases respectively. However, when IECs were pretreated with 1400W and then exposed to TcdA/B, these responses were significantly attenuated (Figure 4.9). In addition, the nitrosylation of HIF-1 α , which was elevated 2.5-fold above control with TcdA/B exposure, was also attenuated with iNOS inhibition (Figure 4.10). Taken together the data strongly support that the nitrosylation and subsequent stabilization of HIF-1 α were dependant on iNOS-generated NO.

C.diff toxin disrupts Caco-2 epithelial monolayer tight junctions

As mentioned previously, C.diff toxins are able to exert their effects on the cytoskeleton (via the Rho family of GTPase proteins) and cause the disruption of tight junctions between adjacent cells. One of the key tight junction proteins found along the periphery of the epithelial cells is known as Zonula Occludens 1 (ZO-1) [78]. The C.diff toxin-induced disruption in the epithelial barrier was measured with immunocytochemistry of ZO-1. Due to the presence of ZO-1 in the tight junction, the relative intensity of ZO-1 immunofluorescence was used as an indicator of cytoskeleton and tight junction integrity (Figure 4.11). Inhibition of iNOS alone appeared to have no effect on cellular structure or barrier function as neither ZO-1 intensity nor overall appearance of the Caco-2 monolayer was altered. As expected, exposure to TcdA/B resulted in noticeable changes to cell morphology as the cells were much smaller with significant rounding occurring at the edges. The continuity of the monolayer was also compromised as large gaps were seen between cells that were not previously present in either control or 1400W treatments. The intensity of ZO-1 at the periphery of the cells was also reduced by approximately 60% with TcdA/B exposure. Interestingly, the combination of the iNOS inhibitor with TcdA/B resulted in the same decrease in intensity seen with TcdA/B alone. Since iNOS has been shown to be responsible for the nitrosylation and stabilization of HIF-1 α , it was anticipated that the inhibition of iNOS would result in increased levels of damage caused by the toxin. However, this was not the case since the relative intensity of ZO-1 was not significantly different with 1400W +

TcdA/B compared to TcdA/B by itself. The 20X magnification is shown to illustrate overall monolayer continuity, and the 40X magnification is shown to illustrate individual cells in terms of ZO-1 distribution and morphology.

Effects of reactive oxygen species on C.diff toxin-mediated modulation of HIF-1 α

From the data presented, it is likely that iNOS-generated NO is indeed a key effector molecule for the modulation of HIF-1 α stabilization and signaling during exposure of Caco-2 cells to C.diff toxin. For this reason, it is also important to consider the role of ROS in this system. It has been identified in previous studies [79] that exposure to C.diff results in elevated concentrations of ROS *in vivo*. As discussed earlier, ROS and NO exert opposing effects as the two groups of molecules are capable of directly inactivating each other in a concentration-dependent manner. Since iNOS is the dominant contributor of NO, it was reasonable to assume that any decrease in the available NO (i.e., for the nitrosylation of HIF-1 α) result from increases in ROS. Studies have previously demonstrated a protective effect for the ROS-scavenging compound, N-acetylcysteine (NAC), in the context of C.diff toxin-induced damage [80]. In this study however, it was proposed that NAC was protecting the cell by acting as a precursor compound to prevent an oxidative imbalance associated with exposure to C.diff toxin. In an effort to investigate another possible mechanism of protection by NAC, it was hypothesized that adding a ROS-scavenging compound could increase the bioavailability of NO and provide needed for the nitrosylation of HIF-1 α . This in turn could result in the

increased downstream signaling activity of HIF-1 and the subsequent protection of the epithelial barrier.

The effect of inducible nitric oxide synthase inhibition on Caco-2 cells exposed to C. difficile toxin

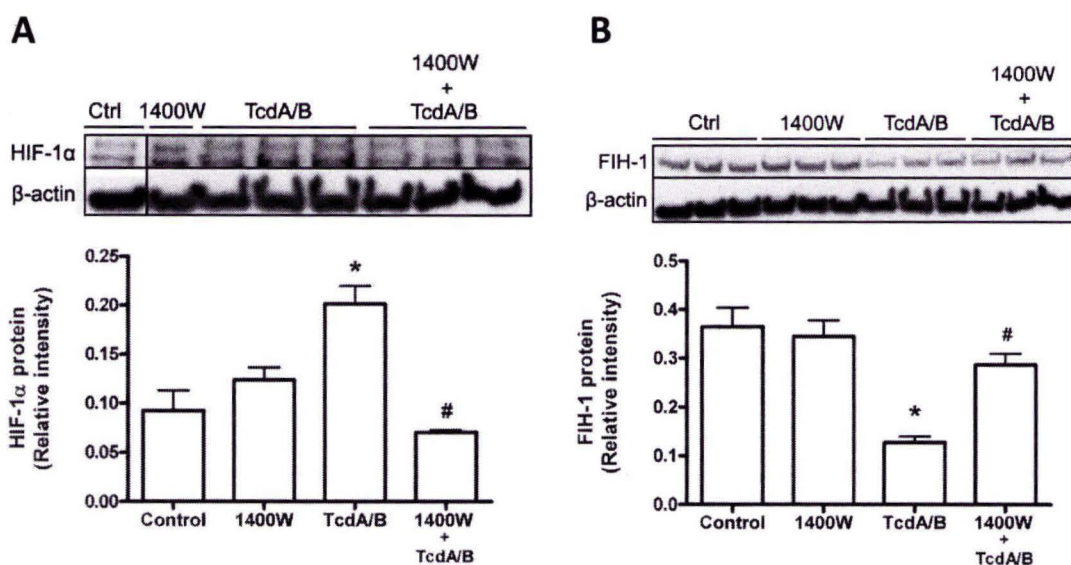


Figure 4.8 – Assessment of iNOS inhibition on HIF-1 α stabilization in Caco-2 cells exposed to *C. difficile* toxin. Caco-2 cells were treated for 4 hours with 1400W (100 μ M), TcdA/B (70 μ g/mL), or a 1 hour pre-treatment with 1400W followed by a 4 hour TcdA/B exposure. Cells were harvested and cytosolic and nuclear extracts were generated (n=3). Cytosolic extracts of each sample were immunoblotted for HIF-1 α (**A**) and FIH-1 (**B**) where expression levels were measured relative to β -actin. Statistical analysis involved a one-way ANOVA followed by Neuman-Keuls post hoc test where * represents $p < 0.01$ relative to control and # represents $p < 0.01$ relative to TcdA/B.

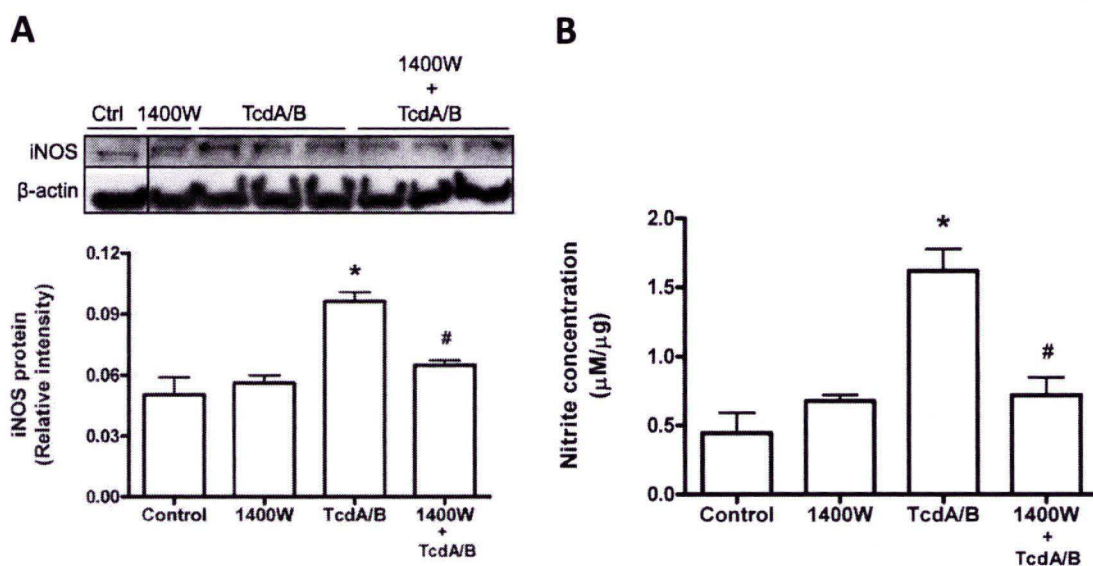


Figure 4.9 – Examination of iNOS-selective inhibition on iNOS expression and nitric oxide concentration in Caco-2 cells exposed to *C. difficile* toxin exposure. Caco-2 cells were treated for 4 hours with 1400W (100 μM), TcdA/B (70 $\mu\text{g}/\text{mL}$), or a 1 hour pre-treatment with 1400W followed by a 4 hour TcdA/B exposure (n=3). **(A)** Cytosolic extracts of each sample were immunoblotted for iNOS where expression levels were measured relative to β -actin. **(B)** NO levels were detected in cytosolic extracts using the colorimetric Griess assay. Detected nitrite concentration in the cells was measured relative to total protein content of the extract used in the assay. Statistical analysis involved a one-way ANOVA followed by Neuman-Keuls post hoc test where * represents $p < 0.01$ relative to control and # represents $p < 0.01$ relative to TcdA/B.

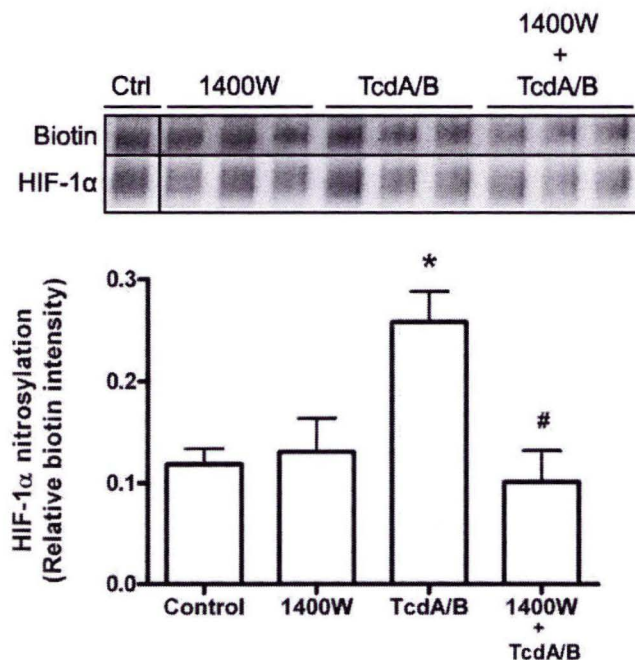


Figure 4.10 - Examination of iNOS inhibition on HIF-1 α nitrosylation (biotinylation) in Caco-2 cells exposed to *C. difficile* toxin. Caco-2 cells were treated for 4 hours with 1400W (100 μ M), TcdA/B (70 μ g/mL), or a 1 hour pre-treatment with 1400W followed by a 4 hour TcdA/B exposure (n=3). HIF-1 α was immunoprecipitated from the nuclear extracts then subjected to the biotin switch assay for measurement of nitrosylation. Statistical analysis involved a one-way ANOVA followed by Neuman-Keuls post hoc test where * represents $p < 0.01$ relative to control and # represents $p < 0.01$ relative to TcdA/B.

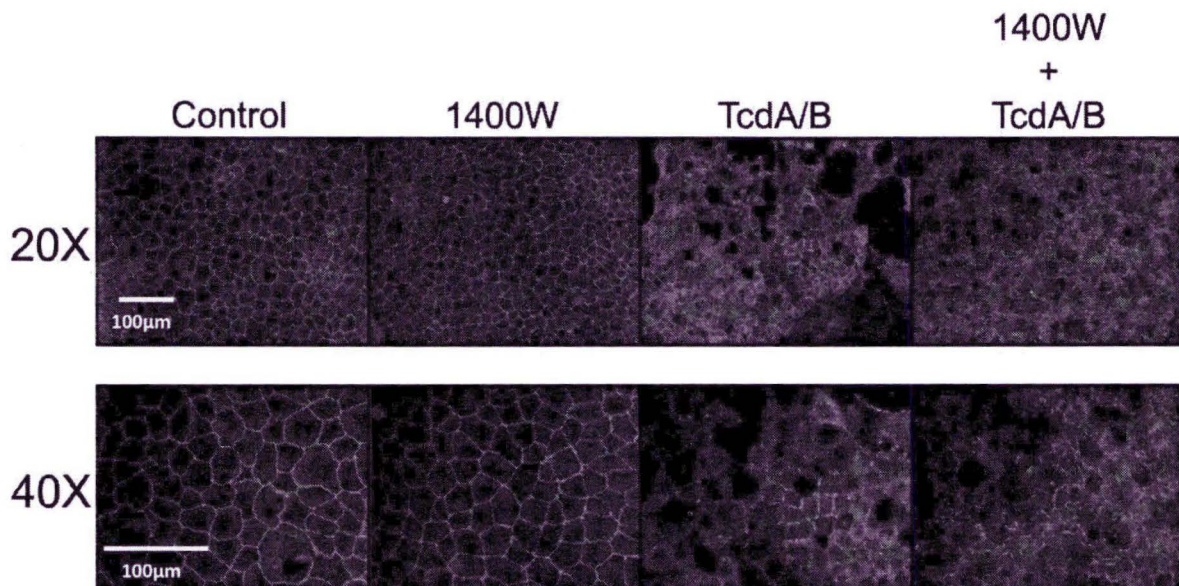


Figure 4.11 - Immunocytochemistry of ZO-1 staining and epithelial monolayer integrity following *C. difficile* toxin exposure and iNOS inhibition – Caco-2 cells were treated for 4 hours with 1400W (100 µM), TcdA/B (70 µg/mL), or a 1 hour 1400W pre-treatment followed by 4 hour TcdA/B exposure. Cell monolayers were immunoblotted for ZO-1 followed by Cy3-conjugated fluorescent secondary antibody. Cells were visualized with a fluorescent microscope. The pictures shown are a representative quadrant from 1 of 3 co-culture preparations.

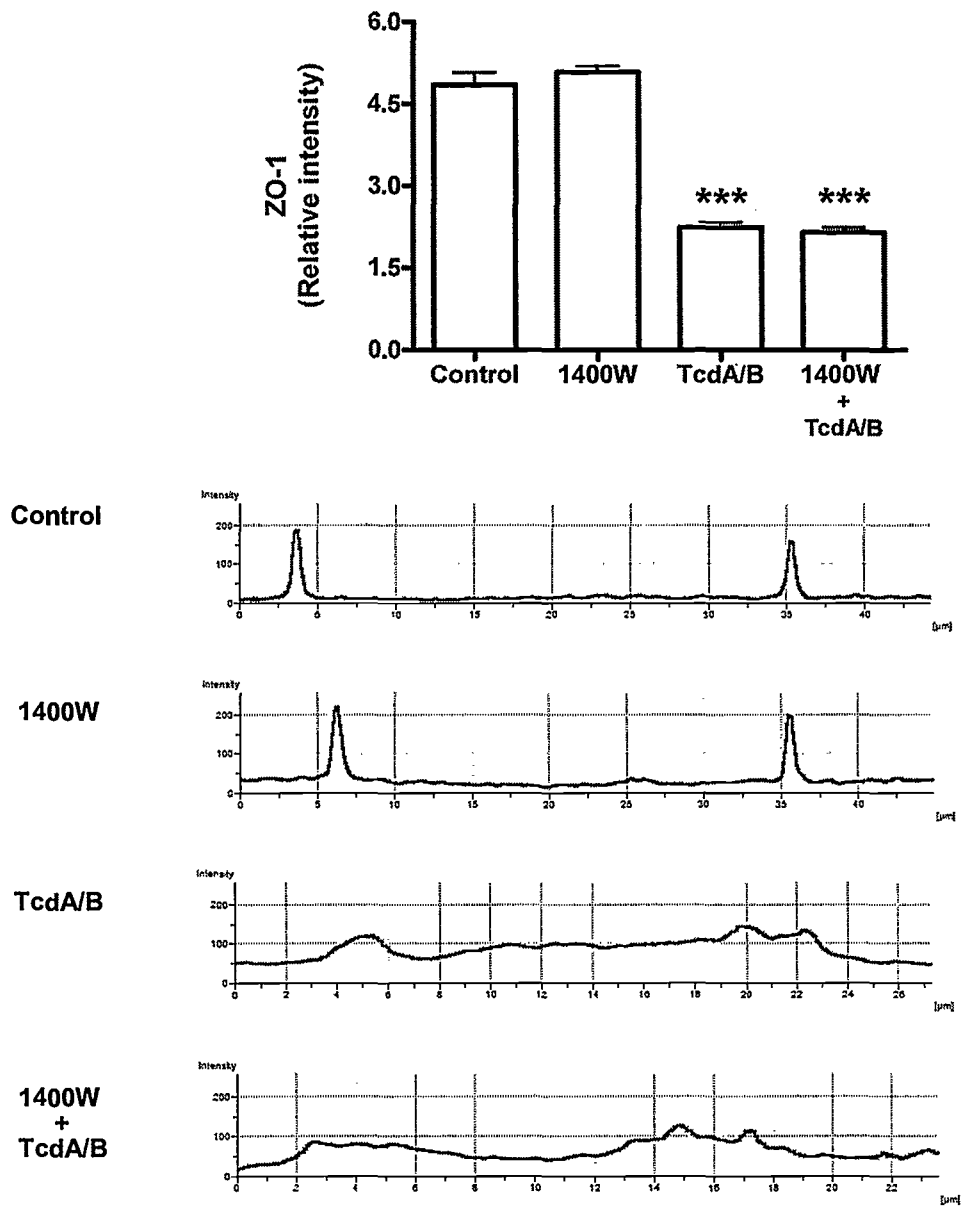


Figure 4.12 – Quantification of Caco-2 epithelial monolayer integrity following *C. difficile* toxin exposure and iNOS inhibition

Figure 4.12 – Relative intensity of ZO-1 fluorescence was quantified using 60 arbitrarily chosen cells from 3 co-culture preparations. The representative intensity profiles (line traces) are shown for each treatment. Statistical analysis involved a one-way ANOVA followed by a Neuman-Keuls post-hoc test where *** represents $p < 0.001$ compared to control.

For the studies investigating the effects of NAC, Caco-2 cells with a constitutive siRNA-mediated knockdown (HIF-KD) of HIF-1 α were used [81]. Using these Caco-2 cells, it would also be possible to determine whether the protective effects of NAC were HIF-1-dependent. Prior to performing any experiments involving NAC or TcdA/B, it was important to confirm that these cells, along with the scrambled siRNA (HIF-Scr) control cells, demonstrated the appropriate HIF-1 α response. It was determined that only the HIF-Scr Caco-2 cells showed the expected increase in HIF-1 α (Figure 4.13) when a HIF-1 α stabilizing compound (CoCl₂, 500 μ M) was applied. It should be noted that these cells do not represent a complete genetic deletion of HIF-1 α ; therefore it is not surprising that some basal levels of HIF-1 α are expressed even in the HIF-KD cells. The siRNA KD in the HIF-KD cells only serves to decrease the amount of HIF-1 α mRNA available for translation. Since HIF-1 α protein is regularly degraded in the normoxic environment, it is possible that both HIF-Scr and HIF-KD cells may demonstrate a similar and negligible baseline of HIF-1 α expression. What makes these cells such an effective tool for monitoring the role of HIF-1 α expression is that different HIF-1 α stabilizers do not increase detectable protein expression in the HIF-KD cell line.

With the Caco-2 cells responding as expected, the cells were exposed to NAC (25 mM) and TcdA/B (70 μ g/mL) and analyzed according to the same parameters described for previous experiments. The HIF-Scr cells demonstrated the same HIF-1 α stabilization and FIH-1 responses as seen previously with TcdA/B exposure alone (Figure 4.14A, A1). NAC alone did not elicit any response from either protein, however NAC + TcdA/B

suppressed the increase in HIF-1 α expression seen with TcdA/B alone. The combination of NAC and TcdA/B however still resulted in the same 2-fold suppression in FIH-1 as seen with TcdA/B alone. Conversely, the HIF-KD cells showed the reverse effect with HIF- α but not FIH-1 (Figure 4.14B, B1), where HIF-1 α expression was suppressed 3-fold below control with TcdA/B, and no change from control with NAC + TcdA/B. FIH-1 experienced the same approximate 2-fold decrease with both TcdA/B and NAC + TcdA/B. Taken together, the data provided by the HIF-Scr cells with respect to FIH-1 (Figure 4.14A1), iNOS, and NO (Figure 4.15A, A1) supports the hypothesis that FIH-1 expression is linked to NO. However, since a 2-fold suppression of FIH-1 was also seen in the HIF-KD cells, it was possible that FIH-1 was being regulated in an NO-independent manner.

Taking the iNOS expression and NO levels into consideration in the HIF-Scr cells (Figure 4.15A, A1), TcdA/B caused a significant increase in both iNOS (30% increase) and NO (3-fold increase) (as seen before, Figure 4.9). Interestingly, both NAC stimulation alone and in combination with TcdA/B caused 2-fold increases in NO concentration. The increases seen in iNOS and NO are both attenuated in HIF-KD cells (Figure 4.15B, B1). Although NO levels are increased with NAC treatments, the proportion of nitrosylated HIF-1 α only appears to be elevated when TcdA/B is present (Figure 4.16A). Although TcdA/B exposure results in a numerically larger (2-fold) increase in nitrosylation, the nitrosylation stimulated by NAC + TcdA/B (1.5-fold increase) is not significantly different. In the HIF-KD cells, the elevation in NO concentration was completely abolished

regardless of the treatment, which coincides with the lack of a measurable increase in nitrosylated HIF-1 α in the HIF-KD cells (Figure 4.16B). On the surface, these findings suggest a possible connection between TcdA/B-stimulated NO production and the expression of HIF-1 α .

Due to the increased susceptibility of HIF-1 α KD cells to TcdA/B (Hirota et al. 2010), cells plated for immunocytochemistry were exposed to a reduced concentration of TcdA/B at 7 μ g/mL (Figure 4.17). For the immunocytochemistry data, the overall appearance of HIF-Scr (Figure 4.17A) and HIF-KD (Figure 4.17B) cells differs with respect to the damage caused by TcdA/B exposure. Although the ZO-1 distribution was noticeably more diffuse with TcdA/B alone and in combination with NAC, HIF-Scr cells appeared to have a much less damaged monolayer compared to HIF-KD cells. In both HIF-Scr and HIF-KD cells, TcdA/B and NAC + TcdA/B treatments resulted in a 60% reduction in ZO-1 intensity. NAC + TcdA/B intensity levels were not significantly different from those of TcdA/B alone in either cell type. Interestingly, exposure to TcdA/B in the presence of NAC did not provide a protective effect on the epithelial barrier as initially hypothesized. As reported earlier (Figure 4.11), TcdA/B treatments elicited changes to cell morphology with Caco-2 cells becoming much smaller with rounded edges. The morphological changes were more apparent in the HIF-KD cells compared to the HIF-Scr cells. Looking at the immunofluorescence data alone, it would seem that the HIF-Scr cells maintained a more cohesive barrier overall, however this did not seem to be reflected in the quantified data. It should be mentioned that in the HIF-

Scr ZO-1 stains, not only was the ZO-1 intensity greater, but so was the background fluorescence. Since the quantification was measured relative to background signal intensity, this could explain why the graphical data did not accurately reflect a protective effect.

Assessment of HIF-1 α siRNA scrambled vs knockdown Caco-2 response to a HIF-1 α stabilizing compound

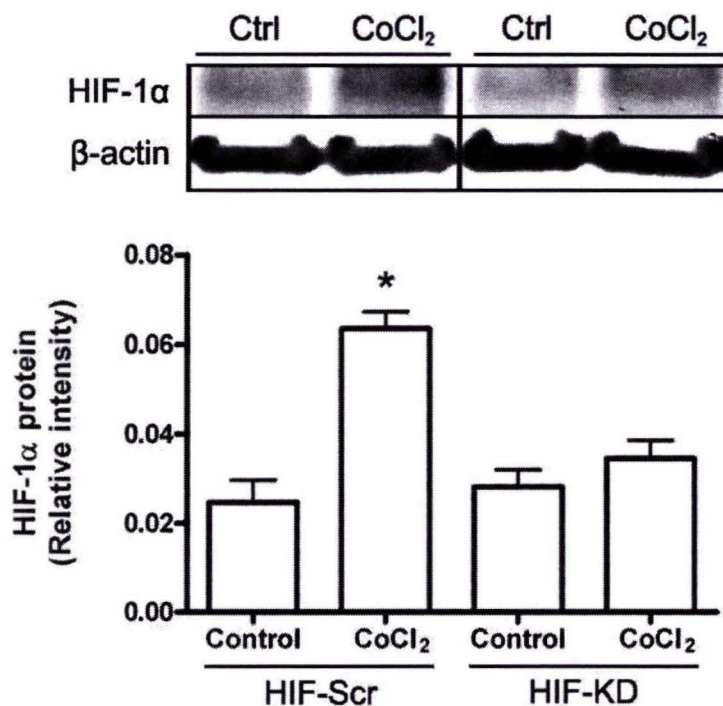


Figure 4.13 – HIF-1 α protein expression in scrambled and knockdown Caco-2 cells upon stimulation with CoCl₂. Scrambled (HIF-Scr) and knockdown (HIF-KD) HIF-1 α siRNA cells were treated with 500 μ M of CoCl₂ for a period of 4 hours. Whole cell extracts were generated and immunoblotted for HIF-1 α (n=3). The expression levels were reported relative to β -actin. Statistical analysis involved a one-way ANOVA with Neuman-Keuls post-hoc test where * represents $p < 0.01$ compared to control.

The effect of N-acetylcysteine on Caco-2 cells with C. difficile toxin exposure (with scrambled and knockdown HIF-1 α siRNA Caco-2 cells)

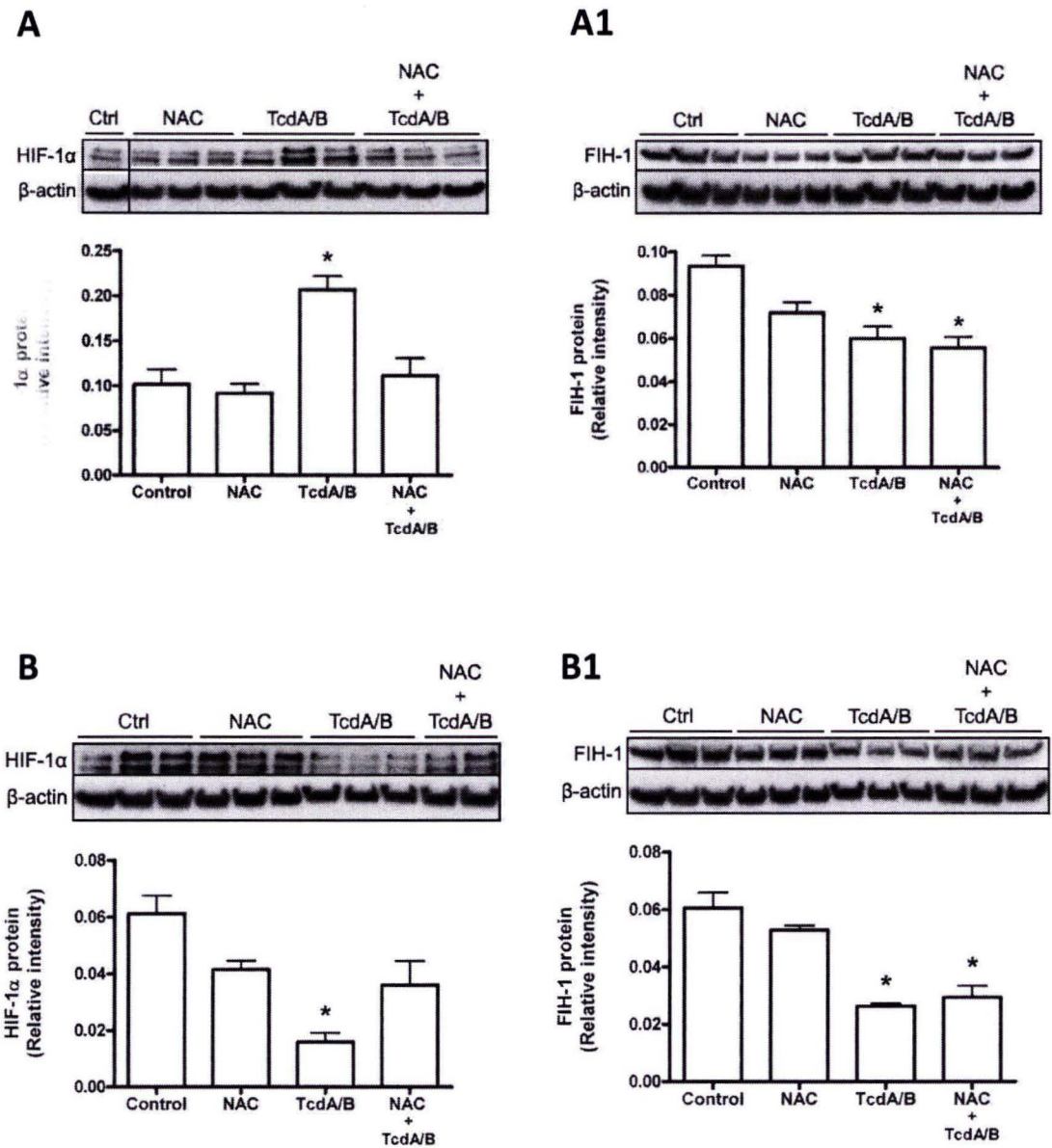


Figure 4.14 – Assessment of N-acetylcysteine on HIF-1 α stabilization in HIF-1 α scrambled (A) and knockdown (B) Caco-2 cells exposed to *C. difficile* toxin

Figure 4.14 – Caco-2 cells (both scrambled and knockdown siRNA cells) were treated for 4 hours with N-acetylcysteine (NAC – 25 mM), TcdA/B (70 µg/mL), or a 1 hour pre-treatment with NAC followed by a 4 hour TcdA/B exposure. Cells were harvested and cytosolic and nuclear extracts were generated (n=3). Cytosolic extracts of each sample were immunoblotted for HIF-1α (**A, B**) and FIH-1 (**A1, B1**) where expression levels were measured relative to β-actin. Statistical analysis involved a one-way ANOVA followed by Neuman-Keuls post hoc test where * represents $p < 0.01$ compared to control.

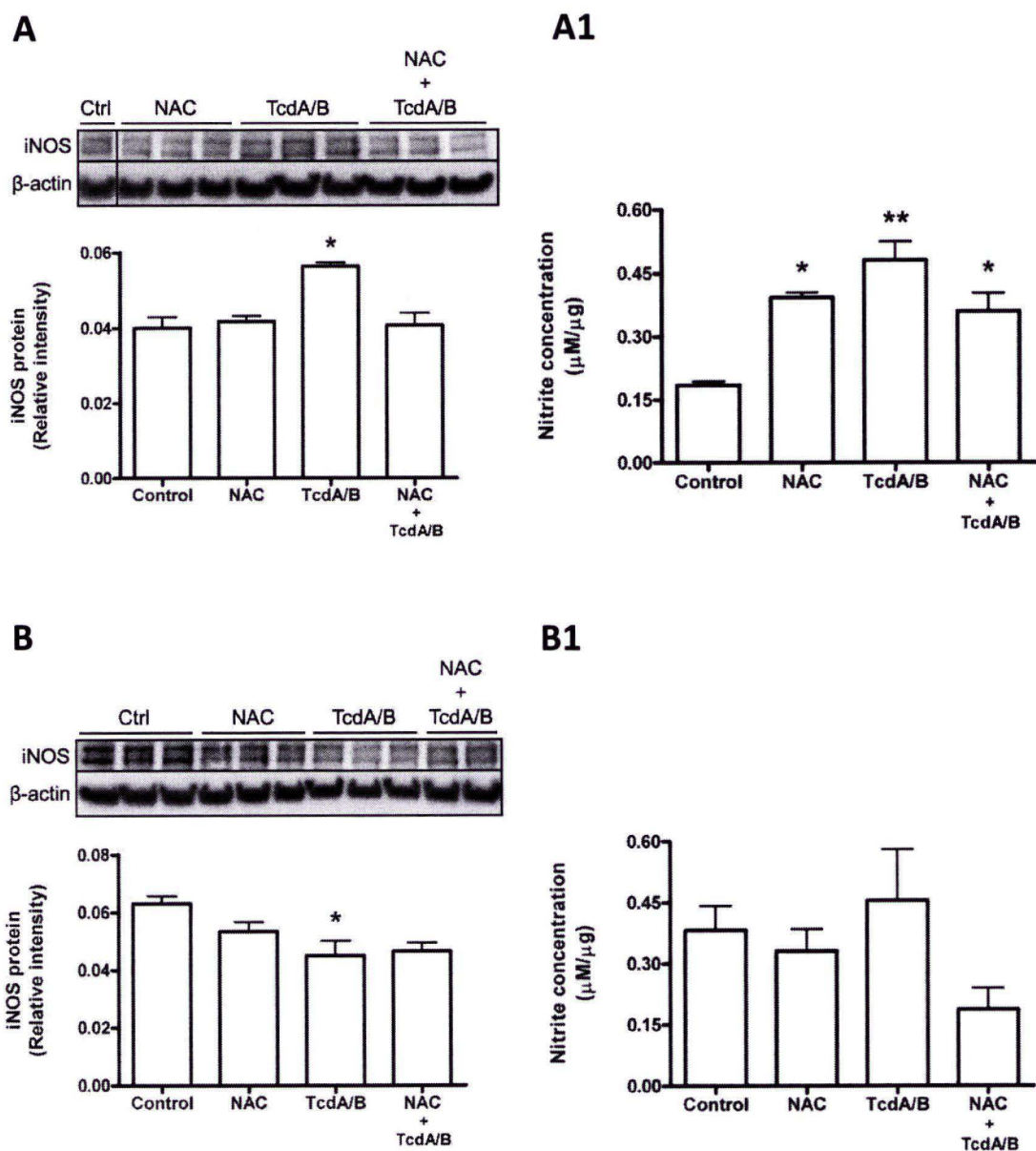


Figure 4.15 – Examination of N-acetylcysteine on iNOS expression and nitric oxide concentration in HIF-1 α scrambled (A) and knockdown (B) Caco-2 cells exposed to *C. difficile* toxin

Figure 4.15 – Caco-2 cells (both scrambled and knockdown siRNA cells) were treated for 4 hours with N-acetylcysteine (NAC – 25 mM), TcdA/B (70 µg/mL), or a 1 hour pre-treatment with NAC followed by a 4 hour TcdA/B exposure. Cells were harvested and cytosolic and nuclear extracts were generated (n=3). **(A, B)** Cytosolic extracts of each sample were immunoblotted for iNOS where expression levels were measured relative to β-actin. **(A1, B1)** NO levels were detected in cytosolic extracts using the colorimetric Griess assay. Detected nitrite concentration in the cells was measured relative to total protein content of the extract used in the assay. Statistical analysis involved a one-way ANOVA followed by Neuman-Keuls post hoc test where * represents $p < 0.01$ and ** represents $p < 0.001$ compared to control.

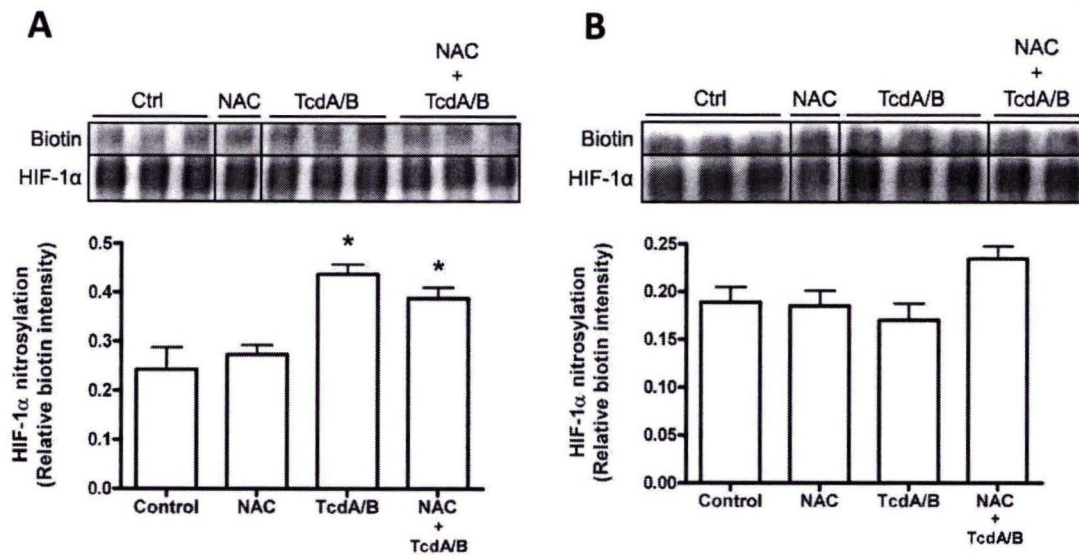


Figure 4.16 – Examination of N-acetylcysteine on HIF-1α nitrosylation (biotinylation) in HIF-1α scrambled (A) and knockdown (B) Caco-2 cells exposed to *C. difficile* toxin.

Caco-2 cells (both scrambled and knockdown siRNA cells) were treated for 4 hours with N-acetylcysteine (NAC – 25 mM), TcdA/B (70 µg/mL), or a 1 hour pre-treatment with NAC followed by a 4 hour TcdA/B exposure (n=3). Cells were harvested and cytosolic and nuclear extracts were generated. HIF-1α was immunoprecipitated from the nuclear extracts then subjected to the biotin switch assay where nitrosylated residues were biotinylated (B). Immunoblot quantification is presented as biotin signal relative to HIF-1α protein levels. Statistical analysis involved a one-way ANOVA followed by Neuman-Keuls post hoc test where * represents $p < 0.01$ compared to control.

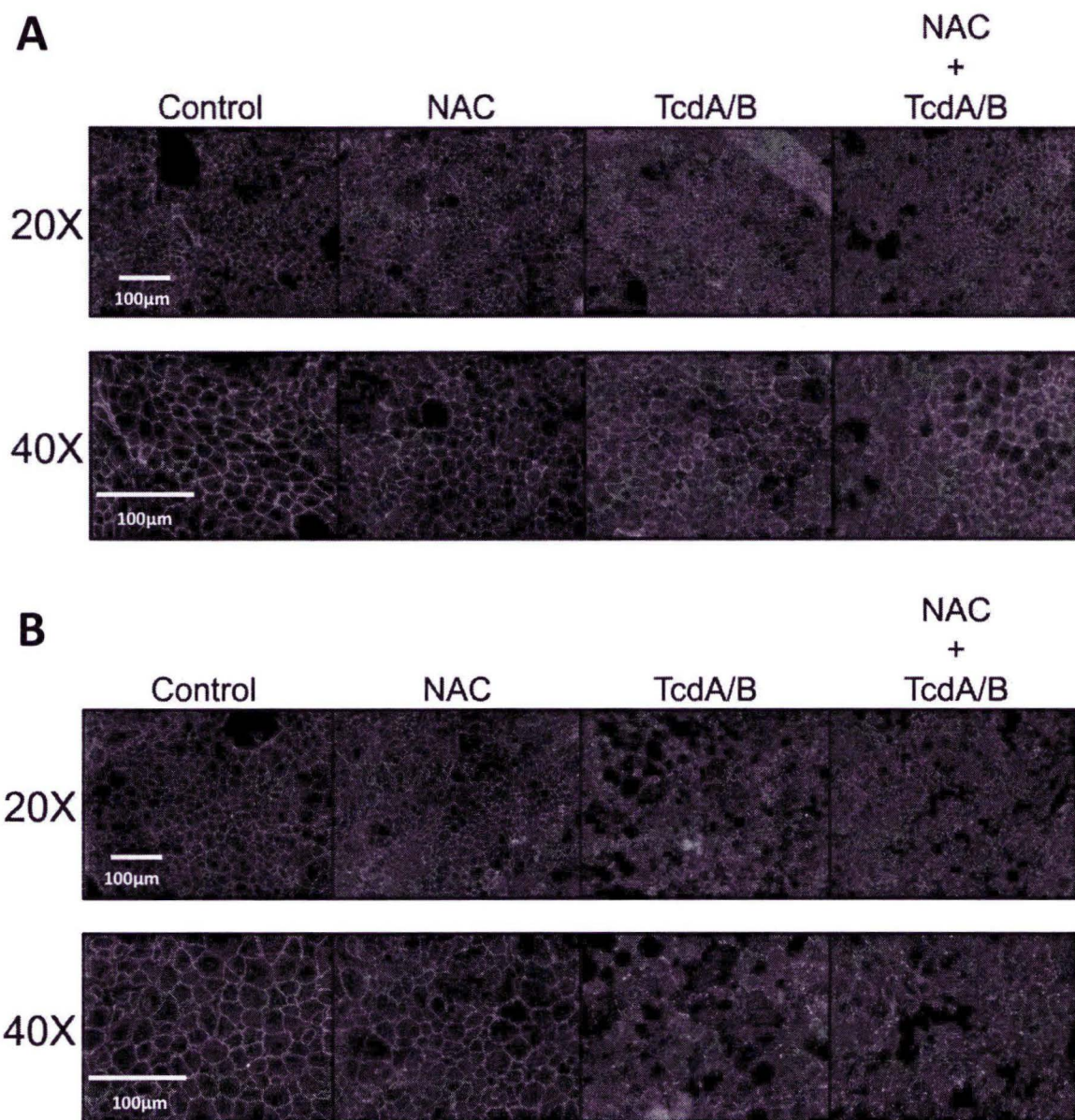


Figure 4.17 – Immunocytochemistry of ZO-1 as an indicator of epithelial monolayer integrity following exposure to *C. difficile* toxin and N-acetylcysteine in HIF-1a scrambled cells (A) and knockdown (B) cells

Figure 4.17 – Caco-2 cells (both scrambled and knockdown siRNA cells) were treated for 4 hours with N-acetylcysteine (NAC – 25 mM), TcdA/B (7 μ g/mL), or a 1 hour NAC pre-treatment followed by 4 hour TcdA/B exposure. Cell monolayers were immunoblotted for ZO-1 followed by Cy3-conjugated fluorescent secondary antibody. Cells were visualized with a fluorescent microscope. The pictures shown are a representative  from 1 of 3 co-culture preparations.

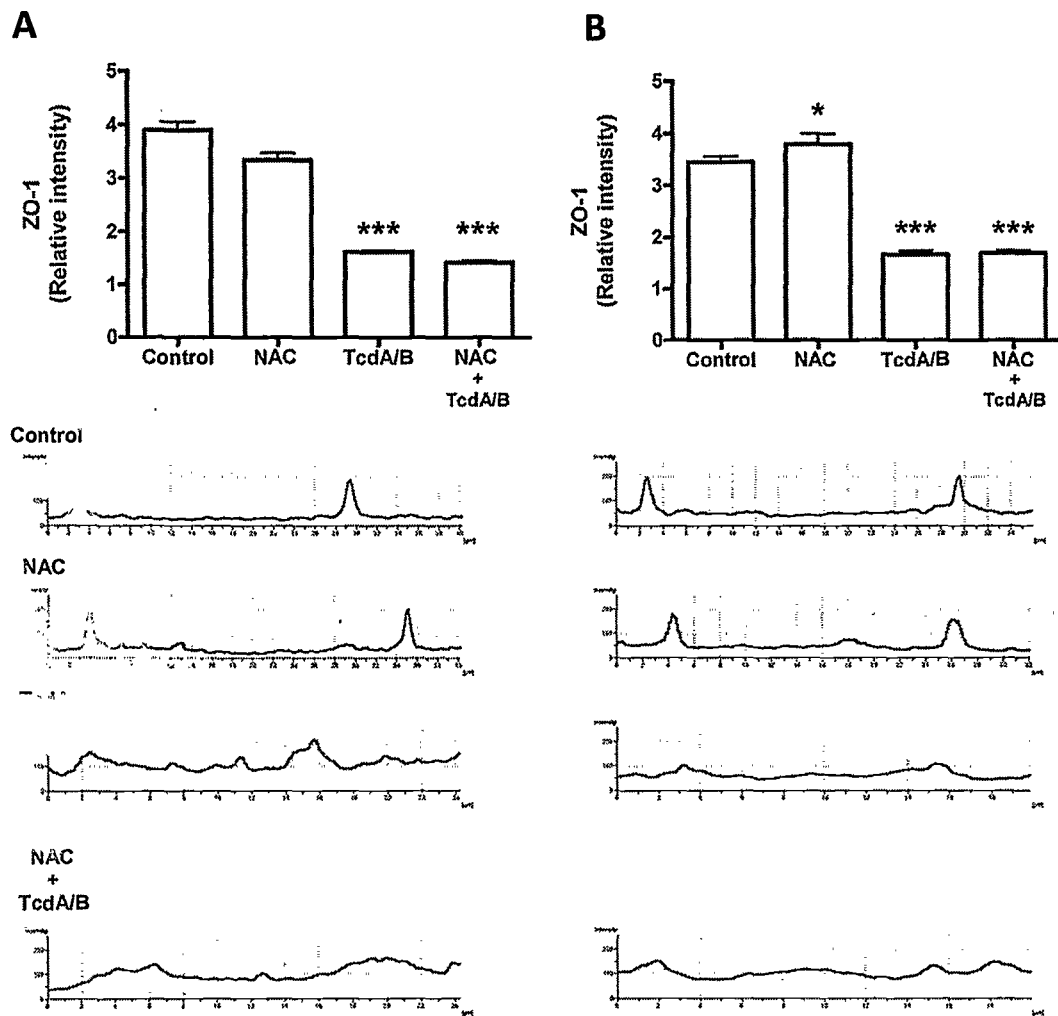


Figure 4.18 - Quantification of Caco-2 epithelial monolayer integrity following *C.difficile* toxin and N-acetylcysteine in HIF-1 α scrambled (A) and knockdown (B) cells

Relative intensity of ZO-1 fluorescence was quantified using 30 arbitrarily chosen cells from 3 co-culture preparations. The representative intensity profiles (line traces) are shown for each treatment. Statistical analysis involved a one-way ANOVA followed by a Neuman-Keuls post-hoc test where * represents $p < 0.05$ and *** represents $p < 0.001$ compared to control.

C.diff toxin modulates HIF-1 α expression via iNOS-generated nitric oxide *in vivo*

The effect of iNOS-generated NO was investigated in an *in vivo* environment with two different models. Initially, studies performed by Hirota et al. 2010 [70], characterized the ileal-loop surgical model of TcdA/B-induced damage in mice. The ileal-loop procedure on wild-type mice showed an approximate 3-fold increase in HIF-1 α expression in mice that were exposed to TcdA/B (Figure 4.19). Using the same procedure, WT mice and iNOS-deficient (iNOS KO) mice were both injected with TcdA/B, and HIF-1 α expression was compared between the two sets of mice (Figure 4.20). Mice that were deficient in iNOS demonstrated a 3-fold decrease HIF-1 α expression compared to WT mice, suggesting that HIF-1 α stabilization was dependent on iNOS *in vivo*. It needs to be said however that there was no PBS vs TcdA/B control performed in the iNOS KO mice, so it is possible that TcdA/B still causes an induction of HIF-1 α compared to basal levels. The experimental procedure was altered from that reported in Hirota et al. 2010 [70]. The amount of TcdA/B injected into the ileal loop was decreased (from 100 μ g to 70 μ g) and the incubation time was shortened due to an increased susceptibility of the iNOS-KO animals to the toxin. The iNOS-KO animals were still noticeably distressed at 3 hours as their movements were very limited and they showed little response to stimulation of the enrichment items in their habitat. A qualitative visual assessment of the ileal tissues after animal sacrifice also revealed differences between WT and iNOS-KO mice. The KO mice appeared to have more intestinal damage as evidenced by increased bleeding and redness of the tissues.

In an effort to more accurately emulate the effects of *C. difficile* toxin *in vivo*, an intra-rectal injection model that directly exposed colonic tissues (as opposed to ileal tissues) to TcdA/B was used (Figure 4.21). With the intra-rectal procedure, mice that were exposed to TcdA/B once again demonstrated a significant 40% increase in HIF-1 α compared to WT mice in harvested colonic tissue samples. This increase in HIF-1 α expression was also correlated with a 40% increase in nitrosylated HIF-1 α , suggesting that the stabilization of HIF-1 α via nitric oxide was also occurring *in vivo*.

Examination of NO-dependent HIF-1 α stabilization in vivo

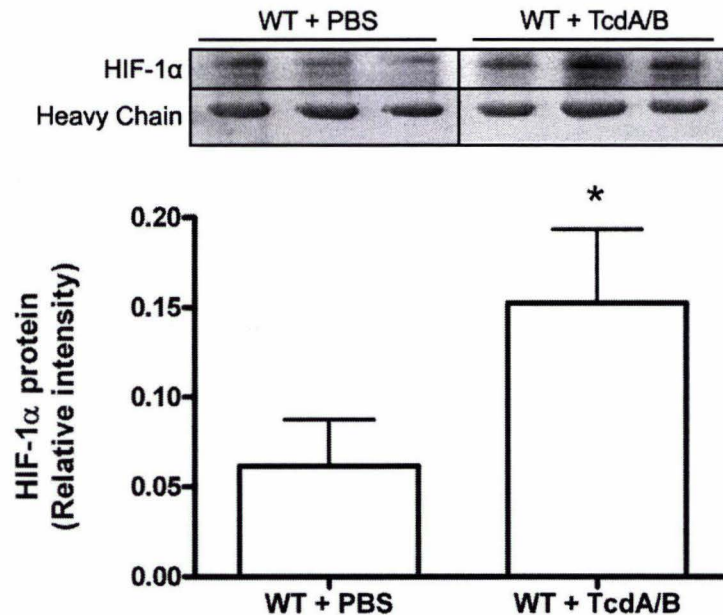


Figure 4.19 - Ileal-loop surgical procedure – HIF-1 α Immunoprecipitation in toxin versus PBS-treated WT mice. The ileal-loop surgical procedure was performed on 12 wild-type (WT) mice where 6 mice were injected with 100 μ L of phosphate-buffered saline (PBS) as a control, and the other 6 mice were injected with 100 μ g of TcdA/B (diluted to 1 μ g/ μ L in sterile PBS). After a 4 hour incubation period, mice were sacrificed and ileal tissues were harvested. HIF-1 α was immunoprecipitated from the tissue homogenates and immunoblotted for HIF-1 α where expression was measured relative to antibody heavy chain. Statistical analysis involved a Student's t-test where * represents $p < 0.05$ compared to PBS treatment.

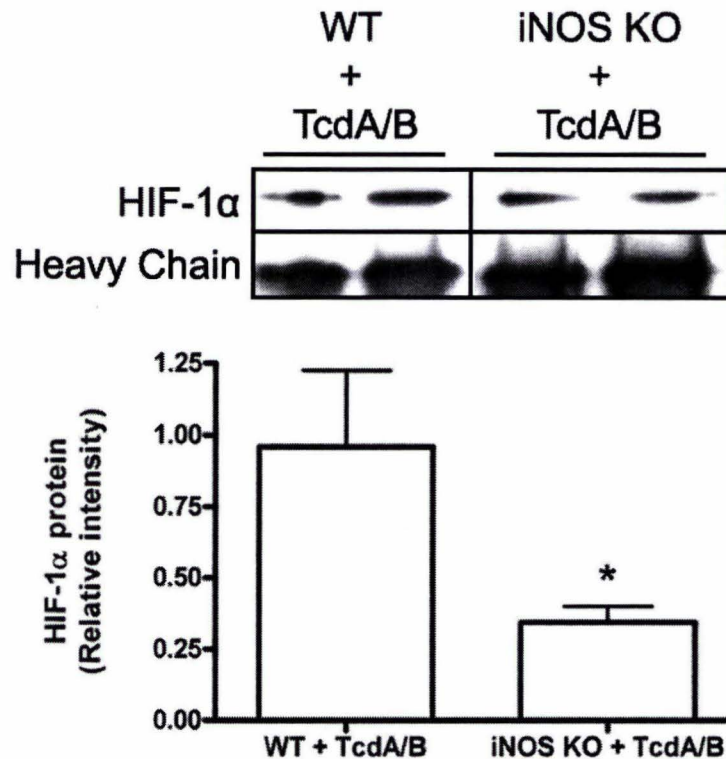


Figure 4.20 - Ileal-loop surgical procedure – HIF-1 α Immunoprecipitation in toxin-treated WT versus iNOS $^{-/-}$ mice. The ileal-loop surgical procedure was performed on 16 wild-type (WT) mice where 8 mice were injected with 100 μ L of phosphate-buffered saline (PBS) as a control, and the other 8 mice were injected with 70 μ g of TcdA/B (diluted to 1 μ g/ μ L in sterile PBS). After a 3 hour incubation period, mice were sacrificed and ileal tissues were harvested. HIF-1 α was immunoprecipitated from the tissue homogenates and immunoblotted for HIF-1 α where expression was measured relative to antibody heavy chain. Statistical analysis involved a Student's t-test where * represents $p < 0.05$ compared to PBS treatment.

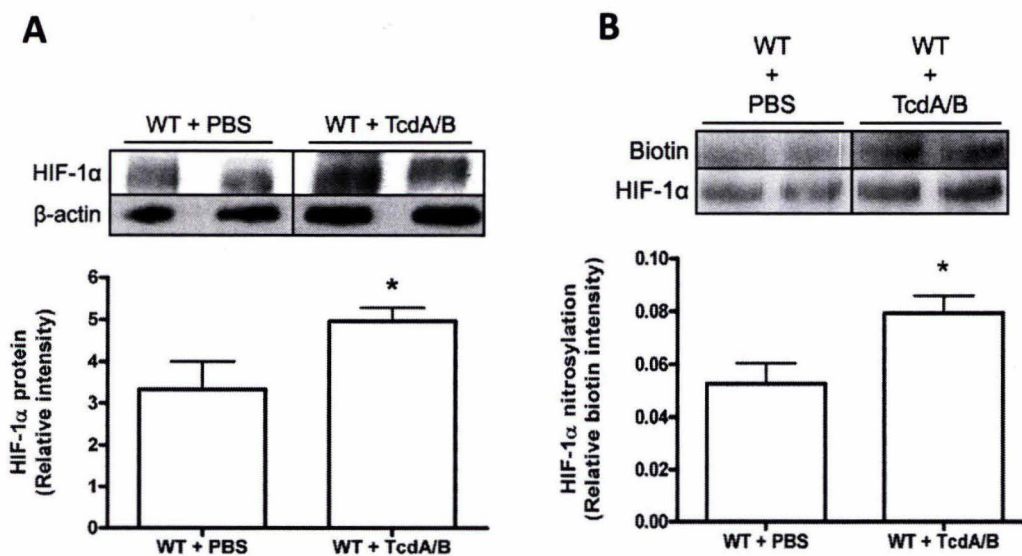


Figure 4.21 - Intra-rectal surgical procedure – HIF-1α protein expression and nitrosylation in PBS versus Toxin-treated C57/Bl6 mice. The intra-rectal surgical procedure was performed on 8 wild-type (WT) mice where 4 mice were injected with 100 μL of phosphate-buffered saline (PBS) as a control, and the other 4 mice were injected with 100 μg of TcdA/B (diluted to 1 μg/μL in sterile PBS). After a 4 hour incubation period, mice were sacrificed and colonic tissues were harvested. Colonic tissue homogenates were immunoblotted for HIF-1α where expression was measured relative to β-actin (**A**). HIF-1α was immunoprecipitated from tissue homogenates and subjected to the biotin switch assay where nitrosylated residues were biotinylated. Immunoblot quantification is presented as biotin signal relative to HIF-1α protein levels (**B**). Statistical analysis involved a Student's t-test where * represents $p < 0.05$ compared to PBS treatment.

5.0

discussion

5.0 Discussion

5.1 Analysis and Interpretation

To reiterate the initial hypothesis, it was proposed that the NO generated as a result of C.diff toxin-induced damage acted as an important signal to stabilize and activate HIF-1 α . In this study, it was demonstrated using both *in vitro* and *in vivo* models of C.diff intoxication that HIF-1 α stabilization occurred via NO that was generated by iNOS. In Caco-2 intestinal epithelial cells, both TcdA/B and TcdB were capable of inducing iNOS expression, which in turn, was associated with subsequent increases in NO concentrations. The elevation in iNOS expression, which occurred after a 4 hour incubation period, was also associated with a significant increase in HIF-1 α protein expression. When cells were pre-treated with the selective iNOS inhibitor, 1400W [77], the increase seen in both iNOS and HIF-1 α was effectively abolished along with the increase in NO itself. Further examination of the HIF-1 α subunit demonstrated that the protein itself was subjected to a post-translational modification (i.e., nitrosylation) when cells were exposed to TcdA/B. In the mouse *in vivo* models, the ileal-loop method of TcdA/B exposure also demonstrated a significant increase in HIF-1 α expression in the ileum of mice that had been exposed to toxin. This increase in HIF-1 α also appeared to be dependent on iNOS since exposure of iNOS-deficient mice to toxin did not elicit increases in HIF-1 α expression relative to WT mice. In the arguably more relevant intra-rectal model of toxin exposure, mice exposed to TcdA/B not only

experienced an increase in HIF-1 α expression but also were found to experience HIF-1 α nitrosylation. These findings suggest that iNOS-generated NO was necessary for the nitrosylation and stabilization of HIF-1 α both *in vitro* and *in vivo* and are particularly important as they represent the first attempt to elucidate the exact mechanism by which HIF-1 α protein levels are elevated in the presence of C.diff toxin. These results confirm and elaborate on previous studies conducted on HIF-1 α in the context of C.diff-induced intestinal injury by Hirota et al. 2010 [70].

Due to the increased susceptibility of HIF-1 α KD Caco-2 cells to TcdA/B, cells plated for immunocytochemistry were exposed to a reduced concentration of toxin at 7 μ g/mL. This increase in susceptibility to *C. difficile* toxin was characterized in previous studies performed by Hirota et al. 2010 [70], that demonstrated an increased susceptibility to TcdA/B in mice that were genetically deficient in HIF-1 α . The increased susceptibility in HIF-1 α ^{-/-} mice was determined via increased histological damage scores (global intestinal trauma) and elevated MPO activity, which represents a measure of neutrophilic infiltration into the tissues and provides a surrogate measure for inflammation [70]. These findings were in general agreement with the immunocytochemistry data presented herein (Figure 4.17) as the overall appearance of HIF-Scr vs HIF-KD Caco-2 cells differs with respect to damage caused by TcdA/B exposure. Although the ZO-1 distribution was noticeably more diffuse with TcdA/B alone and in combination with NAC, the HIF-Scr cells appeared to have less damaged

monolayer when compared to HIF-KD cells. In the aforementioned study by Hirota et al., it was also demonstrated that an inhibition of iNOS resulted in an attenuation of HIF-1 α expression in Caco-2 cells. In our current study, experiments with HIF-1 α -KD cells exposed to TcdA/B have shown an attenuation of iNOS and NO concentration, whereas Hirota et al. have shown an increase in serum NO levels in HIF-1 α ^{-/-} mice (an intestinal epithelium-specific KO) exposed to TcdA/B. These results do not necessarily conflict with our findings as NO levels in our experiments have been taken from the HIF-1 α -deficient epithelial cells themselves, whereas Hirota et al. have looked at global NO present in the serum of the mice. Within the GI tract alone, there are a number of different potential sources of NO which may contribute to an overall increase in systemic NO including macrophages, mast cells, neuronal cells of the myenteric plexus, and smooth muscle cells (reviewed in [82]).

If we focus specifically on iNOS regulation, it has been shown in previous studies that TcdB and other actin cytoskeleton-disrupting agents are capable of inducing iNOS expression [83], [84]. This coincides with our results as we have demonstrated the same events occurring in Caco-2 cells with TcdB treatment. In addition, it was previously shown that the TcdB-mediated induction of iNOS was markedly increased in the presence of cytokines [85]. Within intestinal epithelial cells, Kim et al. demonstrated that TcdA was capable of rapidly inducing cytokine and chemokine production in an NF- κ B-dependent fashion [86]. The increase in NF- κ B activity and subsequent chemokine

production was seen as early as 10 minutes with a peak response occurring after 2 hours of exposure with TcdA. This is a fairly significant finding with respect to our current study as iNOS expression levels were significantly increased (2.5-fold compared to control) after 4 hours of TcdA/B exposure. This suggests that both TcdA and TcdB are involved in the induction of iNOS in our experimental model. The study by Kim et al. [86], along with another conducted by Taylor et al. [87] identified NF- κ B as being a major inducer of cytokine-mediated iNOS expression. However, another study performed by Hattori et al. [84] revealed that iNOS could also be induced by disruption of the actin cytoskeleton in an NF- κ B-independent fashion. It is important to note that this study was conducted using cytoskeletal disrupting agents that did not include TcdA or TcdB. However, since the major action of the Clostridial toxins is to facilitate the disruption of the cytoskeleton, it may be possible for TcdA/B to induce iNOS expression without NF- κ B.

In addition to these mechanisms, the results gathered from HIF-KD Caco-2 cells add yet another dimension to iNOS regulation in the context of C.diff toxin exposure. When treated with TcdA/B alone, HIF-Scr cells demonstrate opposite effects to those observed for the HIF-KD cells. In the Scr cells, significant increases in both HIF-1 α stabilization and iNOS induction were present as with WT Caco-2 cells. As for the cells deficient in HIF-1 α , along with an attenuated HIF-1 α response, iNOS induction was also completely abolished. As discussed previously, HIF-1 regulates the transcription of

downstream gene targets by binding to a specific DNA sequence known as the Hypoxia Response Element (HRE). With HIF-1 activity being implicated in a number of different cellular processes (including epithelial barrier maintenance) [70, 88], it comes as no surprise that iNOS also contains an HRE within its promoter region [89]. Peyssonnaud et al. conducted studies investigating the HIF-1 α -mediated induction of bactericidal factors (which include NO). These studies were performed in mice expressing macrophages that were deficient in HIF-1 α . The HIF null mice harbored greater amounts of colonized bacteria (2-fold increase in bacterial CFUs) compared to WT suggesting their bactericidal response was suppressed by the lack of HIF-1 α [90]. Taken together, these findings provide support for our conclusions which suggest that HIF-1 α may be necessary to induce iNOS expression in colonic epithelial cells in response to C.diff toxin exposure.

While still in the realm of iNOS regulation, an interesting result to consider was the response of HIF-Scr cells with NAC treatment (Figure 4.15A1). This result was rather unexpected as treatment of HIF-Scr cells with NAC alone resulted in increased NO production. To this result, I can only speculate as to the mechanisms that may be involved. One possible explanation may be found with HIF-2 α . The HIF-2 α protein belongs to the HIF- α family and is also an oxygen-regulated protein that responds to hypoxic stabilization. It is fairly similar to HIF-1 α (with a 48% sequence similarity), and it is capable of binding to the same HRE as HIF-1 α on downstream target genes [28]. Although the role of HIF-2 α is tissue specific, its expression and signaling has been

associated with the GI tract. Most recently, a report has implicated the protein in the regulation of iron absorption in rat small intestine epithelial cells [91]. Studies which have utilized NAC in cell cultures have determined that NAC creates a reducing environment [80], and Chen et al. demonstrated that a NAC-induced redox shift favored the expression of HIF-2 α over HIF-1 α in neuroblastoma cells [92]. As a result of the change in redox conditions brought on by NAC, it is possible that the HIF-Scr Caco-2 cells adjust to favor the expression of HIF-2 α over HIF-1 α . While speculative, this possibility would coincide with the lack of HIF-1 α expression seen with this treatment. HIF-2 α , with its HRE-binding capability, may induce iNOS expression to increase NO production. However, due to the absence of cytokines (as TcdA/B is absent) or cytoskeleton disruption, the induction of iNOS may be relatively short-lived, but still sufficient to cause an increase in NO concentration. Due to the presence of inhibitory siRNA in the HIF-KD cells, it's possible that both HIF-1 α and HIF-2 α transcription may be affected, which may explain why the increase in NO is absent in HIF-KD cells with NAC treatment alone. In the study by Ahmad et al. [81], which utilizes the HIF-1 α -KD siRNA cells, there doesn't appear to be any conclusive evidence to suggest that HIF-2 α is unaffected by the siRNA. Although they demonstrate increased HIF-2 α -mediated signaling of a protein in the HIF-1 α -KD cells, there is no evidence to directly connect the two proteins (i.e. there is no immunoblot data showing HIF-2 α expression in HIF-1 α -KD cells). It is also possible that their protein of interest may be more sensitive to HIF-2 α expression, meaning that less HIF-2 α may be required to stimulate a downstream response. Taking these factors

into consideration, it may be possible that the siRNA is interfering with both HIF-1 α and HIF-2 α in our HIF-KD cells.

One interesting finding in our study relates to the interaction between ROS and HIF-1 α . When HIF-Scr cells were exposed to TcdA/B in combination with NAC, the overexpression of HIF-1 α was attenuated. NAC was demonstrated in a number of different experimental models to have a cytoprotective effect by acting as a potent ROS scavenger [93] [94]. There have also been studies in which NAC was shown to be protective against TcdB exposure. Fiorentini et al. hypothesized that the protective effect of NAC resulted from its ability to create a reducing environment. Since NAC is also a precursor for glutathione, they measured the proportion of oxidized glutathione versus reduced glutathione to determine the redox state of the cell. Their findings suggested that TcdB treatment on both human epithelial cells and small intestinal cells created an oxidizing environment (represented by an increase in oxidized glutathione) and that this was rectified with NAC pre-treatment. This shift towards a reducing environment was posited as the mechanism of cytoprotection [80]. These results however seem to contradict the effects that we observe with NAC treatment. In the HIF-Scr cells, pre-treatment with NAC in combination with TcdA/B provided no extra protection since significant differences between ZO-1 immunostaining with TcdA/B alone compared to NAC with TcdA/B were not observed. In addition, HIF-1 α expression was also significantly attenuated with NAC pre-treatment. Assuming that NAC can act

as a potent ROS scavenger in our system, the findings suggest that ROS may be an essential factor in the stabilization of HIF-1 α in the context of C.diff toxin exposure.

Looking at the specific effects of the different C.diff toxins, it has been demonstrated that TcdA is capable of inducing ROS production. Studies performed by Kim et al. in human colonocytes demonstrated that exposure to TcdA caused a significant increase in ROS production in as early as 10 minutes, and this effect seemed to carry over to 90 minutes with ROS levels reaching a maximum of almost 6-fold above control [95]. Looking again at studies of human colonocytes, He et al. also showed an increase in ROS production with TcdA exposure, and this increase was attenuated upon pre-treatment with antioxidants. These studies also investigated the effect of pre-treatment with a potent inhibitor of mitochondrial DNA and RNA synthesis. They discovered that TcdA-induced increases in ROS production were dependent on normal mitochondrial function [18]. In an *in vivo* system, Qiu et al. examined the effects of TcdA in rats using the ileal-loop method of toxin exposure. Not only did TcdA exposure result in the development of enteritis, but more importantly, significant increases in hydrogen peroxide and hydroxyl radical formation were detected in mucosal scrapings [79]. This toxin-mediated induction of ROS seems to be specific for TcdA as there are currently no studies which implicate TcdB as having a direct effect in stimulating the production of ROS. In fact, TcdB has been used in certain studies as an inhibitor of NADPH-oxidase activity [96] due to its ability to inhibit Rac-GTPases, which in turn are

needed to activate NADPH-oxidase-induced ROS generation [97]. Referring back to the study performed by Fiorentini et al., which investigated overall oxidative imbalances with *C.diff* toxins, the key finding indicated that both TcdA and TcdB possessed overlapping effects with respect to the presence of oxidized glutathione [80]. This suggests that TcdB could possibly have a role in ROS generation, although this direct mechanism has yet to be elucidated.

Currently, there is a growing body of evidence to support the hypothesis that ROS play a critical role in the regulation of HIF-1 α during normoxia and hypoxia (reviewed in [98]). Studies performed by Jung et al. have analyzed the effects of exogenous H₂O₂ in a number of different cancer cell lines, including colon carcinoma cells. Their results indicated that in the presence of ROS (i.e., H₂O₂), HIF-1 α expression was elevated and this effect appeared to be the result of AMP-dependent protein kinase (AMPK)-induced increases in HIF-1 α transcription [99]. Although other studies have also demonstrated ROS-induced increases in HIF-1 α transcription, a much more relevant mechanism has also been shown that deals with HIF-1 α protein stabilization. Recent studies performed in melanoma cells have demonstrated that HIF-1 α protein expression was increased during hypoxia in a mitochondrial ROS-dependent fashion. When cells were pre-treated with NAC or mitochondrial inhibitors during hypoxia, both HIF-1 α protein expression and downstream HIF-1 signaling were attenuated [100]. A study performed in human lung epithelial cells demonstrated the same effect using cells

lacking mitochondrial DNA (ρ^0 cells). Hypoxia-induced stabilization of HIF-1 α was suppressed such that ρ^0 cells under hypoxia (1.5% O₂) expressed the same amount of HIF-1 α as WT cells in normoxia (21% O₂) [101]. Finally, an important study performed by Bell et al. investigated this mechanism in both lung epithelial carcinoma cells and osteocarcinoma cells. Once again, using siRNA directed at mitochondria complex III, they demonstrated that ROS-dependent stabilization of HIF-1 α was reliant upon normal functioning mitochondria (specifically, complex III). Also, using antibodies directed against hydroxylated HIF-1 α , they also determined that hydroxylation of the α subunit (presumably in the proline region) was abolished by mitochondrial ROS [102]. This suggested that HIF-1 α stabilization under hypoxia was dependent upon the ability of mitochondrial ROS to prevent PHD enzymes from hydroxylating the regulatory prolines of the α subunit. Experiments performed by Tian et al. have illustrated both PHD enzymes and FIH-1 as requiring iron as a cofactor in order to perform their hydroxylating duties, and each of these enzymes was inhibited in the presence of iron chelating agents [103]. By taking an electron from iron and converting Fe²⁺ to Fe³⁺, PHD and FIH-1 enzymes are able to hydroxylate HIF-1 α . The presence of mitochondrial ROS, however, causes oxidation of iron which subsequently prevents the enzymatic activity of the hydroxylating enzymes [102] [104].

These results have significant implications with regard to our findings. In the HIF-Scr cells, we demonstrated that the stabilization of HIF-1 α in the presence of NAC

with TcdA/B was attenuated such that HIF-1 α levels were similar to those found in control treatments. That being said, the HIF-Scr cells also contained significant amounts of nitrosylated HIF-1 α (1.5-fold above control). This suggests that a greater proportion of HIF-1 α was present in the nitrosylated form. Taking into account the evidence for both NO and ROS stabilization of HIF-1 α , it is possible that in the context of *C. diff* toxin exposure, NO and ROS are acting synergistically to stabilize the HIF-1 α protein. As demonstrated in our experiments both *in vitro* and *in vivo*, nitrosylation of HIF-1 α occurs in the presence of TcdA/B. With the evidence provided by previous studies combined with our own NAC data, it can be posited that TcdA/B may also stimulate an increase in mitochondrial ROS which prevents the hydroxylation of HIF-1 α . This, in turn, would cause an increase in the amount of HIF-1 α available for nitrosylation, which would ultimately result in an overall increase in HIF-1 α protein and subsequent HIF-1 downstream signaling. This coincides with our data as incubation of cells with both NAC and TcdA/B causes a reduction of HIF-1 α expression in the cell, but since NO was still upregulated, a significant reduction in the nitrosylation of HIF-1 α was not observed. So, TcdA/B-induced mitochondrial ROS generation could prevent the hydroxylation-dependent degradation of HIF-1 α such that a greater amount of HIF-1 α could be stabilized via nitrosylation. Despite this newly suggested importance of ROS in the context of *C. diff* toxin exposure, it is important to refer back to our data both in cell cultures and in mice that have demonstrated that HIF-1 α is also very much dependent upon iNOS. An inhibition of iNOS resulted in an abolished HIF-1 α response in our *in*

vitro AND *in vivo* model systems in response to TcdA/B. This effect, at least *in vitro*, was associated with an attenuation of HIF-1 α nitrosylation, where pre-incubation with 1400W caused a complete attenuation of nitrosylation.

With regard to HIF-1 α protein stabilization, it is important not to forget that we're ultimately dealing with a transcription factor; therefore, the presence of HIF-1 α protein is only as significant as the downstream signaling activity it is able to stimulate. With respect to HIF-1 α signaling, FIH-1 as mentioned previously, is a well-known asparagine hydroxylase enzyme that is involved in the suppression of HIF-1 downstream transcriptional activity. Experiments performed in Caco-2 cells demonstrate a possible connection between NO and FIH-1. In our Caco-2 cells that have been exposed to TcdA/B, a significant decrease in FIH-1 expression was also detected. When cells were pre-incubated with 1400W, FIH-1 expression was restored to control levels. This suggests that NO might also be involved in destabilizing FIH-1 and preventing its hydroxylation of HIF-1 α . Studies performed by Park et al., using HeLa cells, have demonstrated that NO donors were actually able to directly inhibit FIH-1, which allowed HIF-1 α to interact with transcriptional co-activators. It was initially suspected that nitrosylation of the Cys-800 site on HIF-1 α protected against this asparagine hydroxylation. However, their data suggested that NO was directly inhibiting FIH-1 itself [27]. These data support our findings concerning FIH-1 regulation in the presence of TcdA/B and 1400W. However, in the HIF-KD cells, NO levels were not altered in any

significant manner, yet FIH-1 expression was still suppressed with both TcdA/B and NAC + TcdA/B treatments. Since NAC alone does not affect FIH-1 expression, it is possible that FIH-1 levels could also be suppressed by TcdA/B in an NO-independent manner. A recent study that Koike et al. performed in smooth muscle cells demonstrated that TcdB was capable of activating membrane-type 1 matrix metalloproteinase (MT1-MMP), a protein that is involved in the breakdown of the extracellular matrix [105]. Another recent study by Sakamoto et al. performed in breast cancer cell lines has demonstrated that MT1-MMP is capable of inhibiting FIH-1 expression, which was consequently shown to stimulate the increased transcription of VEGF (a downstream target of HIF-1 signaling) [106]. This may be important to consider as MT1-MMP expression was shown in colonic epithelial cells [107]. Although this is very much speculation, FIH-1 may be inhibited by TcdB in our model system via MT1-MMP in an NO-independent manner.

It is important to emphasize that there are currently very few studies related to the nitrosylation of HIF-1 α in the context of the GI tract. As such, the findings presented herein represent the first evidence for the nitrosylation of HIF-1 α in the context of C.diff toxin exposure. That being said, if we consider the significance of nitrosylation events occurring within the gut, it is important to analyze the effect of iNOS inhibition on epithelial barrier integrity. According to our ZO-1 immunofluorescence data in Caco-2 cells, pre-treatment with 1400W followed by TcdA/B exposure resulted in no additional damage when compared to TcdA/B exposure alone. In a recent study conducted by

Riaño et al [88], the effects of NO with respect to HIF were investigated in rats that were subjected to intestinal damage via indomethacin (IM). Rats were treated with IM over a period of 24 – 96h in order to induce ulcers in the jejunum. Within this time frame, it was found that iNOS, HIF, Intestinal Trefoil Factor (ITF; a downstream gene target of HIF), and a number of nitrated proteins all reached a peak in terms of their protein expression levels. It was determined that HIF-1 α was being nitrosylated in the animals that were given the IM treatment compared to control animals. Even more interesting, is that when rats were given 1400W in conjunction with IM, this caused a reduction in the amount of HIF-1 α being detected, as well as other nitrated proteins. This attenuation did not significantly modify the damage induced by IM; however, it did serve to impede ITF function with respect to epithelial barrier restitution. This resulted in a delayed healing response in mice treated with both 1400W and IM, compared to those treated with just IM. These findings seem to agree with our study in that iNOS is necessary for the induction of HIF-1 α stabilization via nitrosylation. Also, similar effects in terms of epithelial damage were seen with respect to iNOS inhibition. Both our results and those of Riaño et al. have demonstrated that iNOS inhibition does not result in an overt increase in epithelial damage. These findings may also explain why ZO-1 distribution was not different between TcdA/B treatment alone and NAC + TcdA/B for the HIF-Scr Caco-2 cells. If ROS do in fact stabilize the HIF-1 α subunit, then like iNOS inhibition, the absence of stabilized HIF-1 α via NAC in the presence of TcdA/B may not result in an overt increase in Caco-2 epithelial cell damage. Riaño et al. suggest that the

decrease in HIF-1 α nitrosylation (and subsequent stabilization) was connected to a decrease in barrier restitution via HIF-1-mediated signaling of ITF. Therefore it is possible that the decrease in stabilized HIF-1 α has a greater consequence with respect to downstream signaling and wound healing following C.diff toxin exposure rather than the immediate damage response.

With respect to S-nitrosylation in general, a recent study by Savidge et al. performed in Caco-2 cells and mice have demonstrated that NO was capable of directly nitrosylating C.diff toxins themselves. It was determined that trans-nitrosylation of different cysteine residues, including ones located in the catalytic cysteine protease region, inhibited both autocatalysis and cell entry of the toxin [108]. These studies, along with our current study, demonstrate the increasing importance of NO in mounting a crucial cellular defense response.

In summary, using both *in vitro* and *in vivo* model systems, this thesis provides novel findings that suggest an essential role for iNOS-generated NO in the stabilization of HIF-1 α in the context of C.diff toxin exposure (Summary Figure 2). Additionally, this study is the first to propose a synergistic action for two important stabilization mechanisms of HIF-1 α in the context of C.diff toxin-mediated epithelial damage.

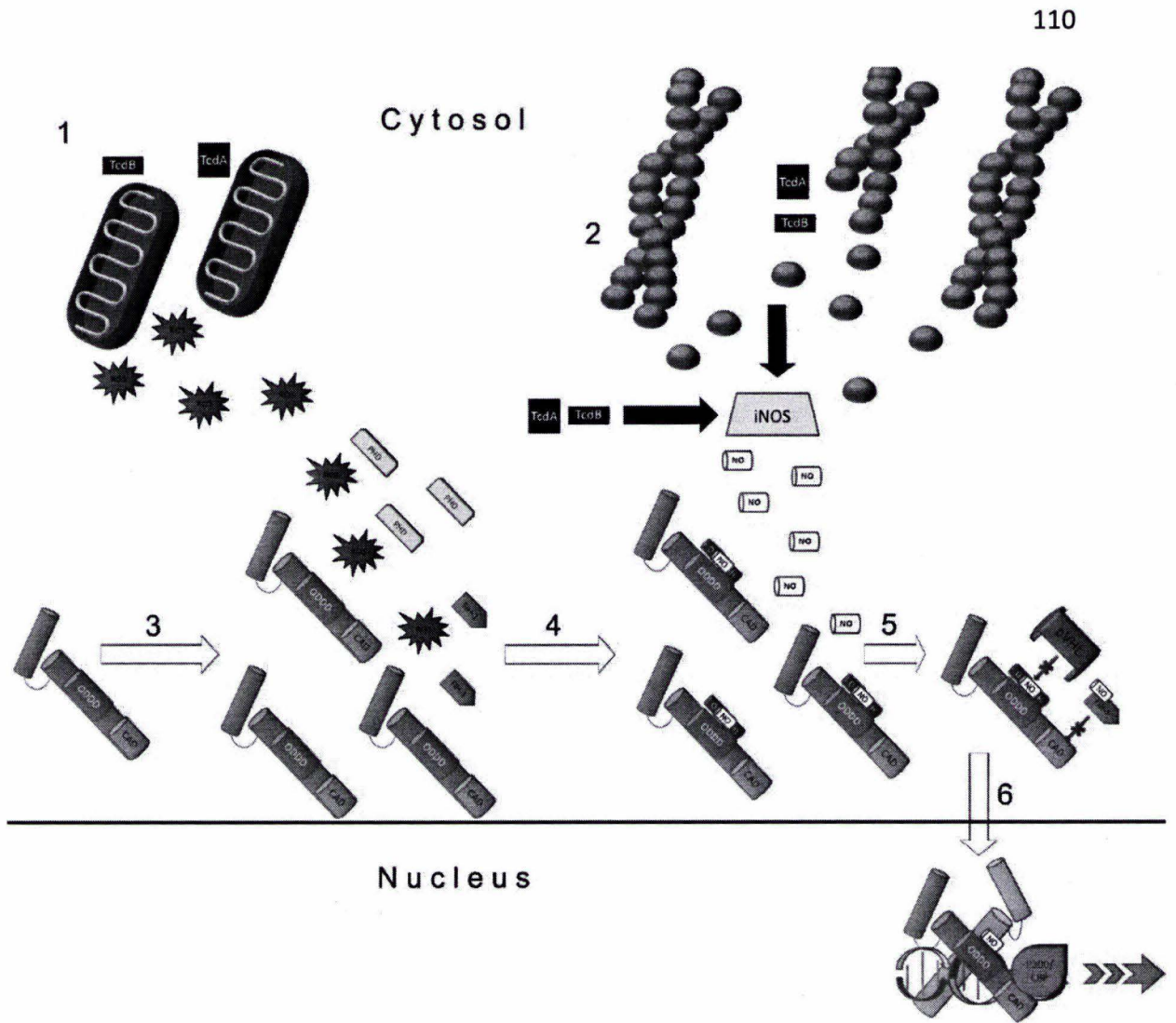
5.2 *Future directions*

The future directions of this study are arguably found in its limitations. This study, for example, does not analyze the specific nitrosylation events that are occurring on HIF-1 α itself. It may be worthwhile to examine which residues are specifically being nitrosylated on HIF-1 α and whether or not certain residues are important for the stabilization of the protein. Riaño et al. for example, detected the presence of both nitrosylated cysteine and nitrosylated tyrosine suggesting that multiple nitrosylation events are occurring on HIF-1 α outside of the well-characterized cysteine residues (i.e., Cys-520 and Cys-800) [88]. This goal could be accomplished using antibodies specific for nitrosocysteine or nitrosotyrosine; however, the most accurate method would be to provide direct identification of post-translational modifications via mass spectrometry.

Another limitation is the lack of mRNA analysis of downstream target genes. HIF-1 α downstream signaling provides important transcriptional regulation of a plethora of genes involved in a number of processes including angiogenesis, erythropoiesis, and cell fate decisions just to name a few [109]. Although we have performed EMSAs and used FIH-1 expression as a surrogate for HIF-1 signaling, verification of direct transcriptional activity would be valuable. This study would benefit immensely with quantitative real-time analysis of mRNA demonstrating increases in HIF-1 downstream barrier protective genes such as VEGF, CD-73, and ITF. Lastly, in order to provide additional supporting evidence for the involvement of a ROS-dependent stabilization

effect, direct analysis of ROS levels both in cell culture and mouse mucosal scrapings would be advantageous. Also, analyzing the hydroxylation of HIF-1 α would help to confirm whether or not stabilization of the α subunit was the primary mechanism involved where ROS is concerned.

In closing, it is my sincere hope that this thesis represents an important piece of a much larger puzzle - one that defines HIF-1 α as an essential therapeutic target in the defense against *Clostridium difficile*-mediated intestinal damage.



Summary Figure 2 – Mechanisms of *Clostridium difficile*-mediated HIF-1 α regulation

Summary Figure 2 – Mechanisms of *Clostridium difficile*-mediated HIF-1 α regulation.

The purpose of this figure is to summarize the mechanisms of HIF-1 α stabilization discussed in the analysis and interpretation. Upon exposure to *Clostridium difficile* (C.diff), toxins are taken up into the cell via receptor-mediated endocytosis. Once inside the cell, C.diff toxin A (TcdA) and C.diff toxin B (TcdB) can initiate an array of different events with respect to HIF-1 α stabilization.

[1] – TcdA stimulates the production of reactive oxygen species (ROS) from the mitochondria

[2] – Both TcdA and TcdB, through their enzymatic activity, begin to glucosylate small GTPase proteins that are involved in maintaining the actin cytoskeleton. Glucosylation of these proteins results in their inactivation and the subsequent disruption of the cytoskeleton. This disruption can lead to the induction of inducible nitric oxide synthase (iNOS), which then begins producing nitric oxide (NO). TcdA and TcdB can also stimulate iNOS activity via NF- κ B.

[3] – HIF-1 α begins to accumulate inside the cell due to the increased concentration of ROS. The mitochondrial ROS causes the oxidation of Fe²⁺, which is needed for the hydroxylation of HIF-1 α . This oxidation of Fe²⁺ to Fe³⁺ suppresses the activity of HIF-1 α hydroxylating enzymes, prolyl hydroxylase (PHD) and Factor inhibiting-HIF-1 (FIH-1 – an asparagine hydroxylase).

[4] – Due to the increase in NO concentration and HIF-1 α protein, more HIF-1 α becomes available for nitrosylation on cysteine residues.

[5] – Nitrosylation of the α subunit results in the stabilization of HIF-1 α by protecting it from interacting with ubiquitinating proteins such as the von Hippel-Lindau protein complex (pVHL). NO is also thought to be capable of interacting with FIH-1 which results in its inactivation. Nitrosylation, however, does not prevent HIF-1 α from being hydroxylated. Therefore it is still possible for proline hydroxylation events to occur after S-nitrosylation.

[6] – S-nitrosylated HIF-1 α is considered stabilized and protected from degradation. It is now capable of entering the nucleus, dimerizing with HIF-1 β , and upregulating the transcription of downstream barrier protective genes.

6.0

references

1. Jaber, M.R., et al., *Clinical review of the management of fulminant clostridium difficile infection*. Am J Gastroenterol, 2008. **103**(12): p. 3195-203; quiz 3204.
2. Lyerly, D.M., H.C. Krivan, and T.D. Wilkins, *Clostridium difficile: its disease and toxins*. Clin Microbiol Rev, 1988. **1**(1): p. 1-18.
3. Voth, D.E. and J.D. Ballard, *Clostridium difficile toxins: mechanism of action and role in disease*. Clin Microbiol Rev, 2005. **18**(2): p. 247-63.
4. Pepin, J., et al., *Clostridium difficile-associated diarrhea in a region of Quebec from 1991 to 2003: a changing pattern of disease severity*. CMAJ, 2004. **171**(5): p. 466-72.
5. Lamontagne, F., et al., *Impact of emergency colectomy on survival of patients with fulminant Clostridium difficile colitis during an epidemic caused by a hypervirulent strain*. Ann Surg, 2007. **245**(2): p. 267-72.
6. Eggertson, L. and B. Sibbald, *Hospitals battling outbreaks of C. difficile*. CMAJ, 2004. **171**(1): p. 19-21.
7. Wilkins, T.D. and D.M. Lyerly, *Clostridium difficile testing: after 20 years, still challenging*. J Clin Microbiol, 2003. **41**(2): p. 531-4.
8. Paredes-Sabja, D., et al., *Germination of spores of Clostridium difficile strains, including isolates from a hospital outbreak of Clostridium difficile-associated disease (CDAD)*. Microbiology, 2008. **154**(Pt 8): p. 2241-50.
9. Iizuka, M. and S. Konno, *Wound healing of intestinal epithelial cells*. World J Gastroenterol, 2011. **17**(17): p. 2161-71.

10. Ulluwishewa, D., et al., *Regulation of tight junction permeability by intestinal bacteria and dietary components*. J Nutr, 2011. **141**(5): p. 769-76.
11. Fasano, A., *Toxins and the gut: role in human disease*. Gut, 2002. **50 Suppl 3**: p. III9-14.
12. Shen, L., et al., *Tight junction pore and leak pathways: a dynamic duo*. Annu Rev Physiol, 2011. **73**: p. 283-309.
13. Wang, F., et al., *Active deformation of apoptotic intestinal epithelial cells with adhesion-restricted polarity contributes to apoptotic clearance*. Lab Invest, 2011. **91**(3): p. 462-71.
14. Madara, J.L., *Intestinal absorptive cell tight junctions are linked to cytoskeleton*. Am J Physiol, 1987. **253**(1 Pt 1): p. C171-5.
15. Furuse, M., *Molecular basis of the core structure of tight junctions*. Cold Spring Harb Perspect Biol, 2010. **2**(1): p. a002907.
16. Genth, H., et al., *Clostridium difficile toxins: more than mere inhibitors of Rho proteins*. Int J Biochem Cell Biol, 2008. **40**(4): p. 592-7.
17. Davies, A.H., et al., *Super toxins from a super bug: structure and function of Clostridium difficile toxins*. Biochem J, 2011. **436**(3): p. 517-26.
18. He, D., et al., *Clostridium difficile toxin A triggers human colonocyte IL-8 release via mitochondrial oxygen radical generation*. Gastroenterology, 2002. **122**(4): p. 1048-57.

19. Laukoetter, M.G., P. Nava, and A. Nusrat, *Role of the intestinal barrier in inflammatory bowel disease*. World J Gastroenterol, 2008. **14**(3): p. 401-7.
20. Lisy, K. and D.J. Peet, *Turn me on: regulating HIF transcriptional activity*. Cell Death Differ, 2008. **15**(4): p. 642-9.
21. Makino, Y., et al., *Transcriptional up-regulation of inhibitory PAS domain protein gene expression by hypoxia-inducible factor 1 (HIF-1): a negative feedback regulatory circuit in HIF-1-mediated signaling in hypoxic cells*. J Biol Chem, 2007. **282**(19): p. 14073-82.
22. Taylor, C.T. and S.P. Colgan, *Hypoxia and gastrointestinal disease*. J Mol Med (Berl), 2007. **85**(12): p. 1295-300.
23. Glover, L.E. and S.P. Colgan, *Hypoxia and metabolic factors that influence inflammatory bowel disease pathogenesis*. Gastroenterology, 2011. **140**(6): p. 1748-55.
24. Brune, B. and J. Zhou, *The role of nitric oxide (NO) in stability regulation of hypoxia inducible factor-1alpha (HIF-1alpha)*. Curr Med Chem, 2003. **10**(10): p. 845-55.
25. Kaelin, W.G., Jr., *The von Hippel-Lindau tumour suppressor protein: O₂ sensing and cancer*. Nat Rev Cancer, 2008. **8**(11): p. 865-73.
26. Hansson, L.O., et al., *Two sequence motifs from HIF-1alpha bind to the DNA-binding site of p53*. Proc Natl Acad Sci U S A, 2002. **99**(16): p. 10305-9.

27. Park, Y.K., et al., *Nitric oxide donor, (+/-)-S-nitroso-N-acetylpenicillamine, stabilizes transactive hypoxia-inducible factor-1alpha by inhibiting von Hippel-Lindau recruitment and asparagine hydroxylation*. *Mol Pharmacol*, 2008. **74**(1): p. 236-45.
28. Semenza, G.L., *Hypoxia-inducible factor 1 (HIF-1) pathway*. *Sci STKE*, 2007. **2007**(407): p. cm8.
29. Tal, R., et al., *Activation of C-transactivation domain is essential for optimal HIF-1 alpha-mediated transcriptional and angiogenic effects*. *Microvasc Res*, 2008. **76**(1): p. 1-6.
30. Frede, S., U. Berchner-Pfannschmidt, and J. Fandrey, *Regulation of hypoxia-inducible factors during inflammation*. *Methods Enzymol*, 2007. **435**: p. 405-19.
31. Frede, S., et al., *Bacterial lipopolysaccharide induces HIF-1 activation in human monocytes via p44/42 MAPK and NF-kappaB*. *Biochem J*, 2006. **396**(3): p. 517-27.
32. Blikslager, A.T., *Life in the gut without oxygen: adaptive mechanisms and inflammatory bowel disease*. *Gastroenterology*, 2008. **134**(1): p. 346-8.
33. Robinson, A., et al., *Mucosal protection by hypoxia-inducible factor prolyl hydroxylase inhibition*. *Gastroenterology*, 2008. **134**(1): p. 145-55.
34. Karhausen, J., et al., *Epithelial hypoxia-inducible factor-1 is protective in murine experimental colitis*. *J Clin Invest*, 2004. **114**(8): p. 1098-106.
35. Brune, B. and J. Zhou, *Nitric oxide and superoxide: interference with hypoxic signaling*. *Cardiovasc Res*, 2007. **75**(2): p. 275-82.

36. Forstermann, U., et al., *Isoforms of nitric oxide synthase. Properties, cellular distribution and expressional control*. *Biochem Pharmacol*, 1995. **50**(9): p. 1321-32.
37. Alican, I. and P. Kubes, *A critical role for nitric oxide in intestinal barrier function and dysfunction*. *Am J Physiol*, 1996. **270**(2 Pt 1): p. G225-37.
38. Moncada, S. and A. Higgs, *The L-arginine-nitric oxide pathway*. *N Engl J Med*, 1993. **329**(27): p. 2002-12.
39. Kubes, P. and D.M. McCafferty, *Nitric oxide and intestinal inflammation*. *Am J Med*, 2000. **109**(2): p. 150-8.
40. Nathan, C. and Q.W. Xie, *Nitric oxide synthases: roles, tolls, and controls*. *Cell*, 1994. **78**(6): p. 915-8.
41. Nathan, C., *Inducible nitric oxide synthase: what difference does it make?* *J Clin Invest*, 1997. **100**(10): p. 2417-23.
42. Moncada, S., R.M. Palmer, and E.A. Higgs, *Biosynthesis of nitric oxide from L-arginine. A pathway for the regulation of cell function and communication*. *Biochem Pharmacol*, 1989. **38**(11): p. 1709-15.
43. Moncada, S., R.M. Palmer, and E.A. Higgs, *The discovery of nitric oxide as the endogenous nitrovasodilator*. *Hypertension*, 1988. **12**(4): p. 365-72.
44. Ignarro, L.J., *Biosynthesis and metabolism of endothelium-derived nitric oxide*. *Annu Rev Pharmacol Toxicol*, 1990. **30**: p. 535-60.

45. Palmer, L.A., B. Gaston, and R.A. Johns, *Normoxic stabilization of hypoxia-inducible factor-1 expression and activity: redox-dependent effect of nitrogen oxides*. *Mol Pharmacol*, 2000. **58**(6): p. 1197-203.
46. Kubes, P., *Nitric oxide modulates epithelial permeability in the feline small intestine*. *Am J Physiol*, 1992. **262**(6 Pt 1): p. G1138-42.
47. Ignarro, L.J., *Biological actions and properties of endothelium-derived nitric oxide formed and released from artery and vein*. *Circ Res*, 1989. **65**(1): p. 1-21.
48. Ignarro, L.J., et al., *Activation of purified soluble guanylate cyclase by endothelium-derived relaxing factor from intrapulmonary artery and vein: stimulation by acetylcholine, bradykinin and arachidonic acid*. *J Pharmacol Exp Ther*, 1986. **237**(3): p. 893-900.
49. Kanwar, S., et al., *Nitric oxide synthesis inhibition increases epithelial permeability via mast cells*. *Am J Physiol*, 1994. **266**(2 Pt 1): p. G222-9.
50. Kolios, G., V. Valatas, and S.G. Ward, *Nitric oxide in inflammatory bowel disease: a universal messenger in an unsolved puzzle*. *Immunology*, 2004. **113**(4): p. 427-37.
51. Kurose, I., et al., *Inhibition of nitric oxide production. Mechanisms of vascular albumin leakage*. *Circ Res*, 1993. **73**(1): p. 164-71.
52. Kubes, P. and S. Kanwar, *Histamine induces leukocyte rolling in post-capillary venules. A P-selectin-mediated event*. *J Immunol*, 1994. **152**(7): p. 3570-7.

53. Clancy, R.M., J. Leszczynska-Piziak, and S.B. Abramson, *Nitric oxide, an endothelial cell relaxation factor, inhibits neutrophil superoxide anion production via a direct action on the NADPH oxidase*. J Clin Invest, 1992. **90**(3): p. 1116-21.
54. Boughton-Smith, N.K., et al., *The induction of nitric oxide synthase and intestinal vascular permeability by endotoxin in the rat*. Br J Pharmacol, 1993. **110**(3): p. 1189-95.
55. Nicholson, S.C., et al., *Lethality of endotoxin in mice genetically deficient in the respiratory burst oxidase, inducible nitric oxide synthase, or both*. Shock, 1999. **11**(4): p. 253-8.
56. De Groote, M.A. and F.C. Fang, *NO inhibitions: antimicrobial properties of nitric oxide*. Clin Infect Dis, 1995. **21 Suppl 2**: p. S162-5.
57. Fang, F.C., *Perspectives series: host/pathogen interactions. Mechanisms of nitric oxide-related antimicrobial activity*. J Clin Invest, 1997. **99**(12): p. 2818-25.
58. Metzen, E., et al., *Nitric oxide impairs normoxic degradation of HIF-1alpha by inhibition of prolyl hydroxylases*. Mol Biol Cell, 2003. **14**(8): p. 3470-81.
59. Winterbourn, C.C., *Reconciling the chemistry and biology of reactive oxygen species*. Nat Chem Biol, 2008. **4**(5): p. 278-86.
60. Turrens, J.F., *Mitochondrial formation of reactive oxygen species*. J Physiol, 2003. **552**(Pt 2): p. 335-44.
61. van der Vliet, A. and A. Bast, *Role of reactive oxygen species in intestinal diseases*. Free Radic Biol Med, 1992. **12**(6): p. 499-513.

62. Swanson, P.A., 2nd, et al., *Enteric commensal bacteria potentiate epithelial restitution via reactive oxygen species-mediated inactivation of focal adhesion kinase phosphatases*. Proc Natl Acad Sci U S A, 2011. **108**(21): p. 8803-8.
63. Wink, D.A., et al., *Nitric oxide protects against cellular damage and cytotoxicity from reactive oxygen species*. Proc Natl Acad Sci U S A, 1993. **90**(21): p. 9813-7.
64. Winterbourn, C.C., et al., *Modeling the reactions of superoxide and myeloperoxidase in the neutrophil phagosome: implications for microbial killing*. J Biol Chem, 2006. **281**(52): p. 39860-9.
65. Beckman, J.S. and W.H. Koppenol, *Nitric oxide, superoxide, and peroxynitrite: the good, the bad, and ugly*. Am J Physiol, 1996. **271**(5 Pt 1): p. C1424-37.
66. Van der Vliet, A., et al., *Role of the epithelium in the control of intestinal motility: implications for intestinal damage after anoxia and reoxygenation*. Agents Actions, 1992. **36**(1-2): p. 159-67.
67. Van der Vliet, A., et al., *Intestinal motility disorder induced by peroxides: possible role of lipid peroxidation*. Res Commun Chem Pathol Pharmacol, 1990. **70**(2): p. 227-43.
68. Dolowschiak, T., et al., *Potentiation of epithelial innate host responses by intercellular communication*. PLoS Pathog, 2010. **6**(11): p. e1001194.
69. Reiter, C.D., R.J. Teng, and J.S. Beckman, *Superoxide reacts with nitric oxide to nitrate tyrosine at physiological pH via peroxynitrite*. J Biol Chem, 2000. **275**(42): p. 32460-6.

70. Hirota, S.A., et al., *Hypoxia-inducible factor signaling provides protection in Clostridium difficile-induced intestinal injury*. *Gastroenterology*, 2010. **139**(1): p. 259-69 e3.
71. Sullivan, N.M., S. Pellett, and T.D. Wilkins, *Purification and characterization of toxins A and B of Clostridium difficile*. *Infect Immun*, 1982. **35**(3): p. 1032-40.
72. Hellman, L.M. and M.G. Fried, *Electrophoretic mobility shift assay (EMSA) for detecting protein-nucleic acid interactions*. *Nat Protoc*, 2007. **2**(8): p. 1849-61.
73. Semenza, G.L. and G.L. Wang, *A nuclear factor induced by hypoxia via de novo protein synthesis binds to the human erythropoietin gene enhancer at a site required for transcriptional activation*. *Mol Cell Biol*, 1992. **12**(12): p. 5447-54.
74. Jaffrey, S.R. and S.H. Snyder, *The biotin switch method for the detection of S-nitrosylated proteins*. *Sci STKE*, 2001. **2001**(86): p. pl1.
75. Tsikas, D., *Analysis of nitrite and nitrate in biological fluids by assays based on the Griess reaction: appraisal of the Griess reaction in the L-arginine/nitric oxide area of research*. *J Chromatogr B Analyt Technol Biomed Life Sci*, 2007. **851**(1-2): p. 51-70.
76. Zehendner, C.M., et al., *Caspase-3 contributes to ZO-1 and Cl-5 tight-junction disruption in rapid anoxic neurovascular unit damage*. *PLoS One*, 2011. **6**(2): p. e16760.

77. Garvey, E.P., et al., *1400W is a slow, tight binding, and highly selective inhibitor of inducible nitric-oxide synthase in vitro and in vivo*. J Biol Chem, 1997. **272**(8): p. 4959-63.
78. Nusrat, A., et al., *Clostridium difficile toxins disrupt epithelial barrier function by altering membrane microdomain localization of tight junction proteins*. Infect Immun, 2001. **69**(3): p. 1329-36.
79. Qiu, B., et al., *Participation of reactive oxygen metabolites in Clostridium difficile toxin A-induced enteritis in rats*. Am J Physiol, 1999. **276**(2 Pt 1): p. G485-90.
80. Fiorentini, C., et al., *N-acetylcysteine protects epithelial cells against the oxidative imbalance due to Clostridium difficile toxins*. FEBS Lett, 1999. **453**(1-2): p. 124-8.
81. Ahmad, A., et al., *Adenosine A2A receptor is a unique angiogenic target of HIF-2alpha in pulmonary endothelial cells*. Proc Natl Acad Sci U S A, 2009. **106**(26): p. 10684-9.
82. Salzman, A.L., *Nitric oxide in the gut*. New Horiz, 1995. **3**(2): p. 352-64.
83. Muniyappa, R., et al., *Inhibition of Rho protein stimulates iNOS expression in rat vascular smooth muscle cells*. Am J Physiol Heart Circ Physiol, 2000. **278**(6): p. H1762-8.
84. Hattori, Y. and K. Kasai, *Disruption of the actin cytoskeleton up-regulates iNOS expression in vascular smooth muscle cells*. J Cardiovasc Pharmacol, 2004. **43**(2): p. 209-13.

85. Witteck, A., et al., *Rho protein-mediated changes in the structure of the actin cytoskeleton regulate human inducible NO synthase gene expression*. Exp Cell Res, 2003. **287**(1): p. 106-15.
86. Kim, J.M., et al., *NF-kappa B activation pathway is essential for the chemokine expression in intestinal epithelial cells stimulated with Clostridium difficile toxin A*. Scand J Immunol, 2006. **63**(6): p. 453-60.
87. Taylor, B.S., et al., *Multiple NF-kappaB enhancer elements regulate cytokine induction of the human inducible nitric oxide synthase gene*. J Biol Chem, 1998. **273**(24): p. 15148-56.
88. Riano, A., et al., *Nitric oxide induces HIF-1alpha stabilization and expression of intestinal trefoil factor in the damaged rat jejunum and modulates ulcer healing*. J Gastroenterol, 2011. **46**(5): p. 565-76.
89. Melillo, G., et al., *A hypoxia-responsive element mediates a novel pathway of activation of the inducible nitric oxide synthase promoter*. J Exp Med, 1995. **182**(6): p. 1683-93.
90. Peyssonnaud, C., et al., *HIF-1alpha expression regulates the bactericidal capacity of phagocytes*. J Clin Invest, 2005. **115**(7): p. 1806-15.
91. Anderson, E.R., X. Xue, and Y.M. Shah, *Intestinal hypoxia-inducible factor-2alpha (HIF-2alpha) is critical for efficient erythropoiesis*. J Biol Chem, 2011. **286**(22): p. 19533-40.

92. Chen, H. and H. Shi, *A reducing environment stabilizes HIF-2alpha in SH-SY5Y cells under hypoxic conditions*. FEBS Lett, 2008. **582**(28): p. 3899-902.
93. Zhang, F., S.S. Lau, and T.J. Monks, *The cytoprotective effect of N-acetyl-L-cysteine against ROS-induced cytotoxicity is independent of its ability to enhance glutathione synthesis*. Toxicol Sci, 2011. **120**(1): p. 87-97.
94. Spagnuolo, G., et al., *Effect of N-acetyl-L-cysteine on ROS production and cell death caused by HEMA in human primary gingival fibroblasts*. Biomaterials, 2006. **27**(9): p. 1803-9.
95. Kim, H., et al., *Clostridium difficile toxin A regulates inducible cyclooxygenase-2 and prostaglandin E2 synthesis in colonocytes via reactive oxygen species and activation of p38 MAPK*. J Biol Chem, 2005. **280**(22): p. 21237-45.
96. Herkert, O., et al., *NADPH oxidase mediates tissue factor-dependent surface procoagulant activity by thrombin in human vascular smooth muscle cells*. Circulation, 2002. **105**(17): p. 2030-6.
97. Heyworth, P.G., et al., *Regulation of NADPH oxidase activity by Rac GTPase activating protein(s)*. Mol Biol Cell, 1993. **4**(11): p. 1217-23.
98. Kietzmann, T. and A. Gorch, *Reactive oxygen species in the control of hypoxia-inducible factor-mediated gene expression*. Semin Cell Dev Biol, 2005. **16**(4-5): p. 474-86.
99. Jung, S.N., et al., *Reactive oxygen species stabilize hypoxia-inducible factor-1 alpha protein and stimulate transcriptional activity via AMP-activated protein*

- kinase in DU145 human prostate cancer cells. Carcinogenesis, 2008. 29(4): p. 713-21.*
100. Comito, G., et al., *HIF-1alpha stabilization by mitochondrial ROS promotes Met-dependent invasive growth and vasculogenic mimicry in melanoma cells. Free Radic Biol Med, 2011. 51(4): p. 893-904.*
 101. Schroedl, C., et al., *Hypoxic but not anoxic stabilization of HIF-1alpha requires mitochondrial reactive oxygen species. Am J Physiol Lung Cell Mol Physiol, 2002. 283(5): p. L922-31.*
 102. Bell, E.L., et al., *The Qo site of the mitochondrial complex III is required for the transduction of hypoxic signaling via reactive oxygen species production. J Cell Biol, 2007. 177(6): p. 1029-36.*
 103. Tian, Y.M., et al., *Differential sensitivity of hypoxia inducible factor hydroxylation sites to hypoxia and hydroxylase inhibitors. J Biol Chem, 2011. 286(15): p. 13041-51.*
 104. Klimova, T. and N.S. Chandel, *Mitochondrial complex III regulates hypoxic activation of HIF. Cell Death Differ, 2008. 15(4): p. 660-6.*
 105. Koike, T., et al., *Activation of MMP-2 by Clostridium difficile toxin B in bovine smooth muscle cells. Biochem Biophys Res Commun, 2000. 277(1): p. 43-6.*
 106. Sakamoto, T., D. Niiya, and M. Seiki, *Targeting the Warburg effect that arises in tumor cells expressing membrane type-1 matrix metalloproteinase. J Biol Chem, 2011. 286(16): p. 14691-704.*

107. Tammali, R., et al., *Aldose reductase inhibition prevents hypoxia-induced increase in hypoxia-inducible factor-1alpha (HIF-1alpha) and vascular endothelial growth factor (VEGF) by regulating 26 S proteasome-mediated protein degradation in human colon cancer cells.* J Biol Chem, 2011. **286**(27): p. 24089-100.
108. Savidge, T.C., et al., *Host S-nitrosylation inhibits clostridial small molecule-activated glucosylating toxins.* Nat Med, 2011. **17**(9): p. 1136-41.
109. Semenza, G.L., *Oxygen sensing, homeostasis, and disease.* N Engl J Med, 2011. **365**(6): p. 537-47.

end

"Your beginnings will seem humble,

So prosperous will your future be."

-Job 8:7